Electronic Supplementary Material (ESI) for RSC Advances.

SUPPORTING INFORMATION

Carbohydrate Structure-Activity Relations of Au-Catalysed Base-Free Oxidations: Gold Displaying a Platinum Lustre

Frits van der Klis,[a,b] Linda Gootjes,[b] Noud Hendrik Verstijnen,[b] Jacco van Haveren,[b] Daniël Stephan van Es,[b] and Johannes Hendrik Bitter[a]

[a]*Wageningen University Biobased Chemistry and Technology, Bornse Weilanden 9, 6708 WG Wageningen, The Netherlands. E-mail: harry.bitter@wur.nl; Tel: +31 317 480 303*

[b]*Wageningen Food & Biobased Research, Bornse Weilanden 9, 6708 WG Wageningen, The Netherlands. E-mail: daan.vanes@wur.nl; Tel: +31 317 481 160*

Section 1. Analysis of freeze dried reaction mixtures

1.1 Galacturonic acid (GalA) oxidation

Fig. S1 shows the ^{13}C-NMR spectra of the lyophilized reaction mixture of the GalA oxidation mixture, and a comparison to GalA (residual starting material), GA (di-acid product), and galactaric acid-1,4-lactone (lactone reference). In the lyophilized sample, remaining GalA and the desired GA products could both be detected. Besides these products, also galactaric acid-1,4-lactone could be clearly identified (triangles in Fig. S1), although at relative low intensity.

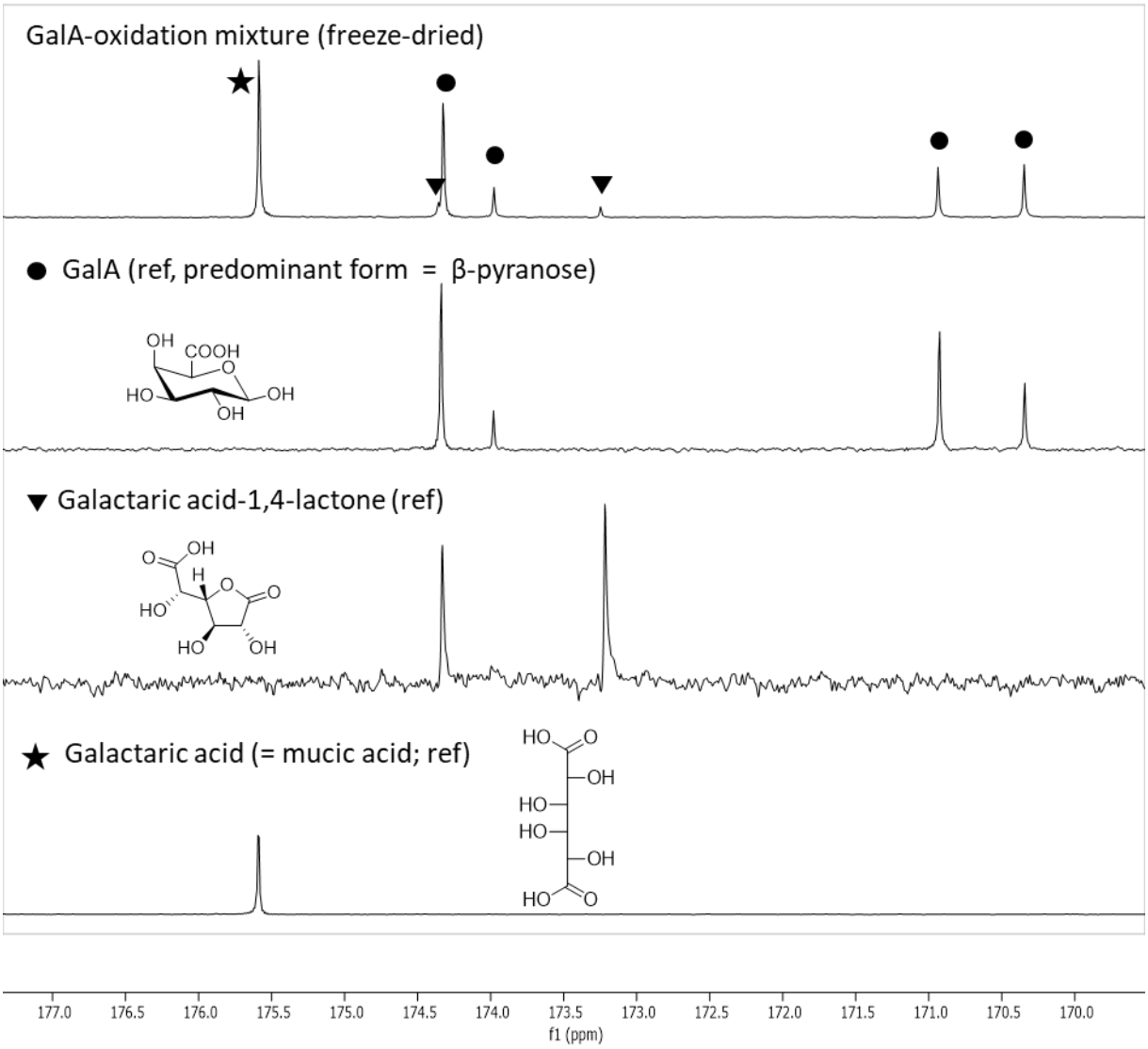

Fig. S1 ^{13}C-NMR's (DMSO-D6) of GalA-reaction mixture, GalA (ref), galactaric acid-1,4-lactone (ref) and GA (ref). Red triangles in GalA-oxidation mixture mark the signals of the galactaric acid-1,4-lactone.

This result confirms the formation of a lactone product under our reaction conditions. It is however surprising to find that the only observed lactone is the galactaric acid-1,4-lactone, while another potential lactone, galactaric acid-1,5-lactone, is not observed.

1.2 Explaining observed 1,4-lactone formation during GalA oxidation

As started in the main article, others already postulated that the oxidation of (other) carbohydrates under alkaline-free conditions proceeds via a hydrogen abstraction mechanism, leading to the lactones as the initial oxidation products.[1, 2] So, hydrogen abstraction of a 5-membered ring (α-/β-furanose) could lead to the observed galactaric acid-1,4-lactone, while hydrogen abstraction of a 6-membered ring (α-r/β -pyranose) would lead to the galactaric acid-1,5-lactone. This raises the question whether the furanose ring is more reactive towards oxidation, or just more prominently present in solution. To guide the reader through the structures, an overview is provided in Fig. S2.

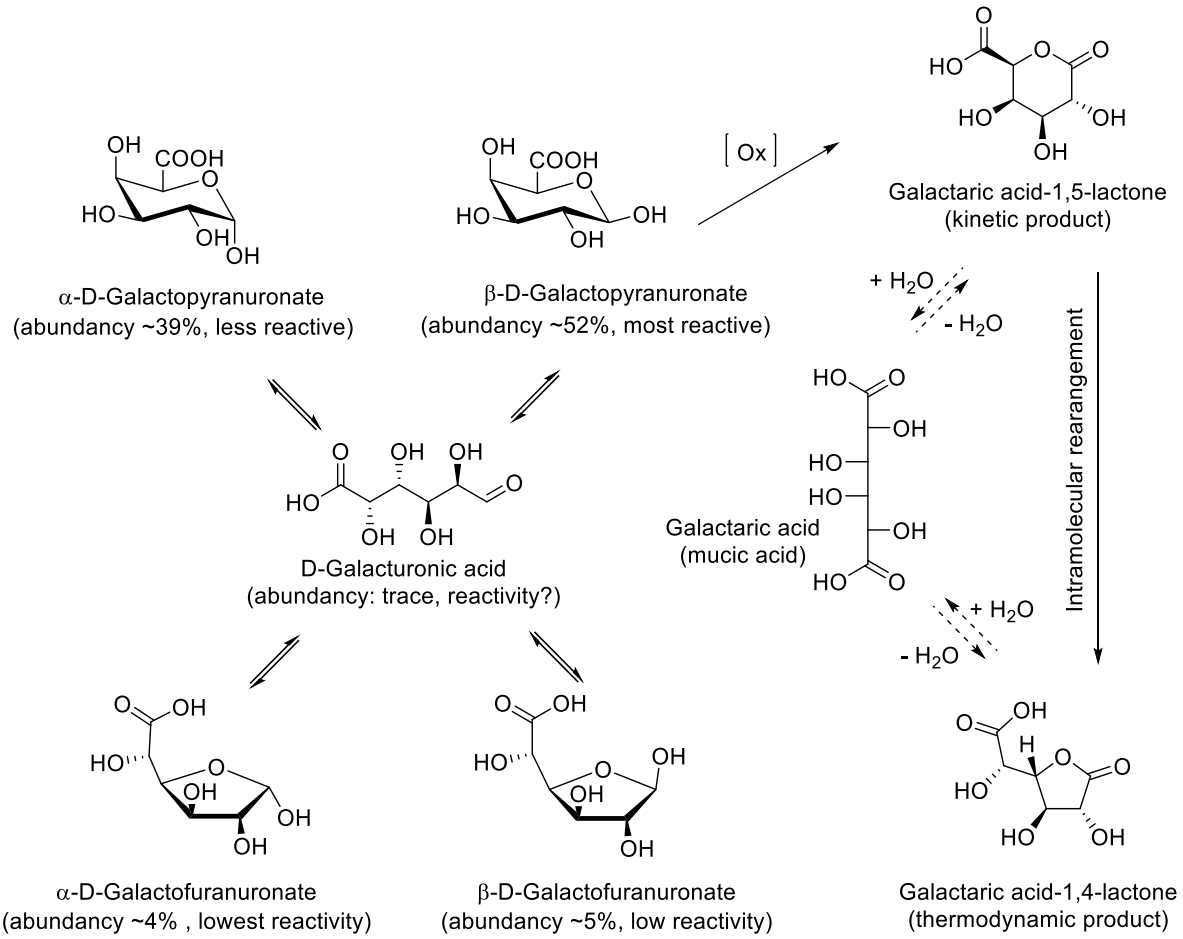

Fig. S2: Galacturonic acid reaction network, showing the galacturonide anomers with their relative abundance and expected reactivity towards oxidation, and the proposed oxidation products in their equilibrium forms.

The starting material GalA exhibits four main conformations in aqueous solution, of which the pyranose forms (β > α) are by far the most predominant species (For further reading, consult literature references in the overview in Table S1). Based on the high relative abundance of the pyranose forms, the 1,5-lactone is therefore still expected to be the predominant initial product, and this cannot explain the sole observation of the 1,4-lactone. The next explanation could be that furanoses are more reactive compared to pyranoses, and thus albeit present at lower concentration, are converted at much faster rate. Unfortunately, for Au-catalysed oxidations over heterogeneous catalysts, to the best of our knowledge there is no data available on the influence of ring structures or anomeric forms on the oxidation kinetics. However, two alternative carbohydrate oxidation reactions could give hints on the reactivity: 1) Aldose bromine oxidations and 2) Electrochemical oxidation of glucose.

1) Pioneering work on the influence of carbohydrate structure on reactivity has been done by Isbell and co-workers in the 1930's.[3-6] They extensively studied the bromine oxidation of aldoses, which led to important insights in reactivity differences: e.g. β-anomers were found much more reactive compared to α-anomers, and pyranoses were more reactive compared to furanoses. It was also found that reactivity at the anomeric centre is influenced by the axial/equatorial orientations of OH-groups of neighbouring positions in the ring.

2) Beden and Largeaud[7, 8] systematically investigated the reactivity of different glucose anomers over Pt-electrodes. These studies showed that the β-glucopyranose form was the most reactive, which is in line with the results of Isbell and co-workers.

So, the β-pyranose is the most prevalent and expected to be the most reactive, and should therefore lead to the (non-observed) galactaric acid-1,5-lactone as the initial product, while experimentally the 1,4-lactone is observed instead. Bouvier *et al.*[9] found that the galactaric acid-1,5-lactone, even under neutral conditions, is readily converted into the galactaric acid-1,4-lactone. This process is believed to proceed spontaneously via an intramolecular rearrangement. Under our conditions, which are acidic in nature (~pH 2.4), this process will be even faster, explaining why the 1,5-lactone is not observed, but might very well still be the initial product.

1.3 Glucose (Glc) oxidation

For the Glc conversion, HPLC analysis showed that the oxidation mixture contained the expected gluconic acid in open form (free acid) and/or gluconic acid-1,5-lactone. However, both compounds elute at the same time in HPLC, and can therefore not be distinguished. Next to that, also gluconic acid-1,4-lactone was detected, a product with a different retention time on HPLC.[10] To confirm the presence of lactones by a separate analysis technique, NMR was recorded of a lyophilized sample in DMSO-D_6, and the results are shown in Fig. S3.

The Glc reaction mixture displayed in Fig. S3 shows a complex mixture of unreacted Glc together with 3 oxidation products: small amounts of gluconic acid (open form),[11] small amounts of gluconic acid-1,4-lactone, and gluconic acid-1,5-lactone as the most predominant product.

To explain the high abundance of the gluconic acid-1,5-lactone in the initial reaction mixture, three factors have to be considered: 1) Glucose conformation (anomeric forms and their mutarotation); 2) Reaction kinetics for the oxidation reaction; and 3) Lactonisation / hydrolysis kinetics of the final product mixture (interconversion of gluconate-lactones and free acid form). A schematic overview of the reaction network is shown in Fig. S4.

1: Glucose conformation: Our oxidation reaction was performed by dissolving commercial available α-D-glucose monohydrate in water, which is a crystalline form of α-D-glucopyranoside (Fig. S3, top left corner). However, upon dissolution glucose undergoes mutarotation, shifting the compositions until an equilibrium is reached. At equilibrium, the most predominant species are the pyranosides, with the β-pyranoside (~62%) prevailing over the α-D-glucopyranoside (~37%).[12-14] Although mutarotation of glucose is a relatively slow process at room temperature, the rates significantly increase at higher temperatures, such as applied under our reaction conditions.[15, 16] At 70 °C, the rate of mutarotation is already in the range of 0.42/s, which is much higher than the oxidation rate.[16]

2: Reaction kinetics for the oxidation reaction: The mechanism for carbohydrate oxidations over Au-catalysts under base-free conditions is proposed to proceed via hydrogen abstraction, leading to lactone formation.[1, 2] Hydrogen abstraction from either α- or β-glucopyranose would therefore lead to the formation of gluconic acid-1,5-lactone, while hydrogen abstraction from either the α- or β-furanosides leads to the formation of gluconic acid-1,4-lactone. Oxidation of the free aldehyde (or its hydrate) could lead directly to gluconic acid.

In our investigation, the main product observed is gluconic acid-1,5-lactone, present in much higher concentration compared to the free acid or the gluconic acid-1,4-lactone. Based on the high preference of the glucose starting material for a pyranoside conformation, the preference for 1,5-lactone product formation might have been expected. However, differences in reactivity of the anomeric forms could not be ignored, since the least abundant species might be the most reactive. Furthermore, the rate of mutarotation is high compared to the rate of oxidation as stated above.[17]

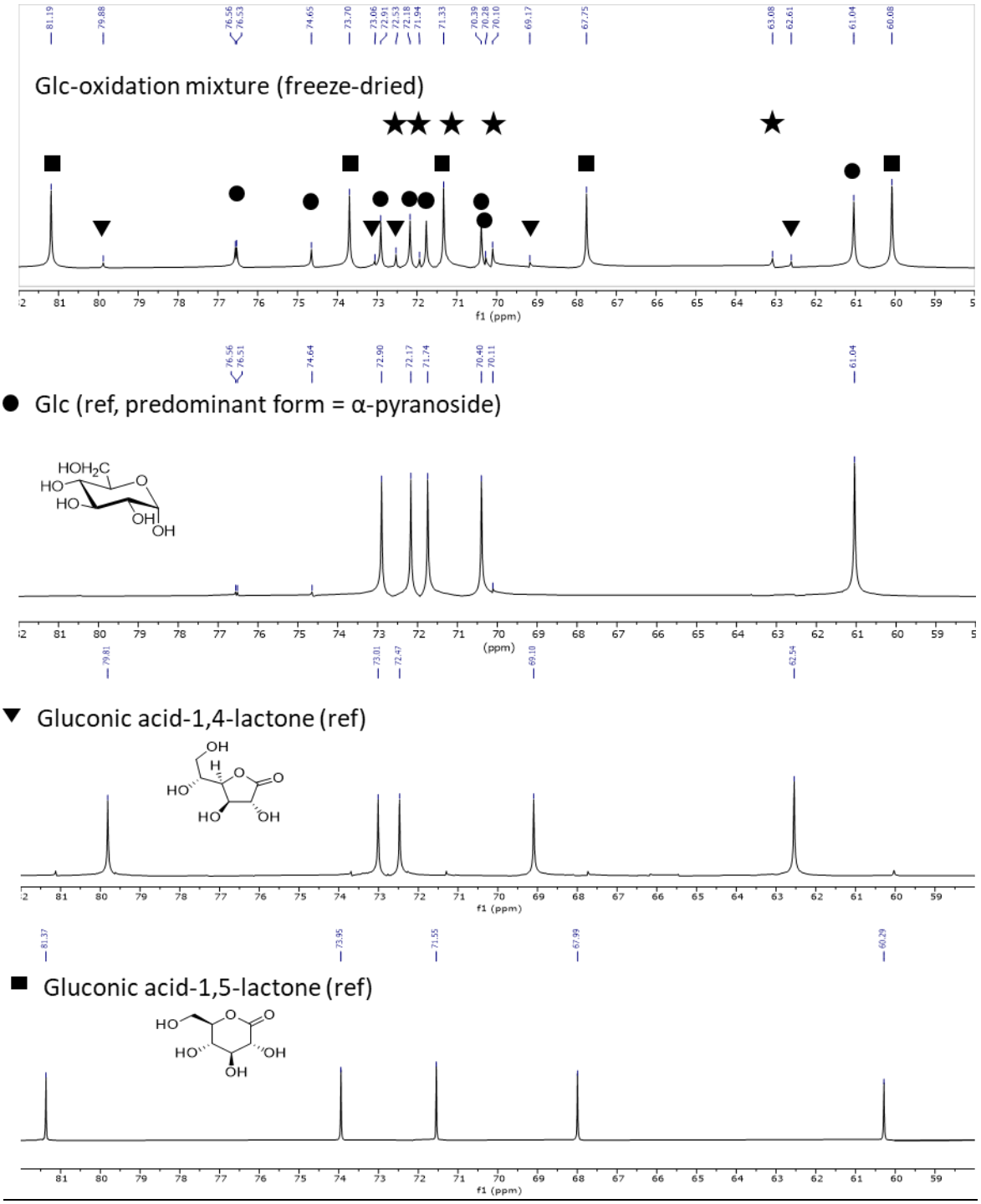

Fig. S3 ^{13}C-NMR's (DMSO-D6) of Glc-reaction mixture, Glc reference (circles), gluconic acid-1,4-lactone reference (triangles), gluconic acid-1,5-lactone reference (squares) and gluconic acid reference (literature values[11] as stars).

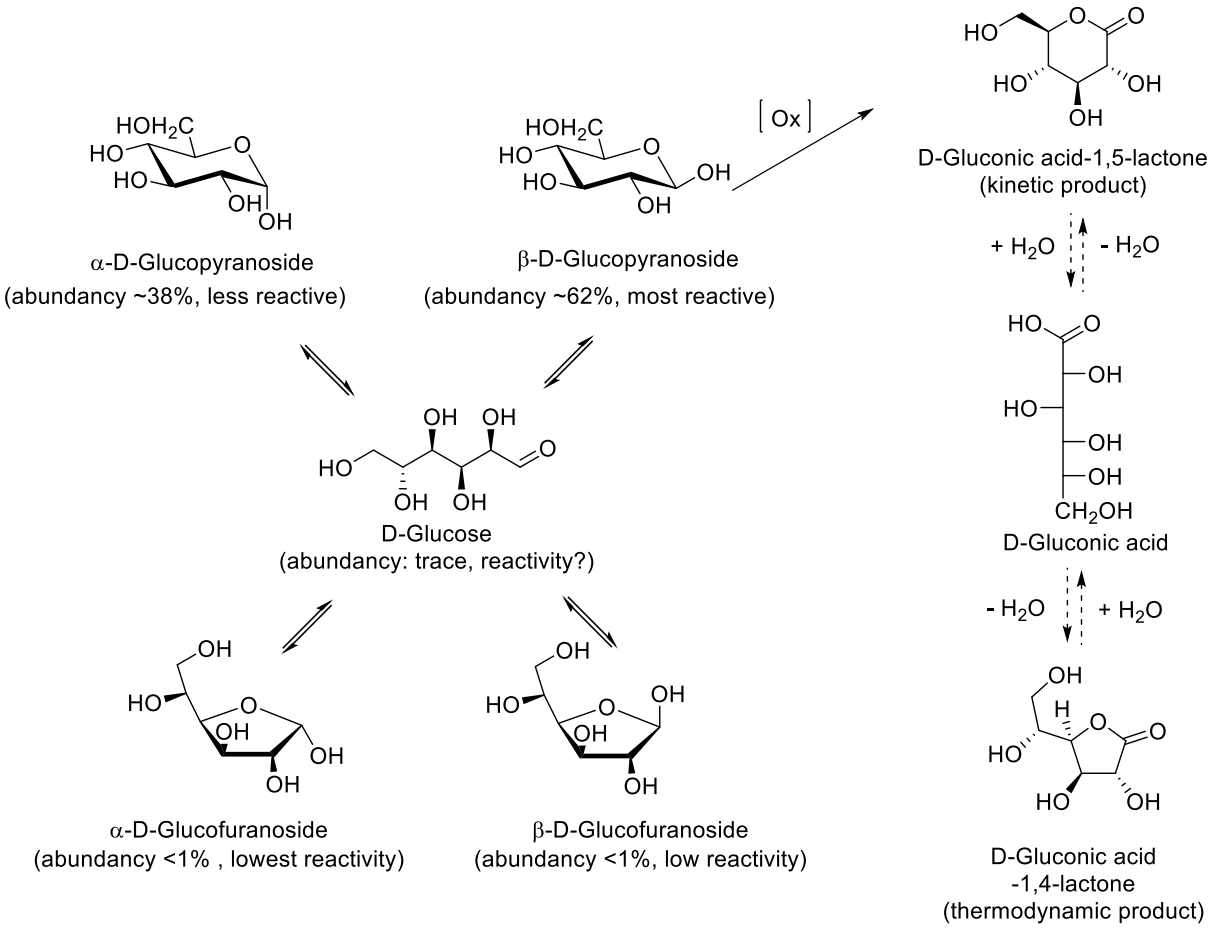

Fig. S4 Glucose reaction network, showing the glucose anomers with their relative abundance and expected reactivity towards oxidation, and the proposed oxidation products in their equilibrium forms.

For Au-catalysed oxidations over heterogeneous catalysts, to the best of our knowledge there is no data available on the influence of anomeric forms on the oxidation kinetics. However, as previously mentioned Beden and Largeaud[7, 8] systematically investigated the reactivity of different glucose anomers over Pt-electrodes, indicating that the β-glucopyranose form is the most reactive, leading to the formation of the 1,5-lactone as the initial product. More recent work on glucose oxidations over Au-electrodes, also propose that the reactions proceeds via the gluconic acid-1,5-lactone.[18, 19]

Nowadays, the correlation between electro-chemistry and heterogeneous catalysis is getting more recognized, in which reactions on the catalyst surface can be regarded as the two half-reactions in an electrochemical cell.[1, 20] Therefore we can assume that the preference for the β-glucopyranose over the α-glucopyranose in electrochemical oxidations, will probably be the same for catalytic Au-oxidations, which is in line with the observed preference for the gluconic acid-1,5-lactone formation.

3: Lactonisation kinetics of the product mixture: So far, the glucose conformational preference, and highest reactivity of the β-pyranose form, were able to explain the observed high concentration of gluconic acid-1,5-lactone. However, the gluconic acid-1,5-lactone itself is also in equilibrium with the 1,4-lactone and gluconic acid (hydrolysis product). So, there is a possibility that the 1,5-lactone is a secondary product which might be formed very rapidly. The lactonization and protonation of gluconic acid was investigated in detail by Zhang et al[21] and Sawyer[22]. They found that gluconic acid lactonisation into the 1,5-lactone proceeds more readily compared to the 1,4-lactone. However, lactone hydrolysis rates are much higher compared to lactone formation rates. A fully equilibrated mixture is reported to contain 67% galactonic acid, 16% 1,5-lactone and 17% 1,4-lactone.[17] So, the high amount of gluconic acid-1,5-lactone compared to trace amounts of gluconic acid and the 1,4-lactone can only be explained if the 1,5-lactone has been formed as the initial product. It should also be noted that the 1,5-lactones are the kinetic products of sugar oxidations, while the 1,4-lactones are the thermodynamic products.[10, 23]

To summarize, based on the composition of the 1,5-gluconic acid-lactone enriched reaction mixture, the most likely reaction cascade is the oxidation of the most predominant and reactive β-D-glucopyranose, via the intermediate gluconic acid-1,5-lactone (kinetic product), into gluconic acid and gluconic acid-1,4-lactone (thermodynamic product).

1.4 Galactose (Gal) oxidation

Analogue to the investigation on glucose, also for Gal conversion, HPLC analysis or the reaction mixture and NMR measurements of a lyophilized sample were performed to indicate the reaction products.

HPLC showed, next to remaining galactose, galactonic acid in open form (free acid) and/or galactonic acid-1,4-lactone, which both elute at the same time and therefore cannot be distinguished. Although we attempted to synthesize the galactonic acid-1,5-lactone as a reference, we were unable to reproduce the literature procedures.[9]

NMR of the lyophilized sample is show in Fig. S5. The major compound was galactonic acid (open form), the 1,4-lactone was found in small amount, while the 1,5-lactone could not be detected.

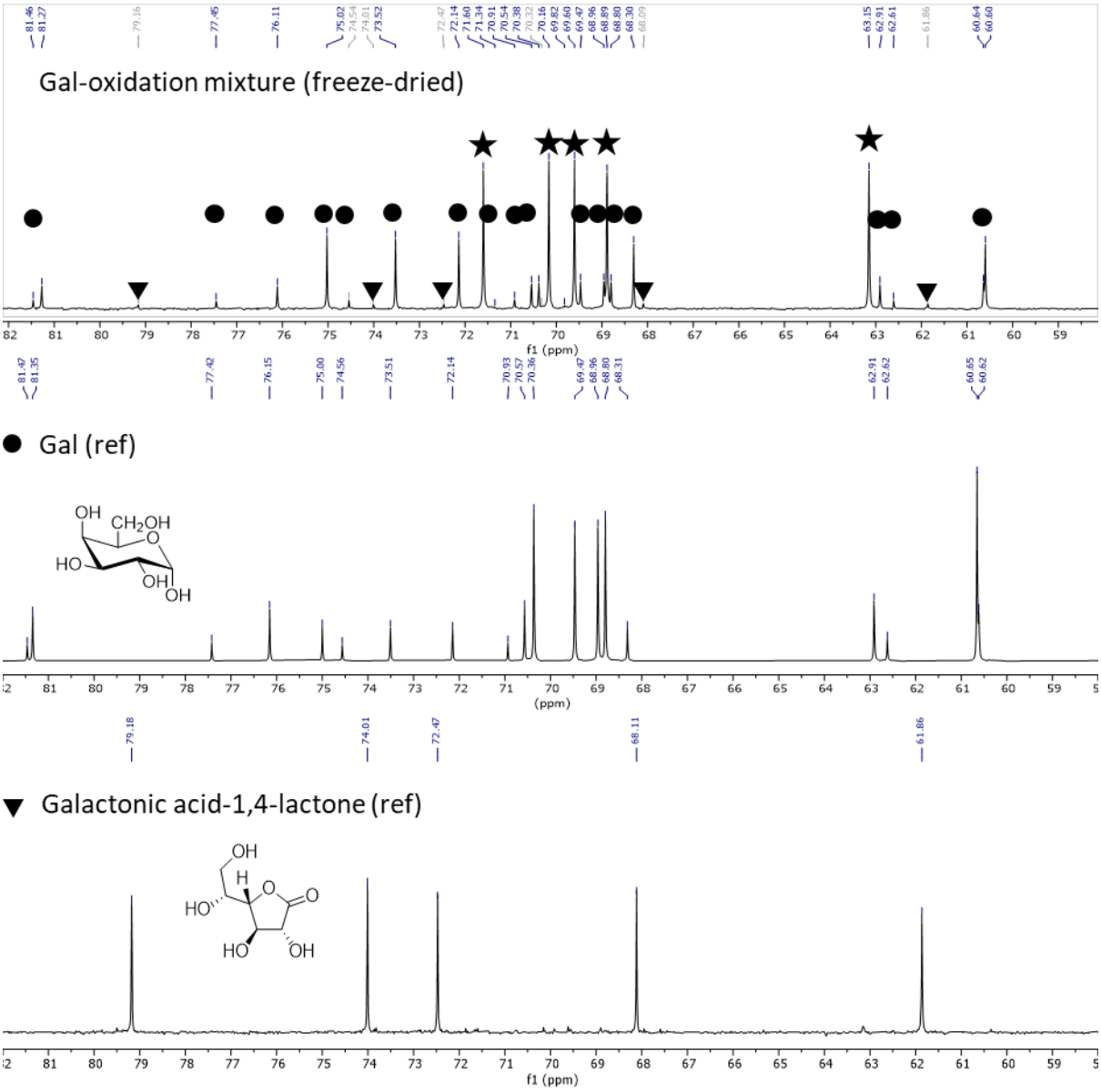

Fig. S5 ^{13}C-NMR's (DMSO-D6) of Gal-reaction mixture, Gal reference (circles), galactonic acid-1,4-lactone reference (triangles), and galactonic acid reference (literature values[11] as stars).

Previous investigations on the thermodynamics of aldonic acids and lactones have already observed differences between the stability of Glc- and Gal-lactones: Felty[17] studied the bromine oxidation of D-glucose and D-galactose. The oxidation of galactose was found to proceed predominantly via the β-D-galactopyranose, since under the applied conditions the mutarotation was slow enough to observe enrichment in α-D-galactopyranose (a schematic overview of the structures is provided in Fig. 6 to guide the eye). The study by Felty also showed that the initial product was the 1,5-lactone. Studying the equilibrium mixture of the open form and the two lactones, the following equilibrium was found: 1,4-lactone > galactonic acid >> 1,5-lactone.

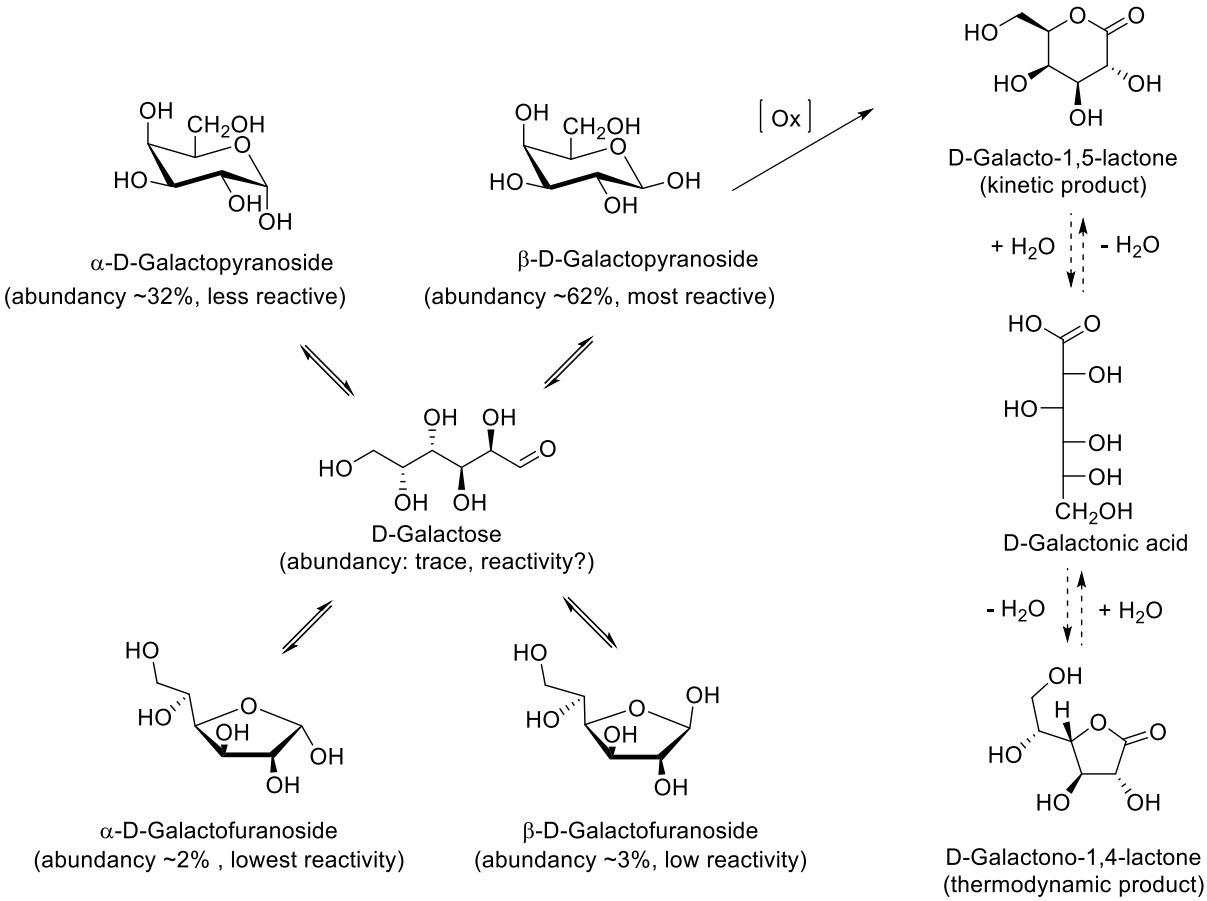

Fig. S6 Galactose reaction network, showing the galactose anomers with their relative abundance and expected reactivity towards oxidation, and the proposed oxidation products in their equilibrium forms.

The observed product mixture in our study showed however predominantly the free galactonic acid, and has therefore not reached equilibrium. This supports the pathway proposed in Fig. S6, since if the 1,4-lactone would have been formed as the initial product, the proportion of this compound in the reaction mixture would have remained high due to the favourable equilibrium. Combined with the previous obtained results for glucose oxidation, it seems likely that the formation of the free galactonic acid (via hydrolysis of the lactone) is occurring in solution rather than on the catalyst surface.

Table S1 Literature values for the equilibrium conformations of carbohydrates in solution

Carbohydrate	***Temp (° C)***	***α-Furanose***	***β-Furanose***	***α-Pyranose***	***β-Pyranose***	***Open***	***Reference***
D-Galactose	15	1.2	2.5	33	64	-	Sinnott[14]
D-Galactose	25	1.8	3.1	32	62	-	Sinnott[14]
D-Galactose	30	2.3	3.7	31.2	62.8	0.006	Sinnott[14]
D-Galactose	31	2.5	3.5	30	64	0.02	Lindhorst,[13] Collins[12]
D-Galactose	35	4	3	29	64	-	Sinnott[14]
D-Glucose	30	0.11	0.28	37.6	62	0.006	Sinnott[14]
D-Glucose	31	-	0.14	38	62	0.02	Collins[12]
D-Glucose	31	-	-	38	62	-	Sinnott[14]
D-Glucose	31	0.5	0.5	38	62	0.002	Lindhorst[13]
D-Glucose	44	0.14	-	37	63	-	Sinnott[14]
D-Glucuronic acid	RT	~7% total furanose		~93%; A:β = 44:56			Kerins[24]
D-Galacturonic acid	25	3.8	5.4	38.5	52.3	-	Stojkovski,[25] Ramos,[26] Jaques[27]
D-Galacturonic acid	40	4.7	6.3	37.5	51.6	-	Stojkovski,[25] Ramos,[26] Jaques[27]
D-Galacturonic acid	60	6.3	9.4	35.4	48.8	-	Stojkovski,[25] Ramos,[26] Jaques[27]
D-Galacturonic acid	80	9.4	14.2	32.3	44.1	-	Stojkovski,[25] Ramos,[26] Jaques[27]

Table S2 (Relative) oxidation rates for various carbohydrates from literature

Carbohydrate	**Catalyst**	**Rate (varying units)**	**Reference**
D-Glucose	0.45% Au/TiO_2	56 mmol min^{-1} g_{Au}^{-1}	Mirescu,[28] Prusse[29]
D-Galactose	0.45% Au/TiO_2	34 mmol min^{-1} g_{Au}^{-1}	Mirescu,[28] Prusse[29]
D-Glucose	4.6% Pd/Al_2O_3	15 mmol min^{-1} g_{Pd}^{-1}	Mirescu[28]
D-Galactose	4.6% Pd/Al_2O_3	18 mmol min^{-1} g_{Pd}^{-1}	Mirescu[28]
D-Glucose	5% Pt/Al_2O_3	5 mmol min^{-1} g_{Pt}^{-1}	Mirescu[28]
D-Galactose	5% Pt/Al_2O_3	7 mmol min^{-1} g_{Pt}^{-1}	Mirescu[28]
D-Glucose	5% Rh/C	1.3 mL H_2 min^{-1}	de Wit[30]
D-Galactose	5% Rh/C	2.4 mL H_2 min^{-1}	de Wit[30]
D-Glucose	5% Pt/C	1 mL H_2 min^{-1}	de Wit[30]
D-Galactose	5% Pt/C	1.7 mL H_2 min^{-1}	de Wit[30]
D-Glucuronic acid	5% Pt/C	0.2 mL H_2 min^{-1}	de Wit[30]
D-Galacturonic acid	5% Pt/C	0.3 mL H_2 min^{-1}	de Wit[30]
D-Glucose	1.8 (±0.15)% Au/Al_2O_3	391 mmol g_{Au}^{-1} min^{-1}	Rautiainen[31]
D-Galactose	1.8 (±0.15)% Au/Al_2O_3	276 mmol g_{Au}^{-1} min^{-1}	Rautiainen[31]
D-Glucuronic acid	1.8 (±0.15)% Au/Al_2O_3	297 mmol g_{Au}^{-1} min^{-1}	Rautiainen[31]
D-Galacturonic acid	1.8 (±0.15)% Au/Al_2O_3	286 mmol g_{Au}^{-1} min^{-1}	Rautiainen[31]

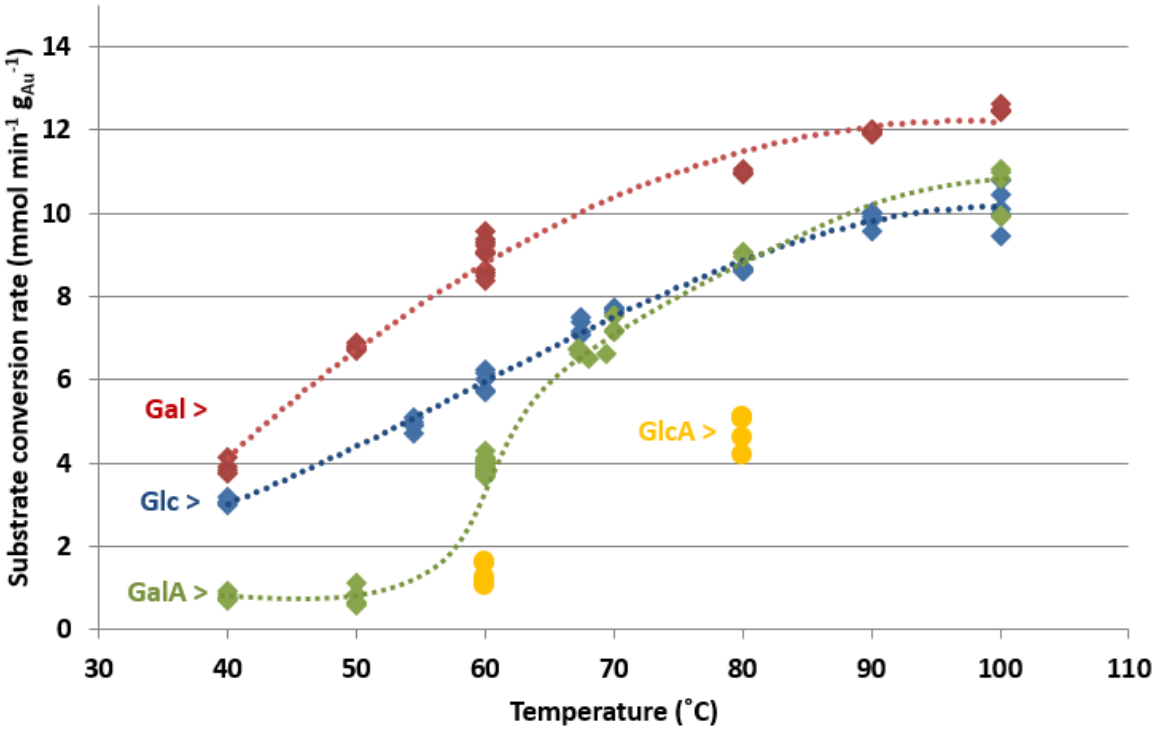

Fig. S7 Substrate conversion rate as a function of reaction temperature; Gal (red), Glc (blue), GalA (green) and GlcA (yellow). Dots represent experimental data points, the dotted lines are added as a visual reference to guide the eye over the general conversion trends. Reaction conditions: Au/TiO_2 catalyst, substrate concentration = 0.1M (10 mL min^{-1}), oxygen (10 bar pressure, 50 mL min^{-1}).

Section 2. Synthesis and characterisation of reference compounds

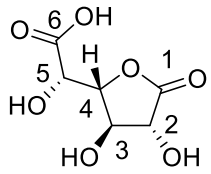

Galactaric acid-1,4-lactone (1) The procedure is adapted from a previously reported literature method.[32] A 400 mL beaker was filled with 150 mL demineralized water, a magnetic stirring bar, and was placed on a magnetic stirring plate. Under stirring at 300 rpm, the water was boiled, and mucic acid (3.164 g, 15.1 mmol) was added resulting in a white suspension. After ca. 30 minutes the suspension turned into a clear solution. Again fresh mucic acid (3.268, 15.6 mmol) was added, resulting in a white suspension. After 2 hours the additional mucic acid was still not completely dissolved. The suspension was transferred to a round bottom flask and concentrated using a rotary evaporator at 50 °C, leaving a white solid. The solid was extracted with acetone, and filtrated over filtration paper to remove residual solids (unreacted mucic acid). The acetone-phase containing the desired lactone was dried over magnesium sulphate for 20 min. The mixture was then filtered over Celite and the acetone solvent was removed by a rotary evaporator. The resulting sticky beige solid was further dried to constant weight in an vacuum oven at 40 °C, resulting in a beige solid (yield: 2.59 g, 43.6 % of theory).

HPLC (UV and RI) of this product is provided in the HPLC overview at the end of this document (Fig. S50).

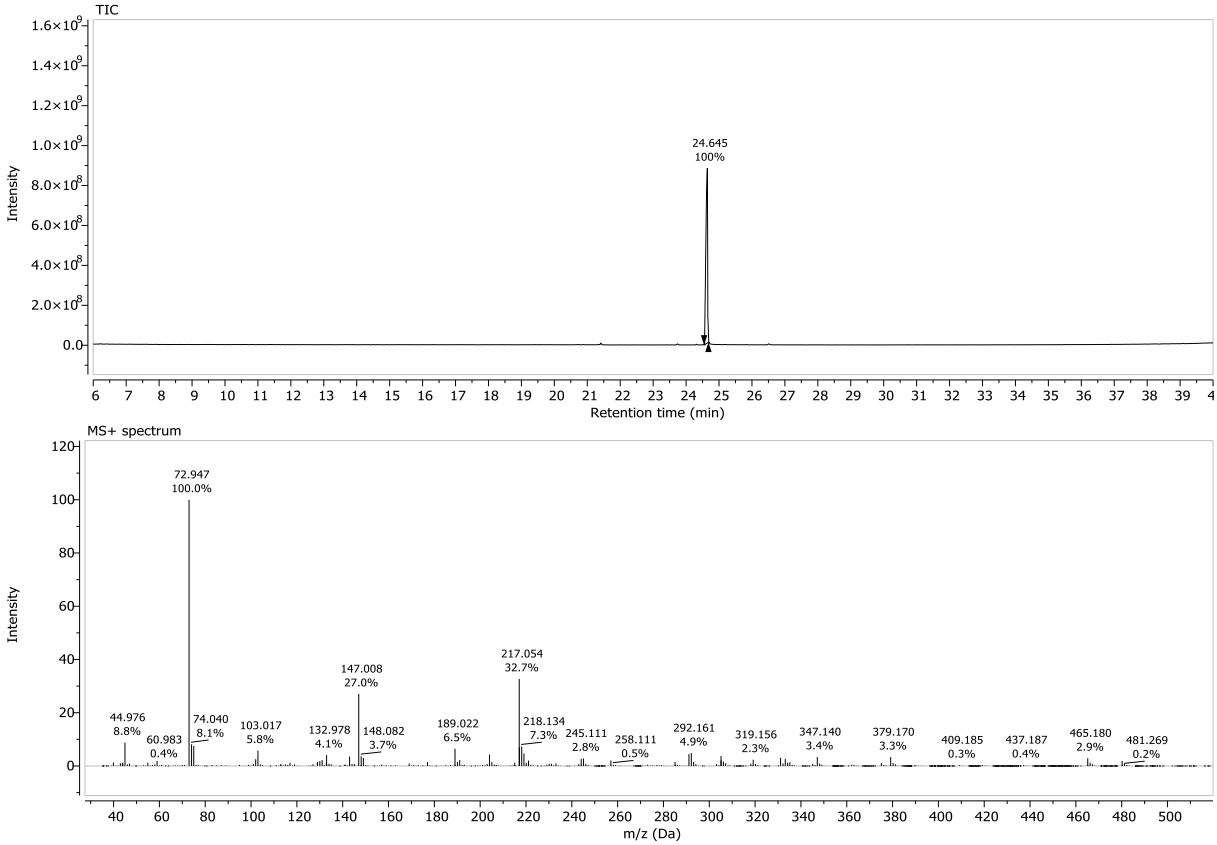

Fig. S8 GC-MS (silylated sample in pyridine) of **1** : RT = 24.65 min. MS (GC-MS, 70 eV): *m/z* (%) = 480 (1.9) [M^+], 465 (2.9), 379 (3.3), 347 (3.4), 292 (4.9), 217 (32.7), 147 (27), 73 (100).

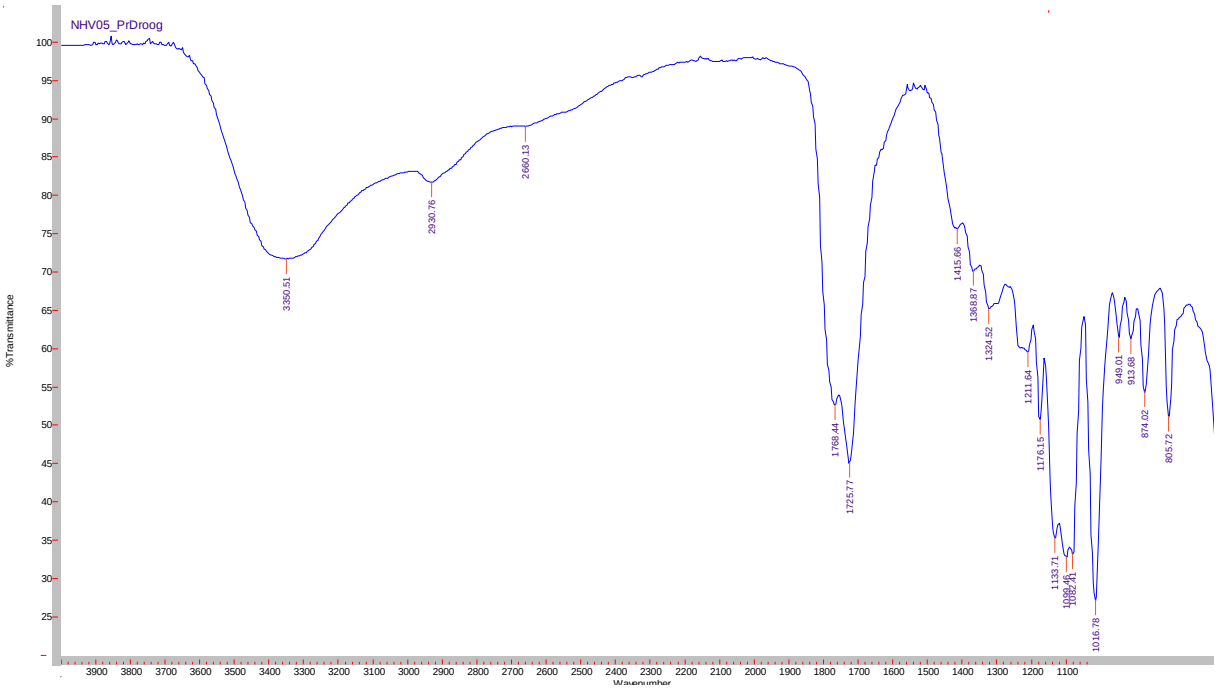

Fig. S9 FT-IR of **1**: Carbonyl signals correspond to a combination of a γ-lactone (1768 cm^{-1}) and a carboxylic acid (1726 cm^{-1}).

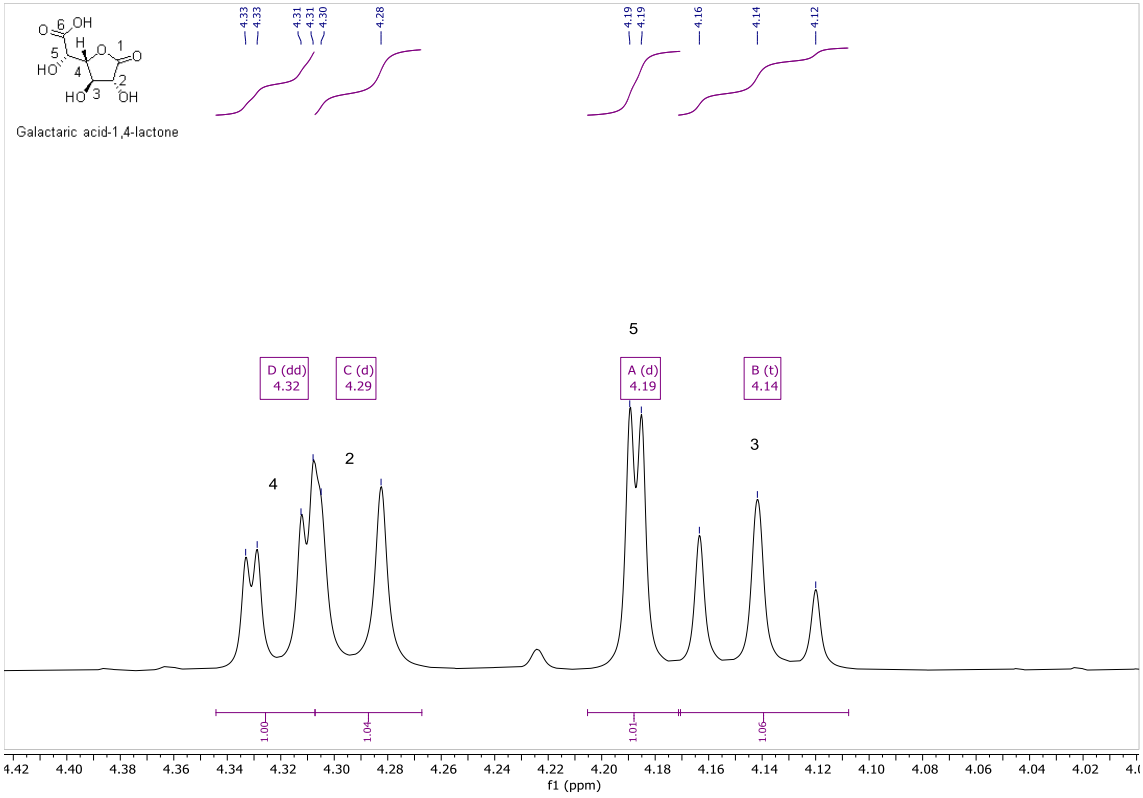

Fig. S10 ^{1}H NMR of **1** (400 MHz, DMSO) δ ppm: 4.32 (dd, *J* = 59.2, 1.8 Hz, 1H), 4.31 – 4.26 (m, 1H), 4.19 (d, *J* = 1.7 Hz, 1H), 4.14 (t, *J* = 8.7 Hz, 1H).

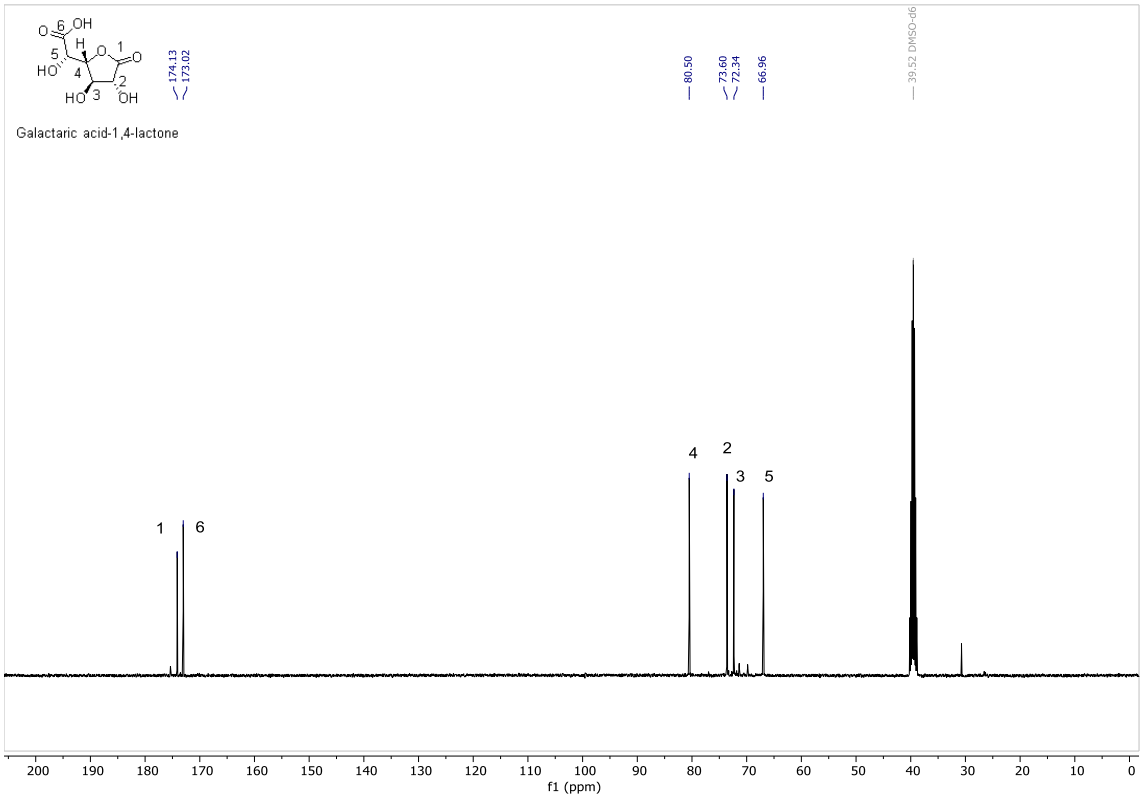

Fig. S11 ^{13}C-NMR of **1** (100.62 MHz, DMSO-D6) δ(ppm): 66.96, 72.33, 73.60, 80.50, 173.02, 174.13.

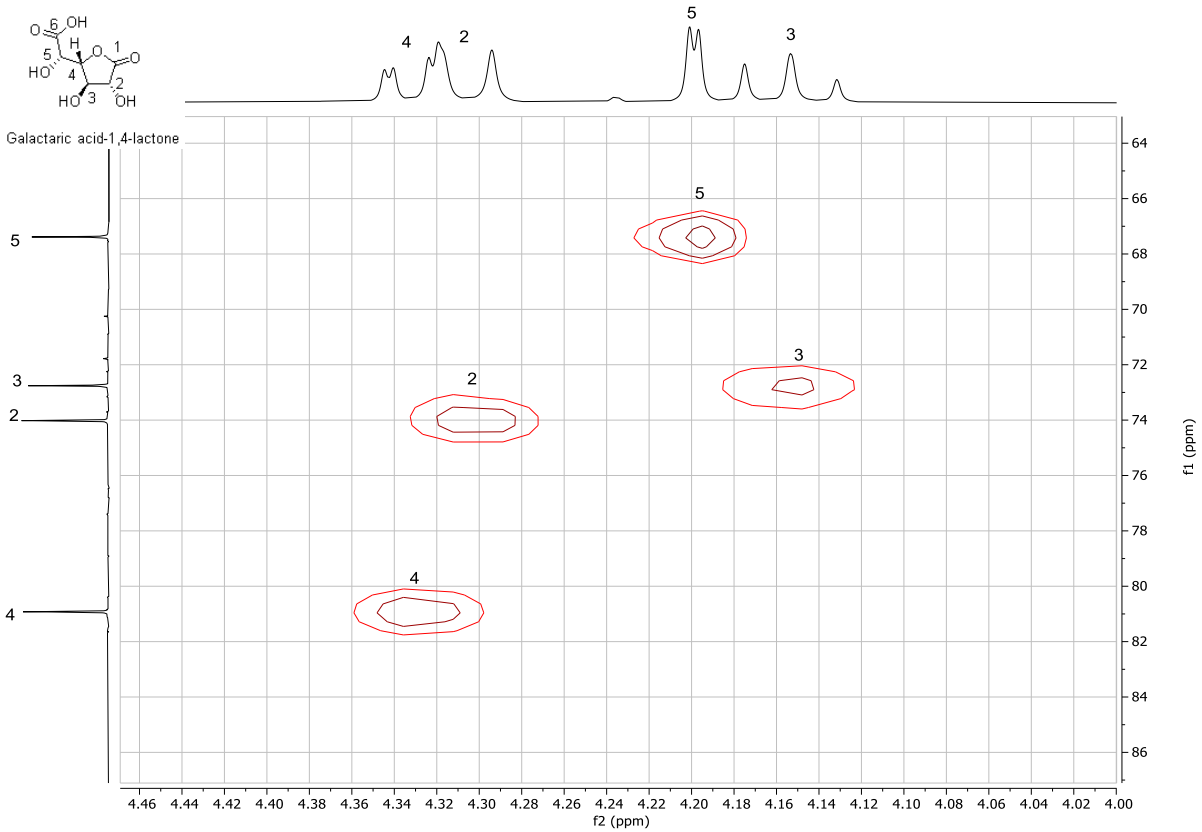

Fig. S12 HSQC-NMR of **1** (DMSO-D6)

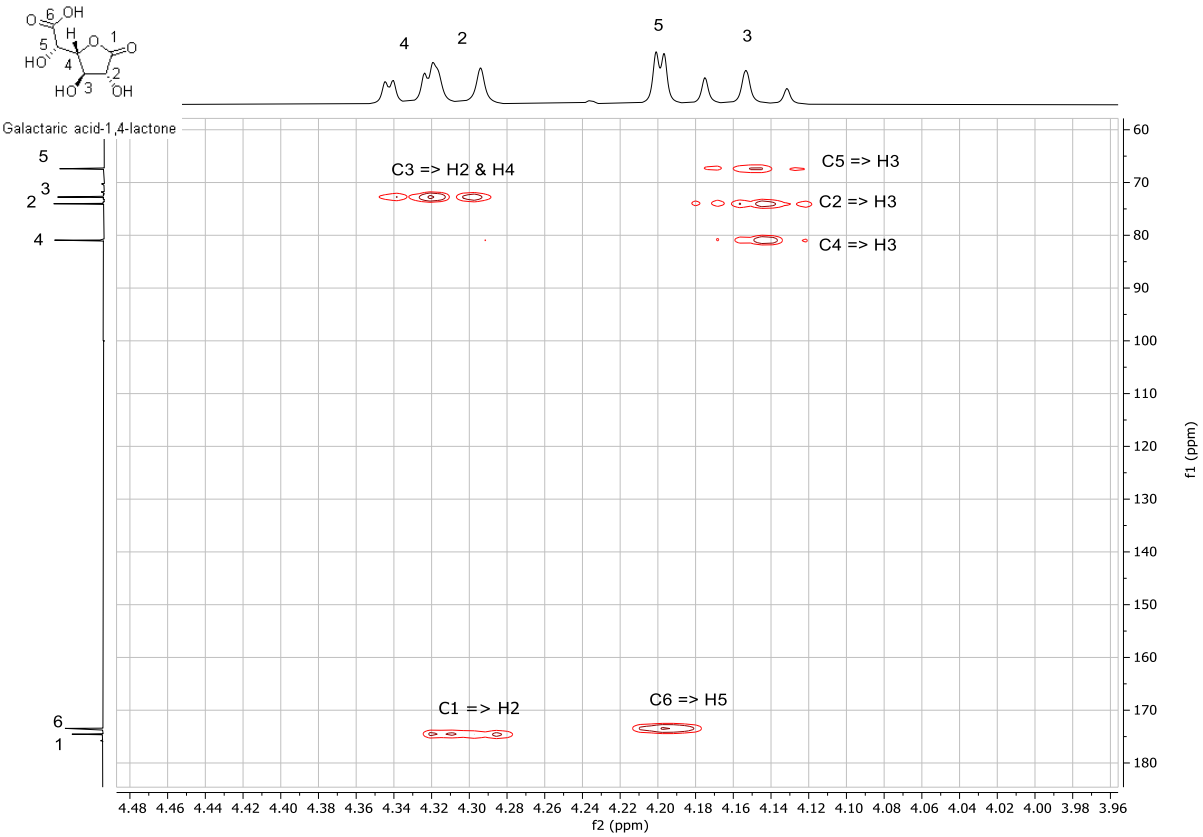

Fig. S13 HMBC-NMR of **1** (DMSO-D6)

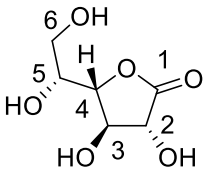

Galactonic acid-1,4-lactone (2) The procedure is adapted from a previously described method.[33] A 250 mL 3-neck flask was equipped with a magnetic stirrer, a reflux condenser, and a pressure equalizing dropping funnel. D-Galactose (10.092 g, 56.0 mmol, 1.0 eq.) and sodium bicarbonate (9.289 g, 110.6 mmol) were dissolved in 100 mL water. Bromine (9.7 g, 60.7 mmol, 1.08 eq.) was added dropwise to the solution at room temperature under firm stirring. The clear light yellowish solution turned into a clear orange mixture. After 48 hours, sodium bisulphite (591 mg, 5.7 mmol) was added to quench the excess of bromine. Immediately the solution turned colourless. After 10 minutes, the mixture was transferred to a 250 mL round bottom flask and the solvent was evaporated using the rotary evaporator. The white solid was dried in a vacuum oven in the presence of Sicapent.

The crude product (23.012 g) was sticky and had become dark brown during drying. The solid was extracted with 4 x 75 mL absolute EtOH and the remaining brown suspension was filtrated over Celite. The ethanolic phase was evaporated using the rotary evaporator. The remaining solid was treated with 150 mL acidic water (4 mL concentrated HCl to 1 L water). The beige mixture was concentrated with the rotary evaporator and dried overnight in the vacuum oven in the presence of Sicapent. Again the product turned dark brown to black (10.224 g).

For purification, 8.4 g of the solid was dissolved in a minimal amount of pyridine, and coated on silica. The silica-coated product was transferred to a 50 g silica column, and eluted with EtOAc/EtOH (9/1, v/v) was used as eluent. The desired fractions were combined and concentrated on a rotary evaporator, followed by drying in a vacuum oven, resulting in a yellowish/ brown syrup (3.007 g).

Amberlite IR-120 (11.4 g) was washed with water using sonication, to remove pollutions. The product (3.007 g) was dissolved in water (50 mL), and the solution was added to the IE-resin. The mixture was filtrated over filter paper, and transferred to a 100 mL round bottom flask. The solution was concentrated using a rotary evaporator (40 °C), and dried in the vacuum oven (40 °C) in the presence of Sicapent. The final product was obtained as a beige sticky solid (yield: 1.427 g, 14,3 % of theory). HPLC (UV and RI) of this product is provided in the HPLC overview at the end of this document (Fig. S53).

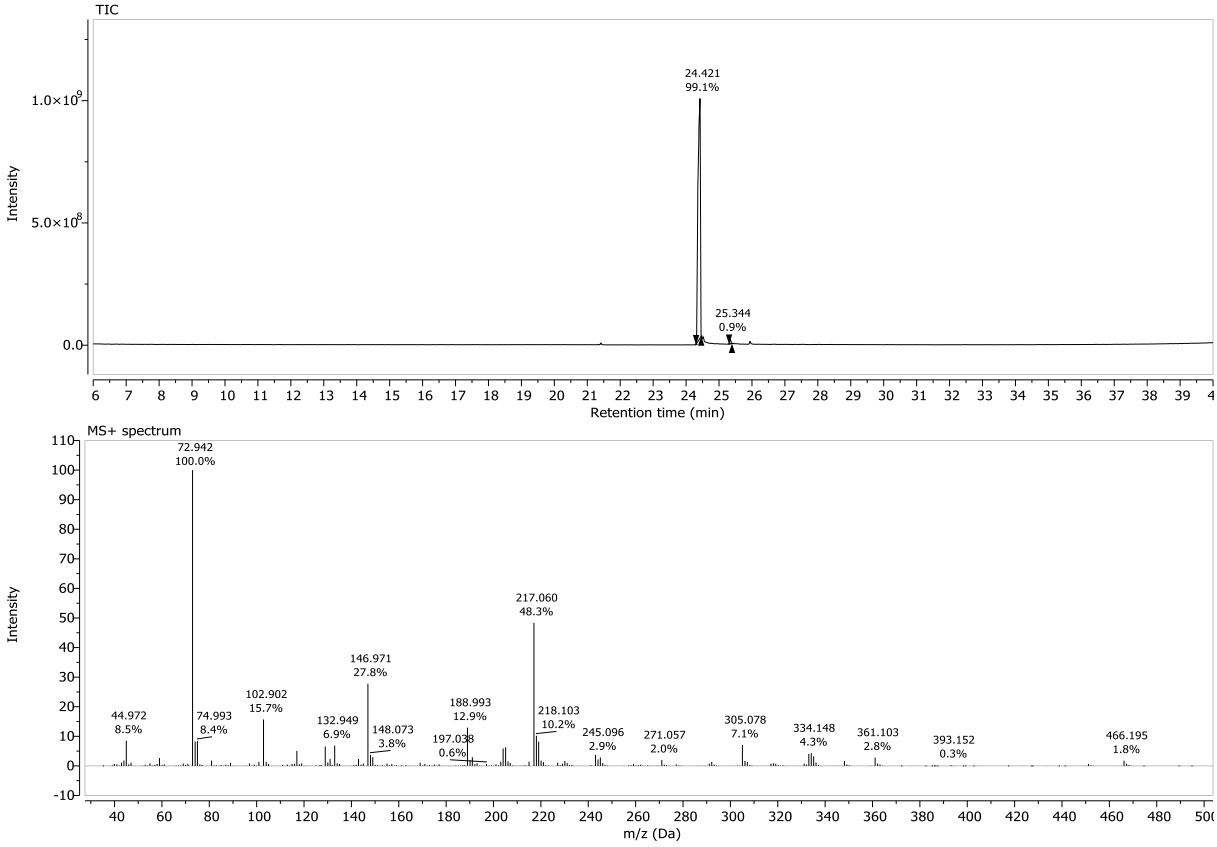

Fig. S14 GC-MS of **2** (silylated sample in pyridine): RT = 24.42 min. MS (GC-MS, 70 eV): *m/z* (%) = 466 (1.8) [M^+], 361 (2.8), 305 (7.1), 245 (2.9), 217 (48.3), 147 (27.8), 73 (100).

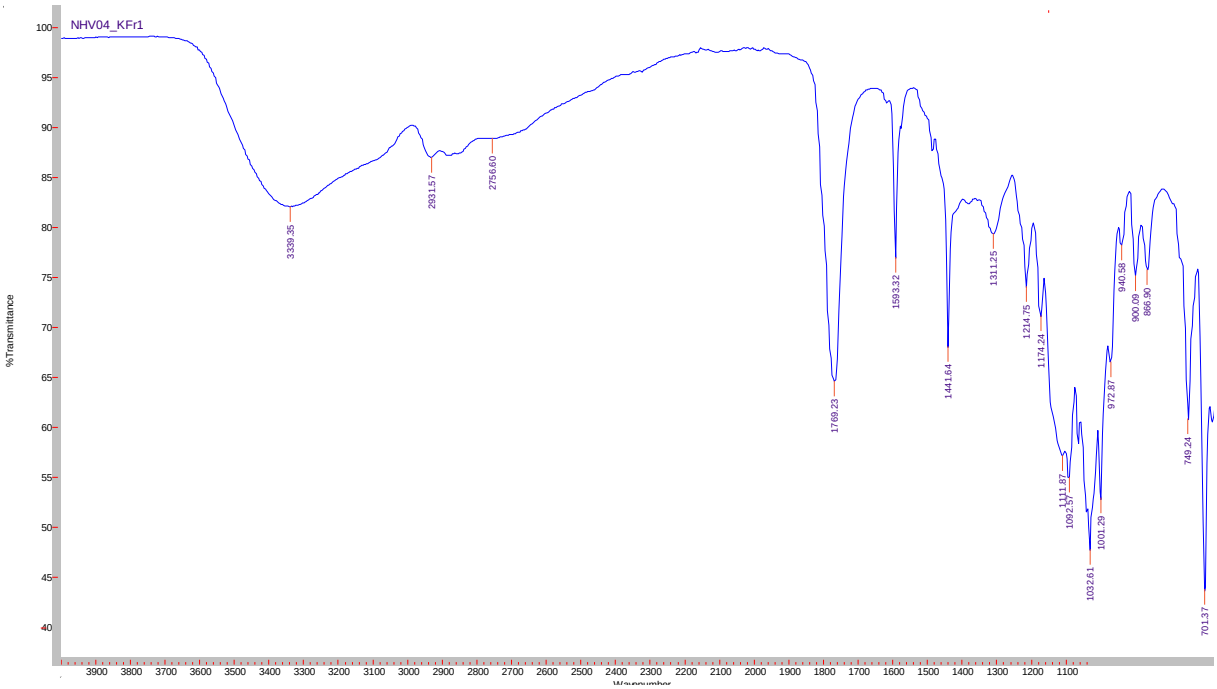

Fig. S15 FT-IR of **2**: Carbonyl signals correspond to a γ-lactone (1769 cm^{-1}).

The NMR values for this product in D_2O have been previously published by El Khadem[34] and Lemau de Talancé.[33] Based on our own measurements in DMSO-D6, we confirm the previously reported assignments for the ^{13}C-NMR, but came to the conclusion that the original assignment for the ^{1}H-spectrum was incorrect in the oldest literature. Based on our HSQC and HMBC spectra, we agree with Lemau de Talancé *et al.* that the original assignment of H3 and H4 have to be switched.

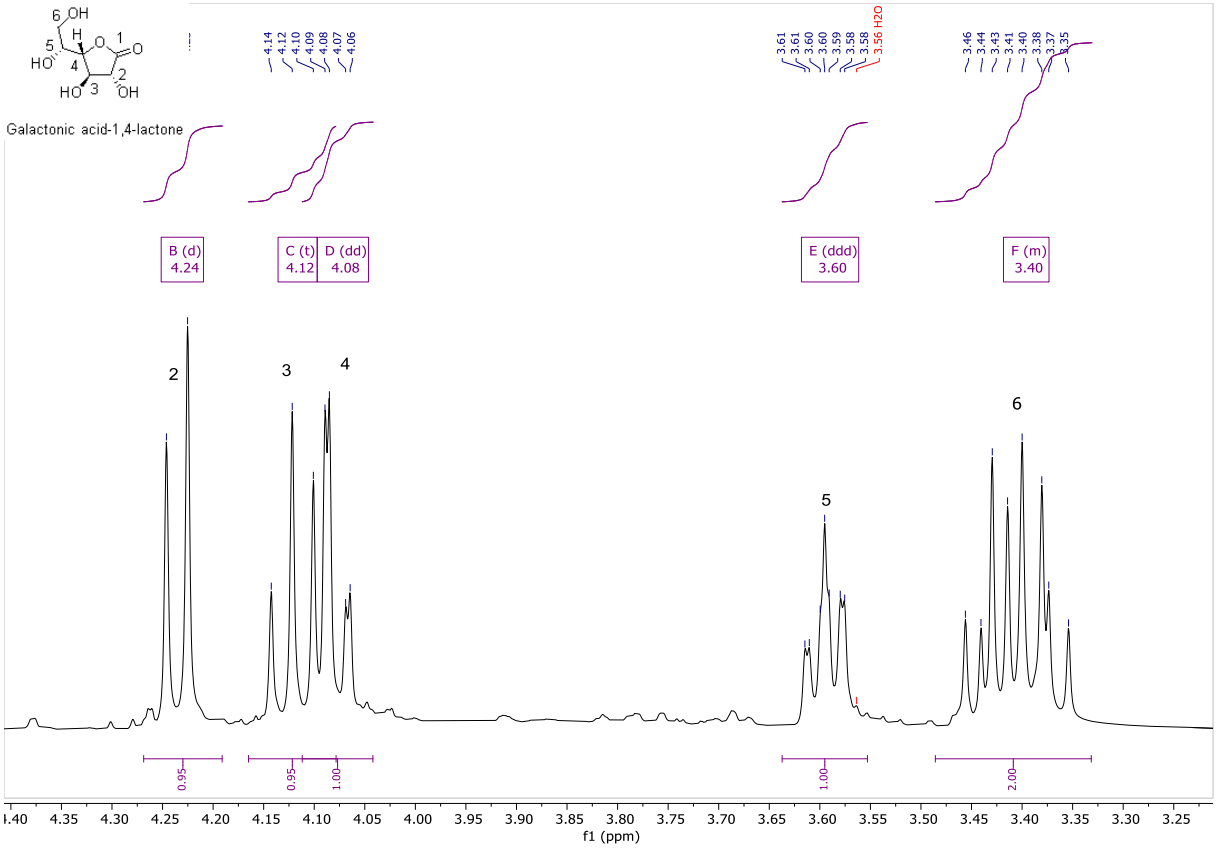

Fig. S16 ^{1}H NMR of **2** (400 MHz, DMSO) δ ppm: 4.24 (d, J = 8.4 Hz, 1H), 4.12 (t, J = 8.3 Hz, 1H), 4.08 (dd, J = 8.2, 1.8 Hz, 1H), 3.60 (ddd, J = 7.9, 6.1, 1.8 Hz, 1H), 3.49 – 3.33 (m, 2H).

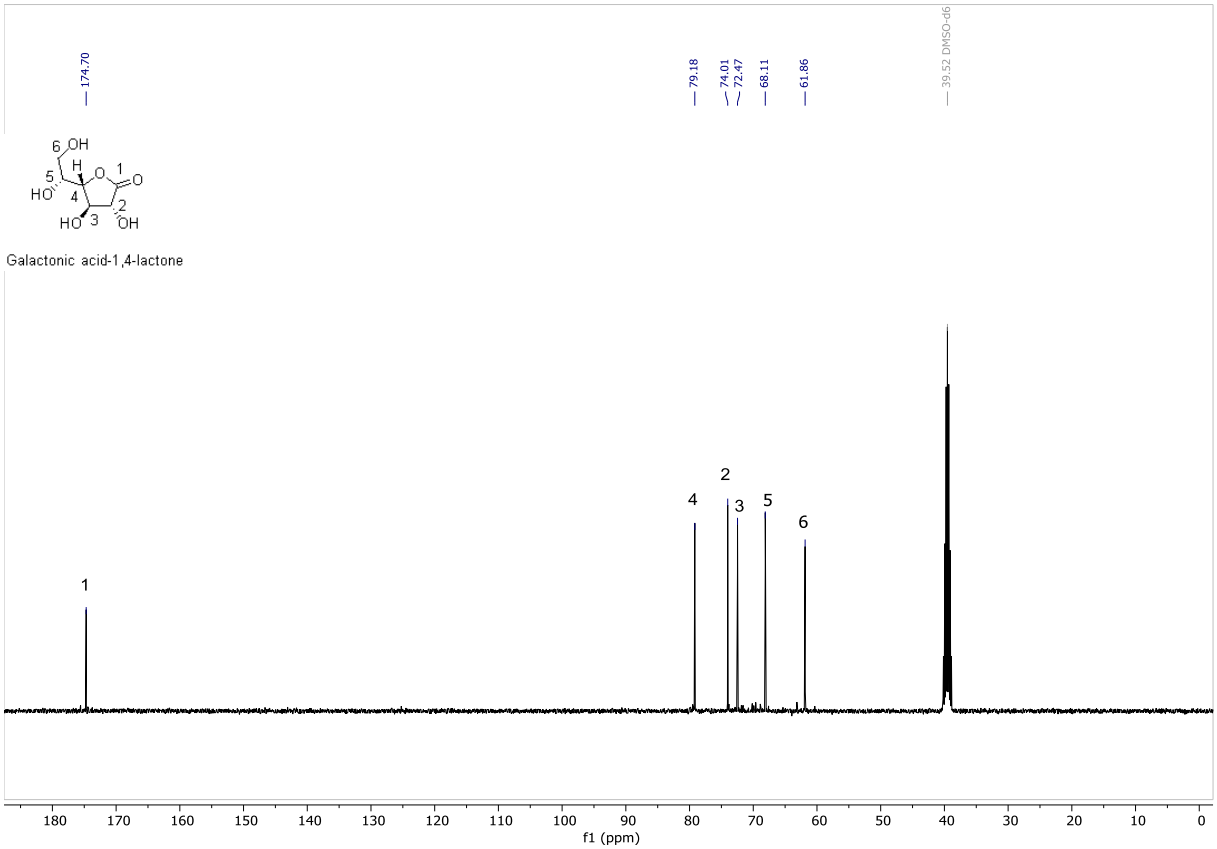

Fig. S17 ^{13}C-NMR of **2** (100.62 MHz, DMSO-D6) δ(ppm): 61.86, 68.11, 72.47, 74.01, 79.18, 174.70.

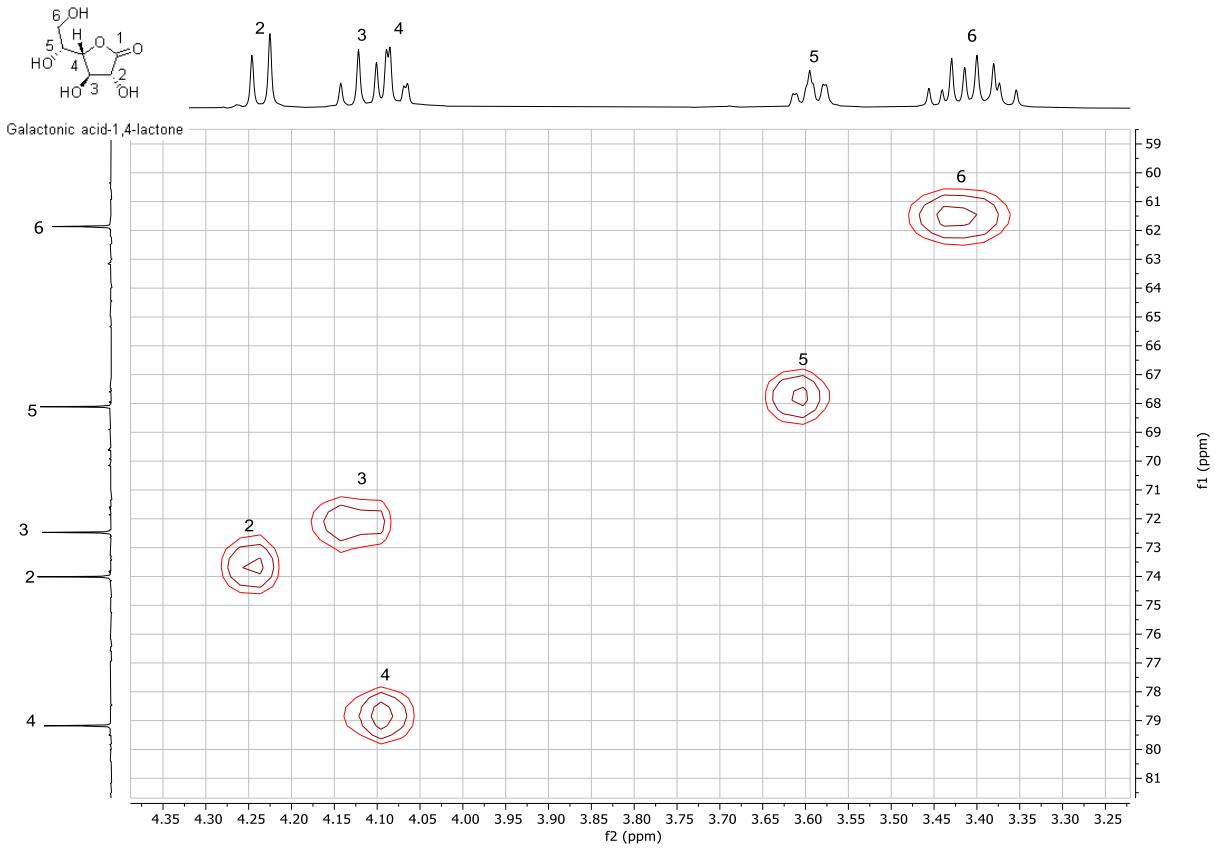

Fig. S18 HSQC-NMR of **2** (DMSO-D6)

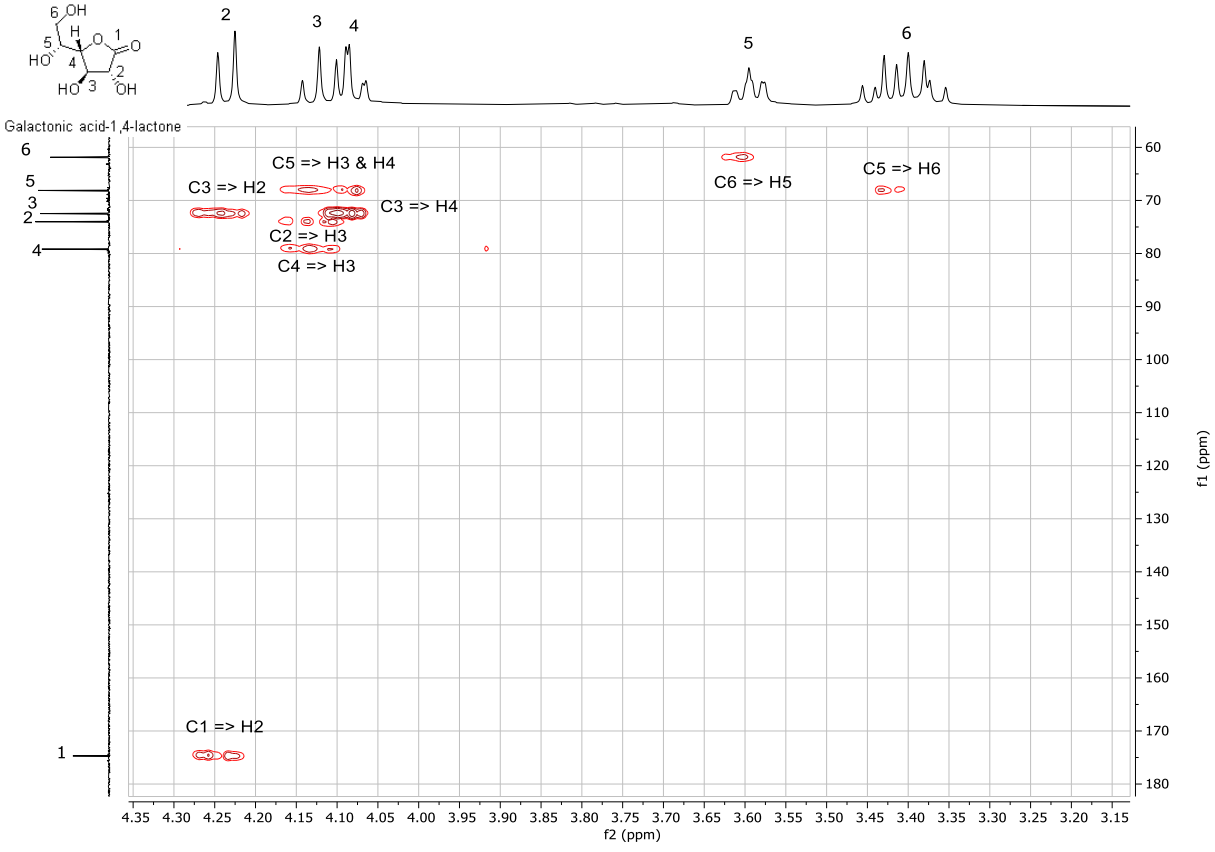

Fig. S19 HMBC-NMR of **2** (DMSO-D6)

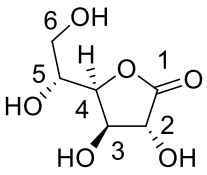

Gluconic acid-1,4-lactone (3) The procedure is adapted from a previously described method.[35] A 50 mL round bottom flask was equipped with a condenser and a magnetic stirrer. D-gluconic acid-1,5-lactone (4.967 g, 27.9 mmol) was suspended in glacial acetic acid (10 mL). The mixture was refluxed for 75 min., resulting in a clear solution. The solution was cooled in the refrigerator for 3 days to allow crystallization. The resulting white crystals were filtered over a type-3 glass filter. The crystals were washed with glacial acetic acid, followed by EtOH and Et_2O. Most of the crystals dissolved in EtOH and Et_2O, and to recover the product the solvents were evaporated with the rotary evaporator. The remaining thick colourless syrup was allowed to crystalize at RT for a week. The crystals were suspended in glacial acetic acid using sonication, and the suspension was filtered over a type-3 glass filter. After the residue was washed with glacial acetic acid, the residue was carefully washed with a small amount of cold EtOH and Et_2O. The product was dried in a vacuum oven overnight at 40 °C. The product was obtained as a white solid (yield: 207 mg; 4.2 % of theory); mp. 127.8 – 130.1 °C; lit.[35] mp. 133 – 135 °C.

HPLC (UV and RI) of this product is provided in the HPLC overview at the end of this document (Fig. S56).

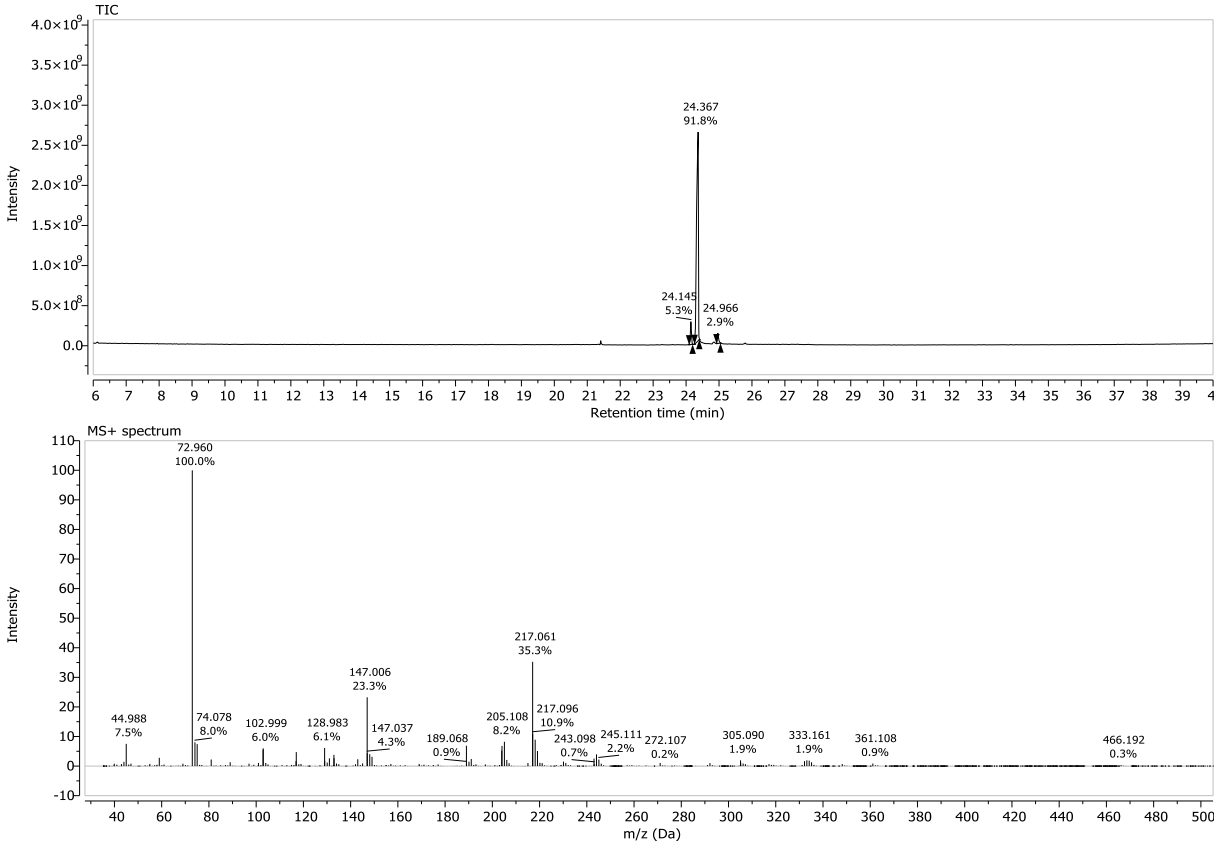

Fig. S20 GC-MS of **3** (silylated sample in pyridine): RT = 24.37 min. MS (GC-MS, 70 eV): *m/z* (%) = 466 (0.3) [M^+], 333 (1.9), 305 (1.9), 245 (2.2), 217 (35.3), 205 (8.2), 147 (23.3), 129 (6.1), 103 (6.0), 73 (100).

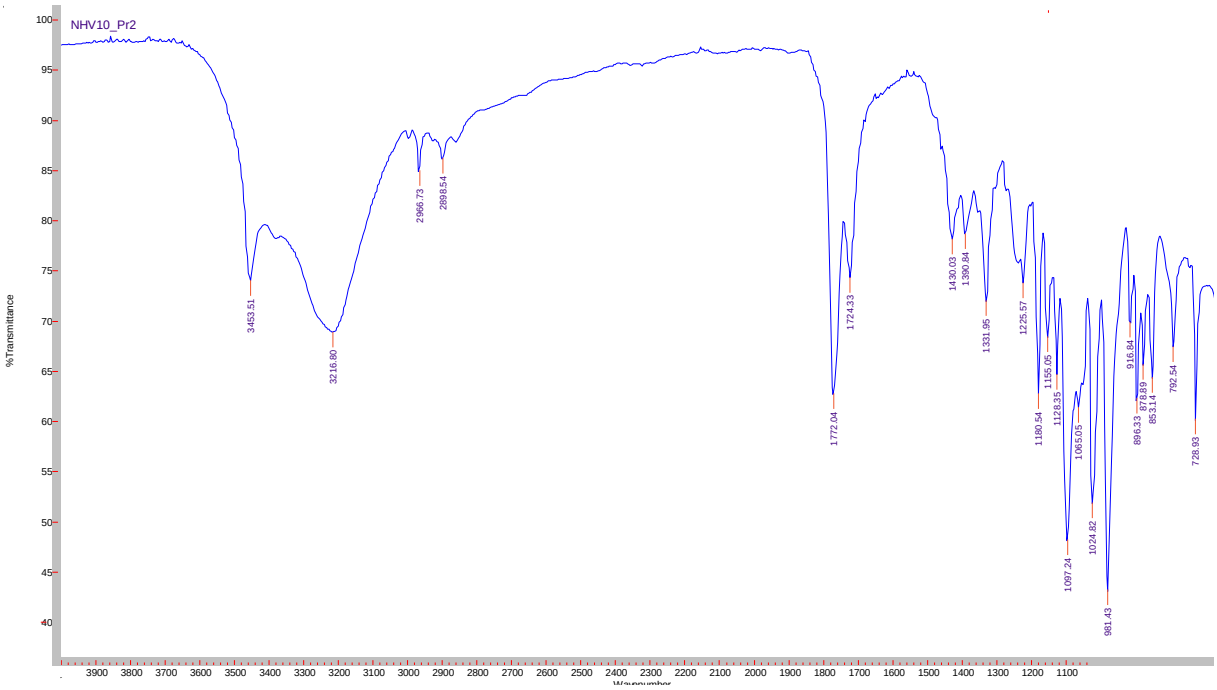

Fig. S21 FT-IR of **3**: Carbonyl signal correspond to a γ-lactone (1772 cm^{-1}), the signal at 1724 corresponds to the presence of residual acetic acid in the product.

$^{1}H/^{13}C$-NMR spectra confirmed the product still contained a small amount of acetic acid. The ^{1}H-NMR assignments matched those reported in literature.[36] Unfortunately, no ^{13}C assignments in DMSO-D6 were found in literature for comparison, but assignments could made based upon COSY, HSQC and DEPT.

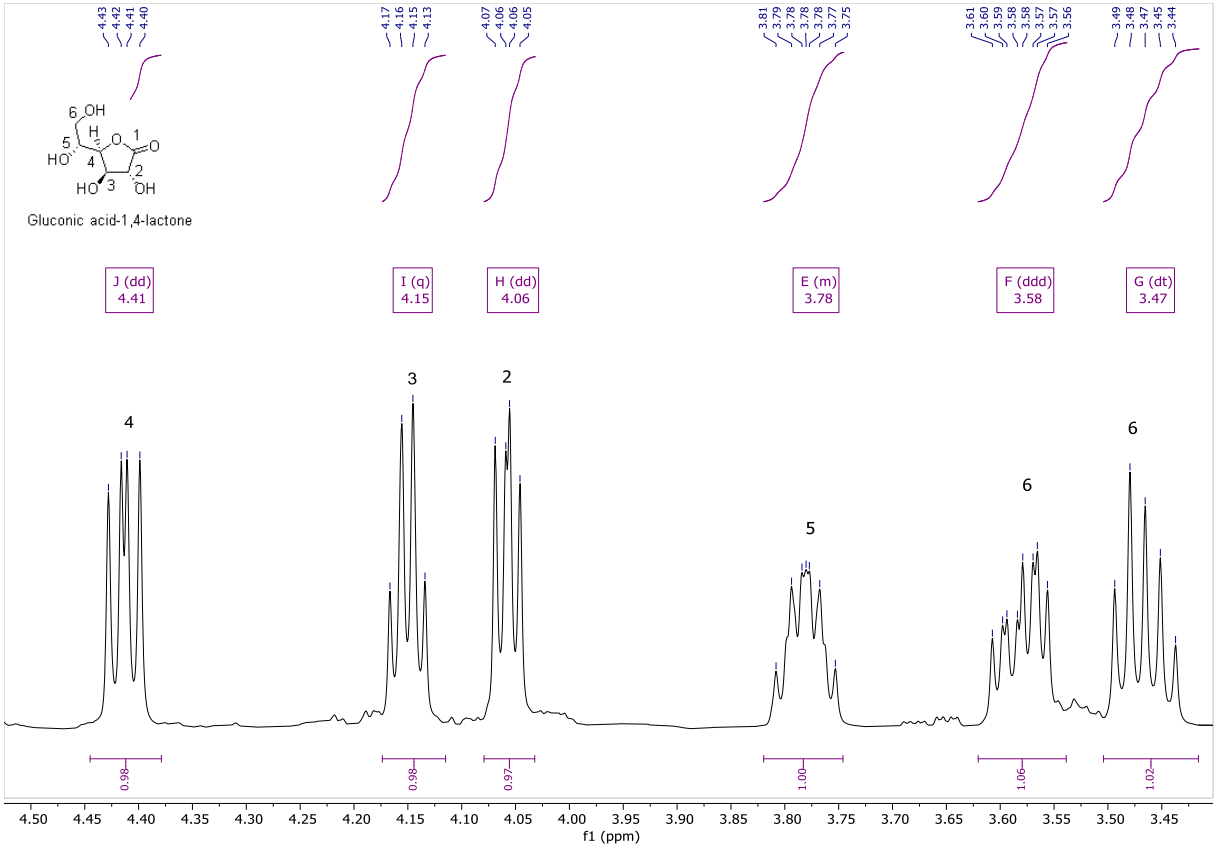

Fig. S22 ^{1}H NMR of **3** (400 MHz, DMSO) δ ppm: 4.41 (dd, *J* = 6.9, 4.8 Hz, 1H), 4.15 (q, *J* = 4.4 Hz, 1H), 4.06 (dd, *J* = 5.3, 3.9 Hz, 1H), 3.82 – 3.75 (m, 1H), 3.58 (ddd, *J* = 11.1, 5.4, 3.8 Hz, 1H), 3.47 (dt, *J* = 11.3, 5.7 Hz, 1H).

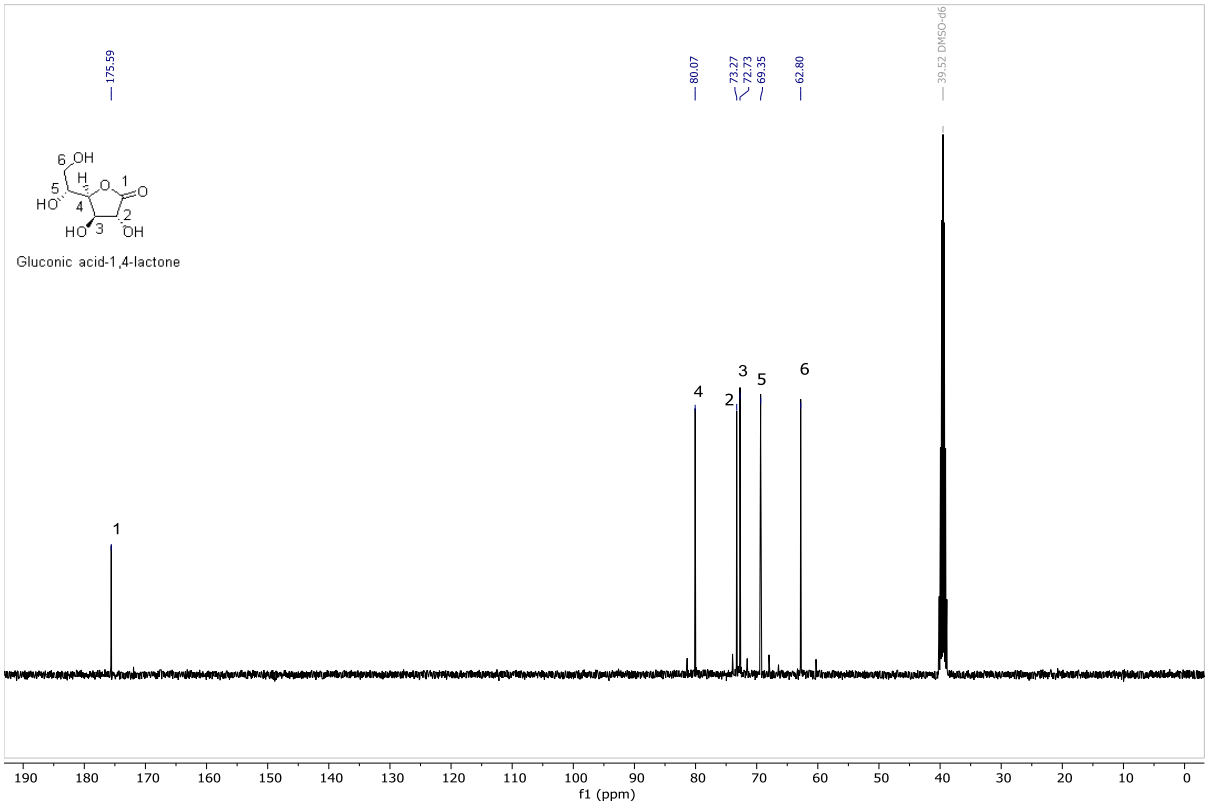

Fig. S23 ^{13}C-NMR of **3** (100.62 MHz, DMSO-D6) δ(ppm): 62.80, 69.35, 72.73, 73.27, 80.07, 175.59.

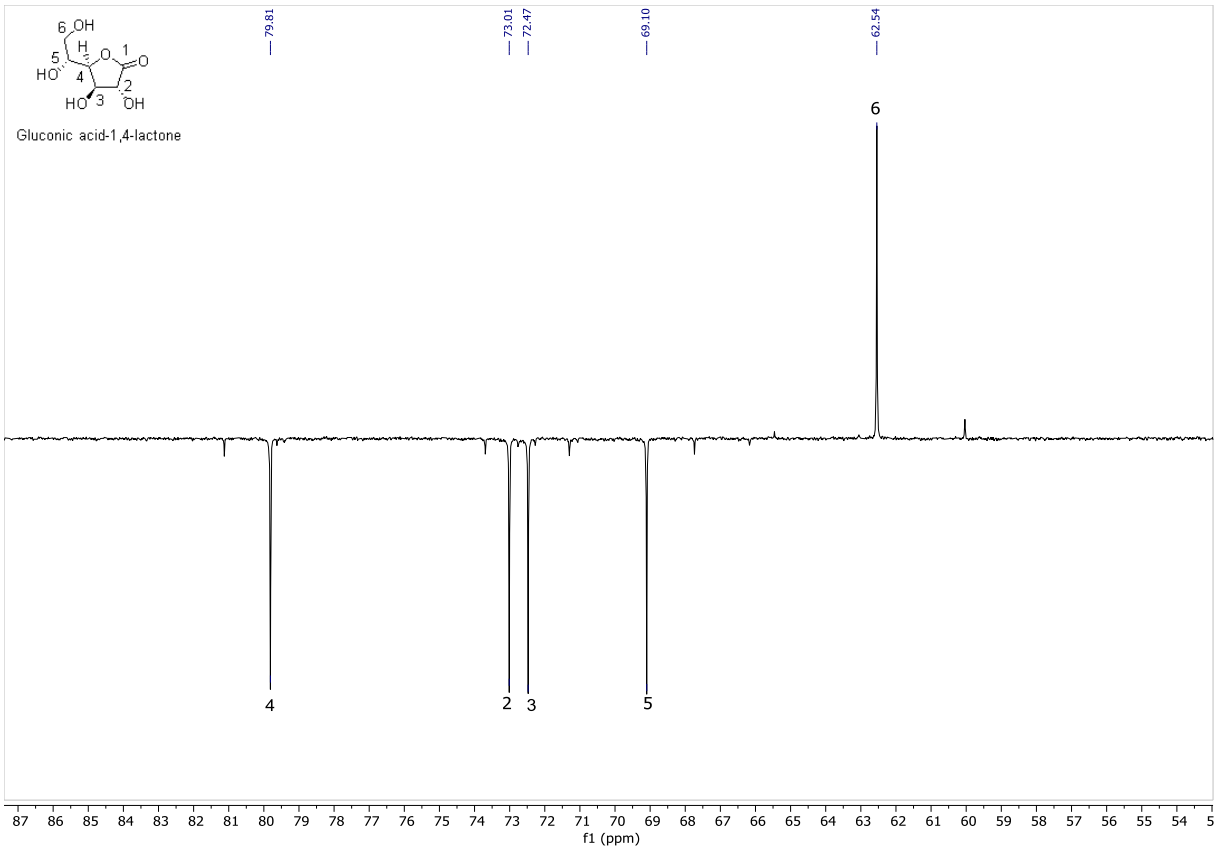

Fig. S24 DEPT-NMR of **3** (DMSO-D6)

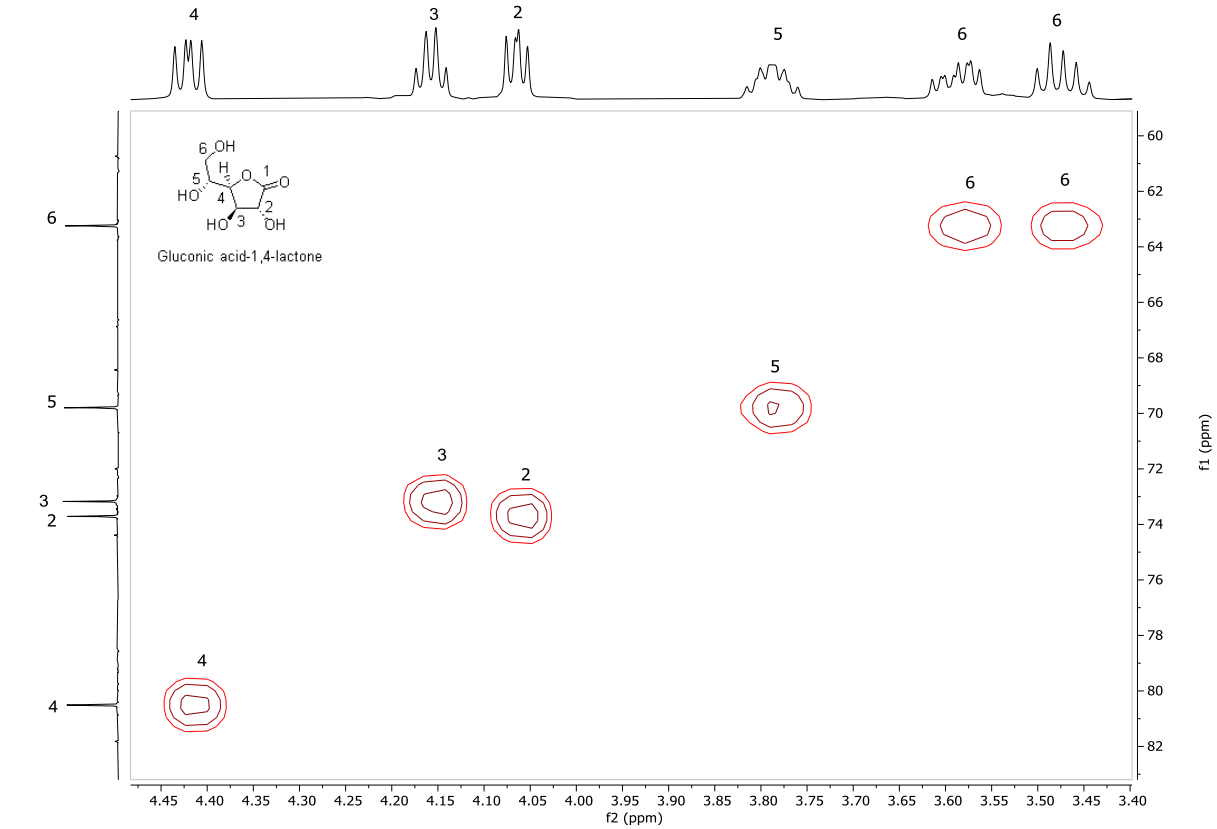

Fig. S25 HSQC-NMR of **3** (DMSO-D6)

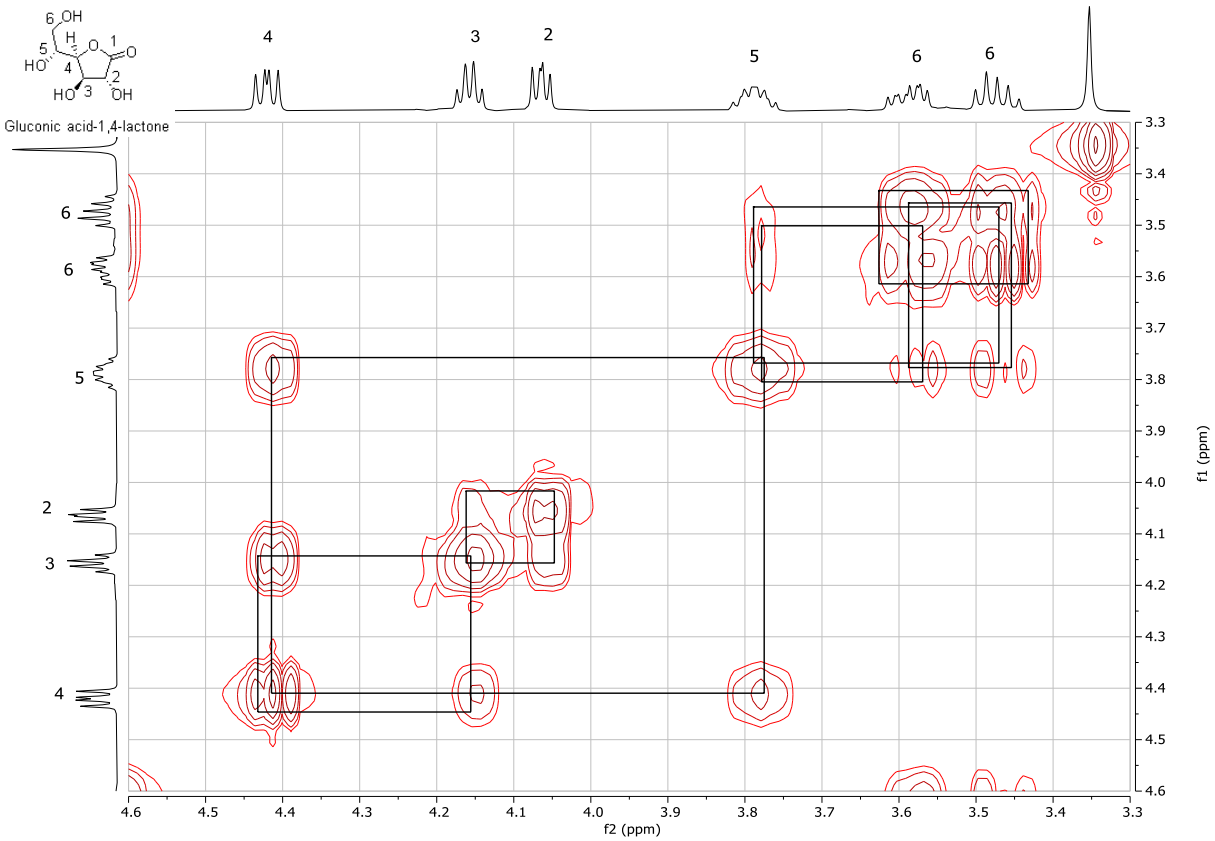

Fig. S26 COSY-NMR of **3** (DMSO-D6)

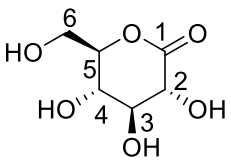

Gluconic acid-1,5-lactone (4) The following spectra were recorded from commercially sourced delta-gluconolactone. HPLC (UV and RI) of this product is provided in the HPLC overview at the end of this document (Fig. S57).

NMR spectra were recorded, and the signals were assigned. The ^{1}H-NMR assignments differ from those earlier reported by Bierenstiel.[37] The ^{1}H signals of H-3 and H-4 closely overlap, resulting in a difficult assignment for C-3 and C-4. However, on basis of the HSQC and HMBC spectra, we propose a different assignment.

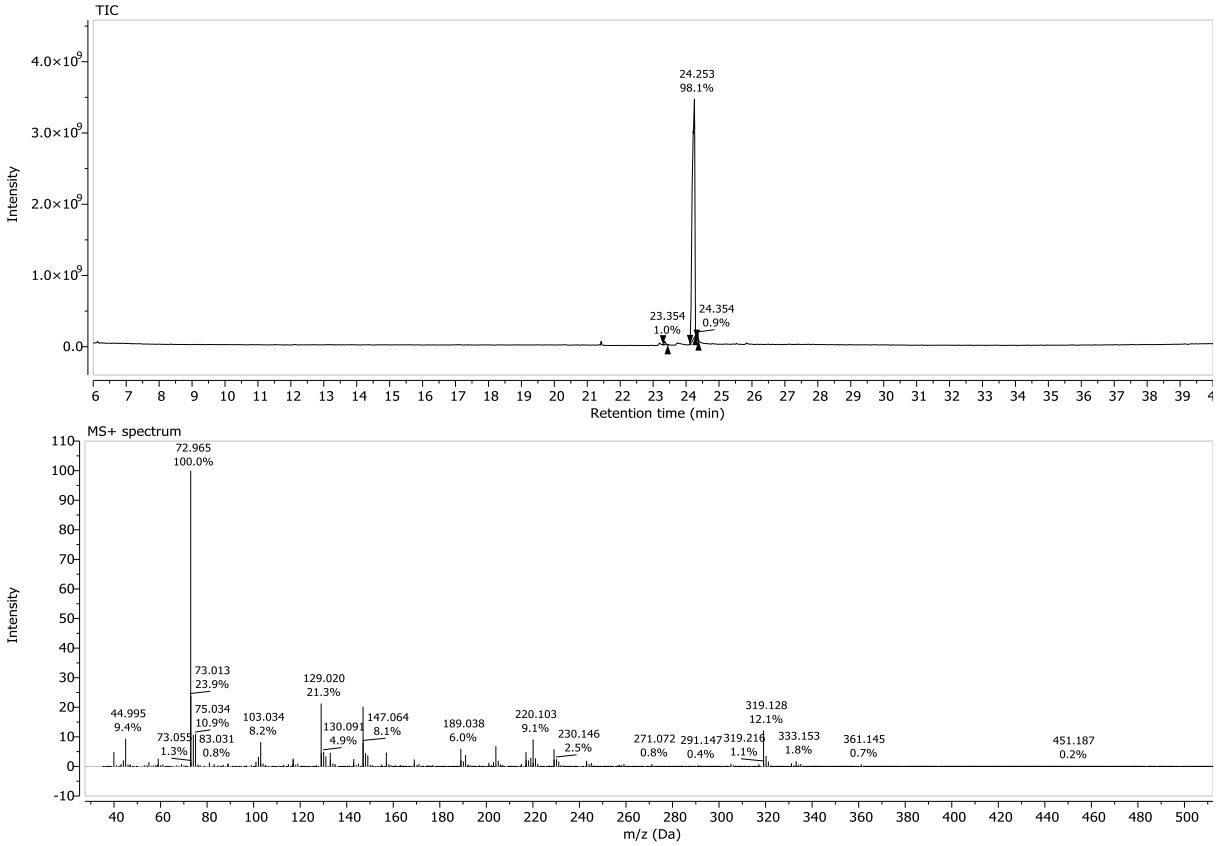

Fig. S27 GC-MS of **4** (silylated sample in pyridine): RT = 24.25 min. MS (GC-MS, 70 eV): *m/z* (%) = 466 (0.1) [M^{+}], 451 (0.2), 333 (1.8), 319 (12.1), 271 (0.8), 220 (9.1), 189 (6.0), 147 (8.1), 129 (21.3), 73 (100).

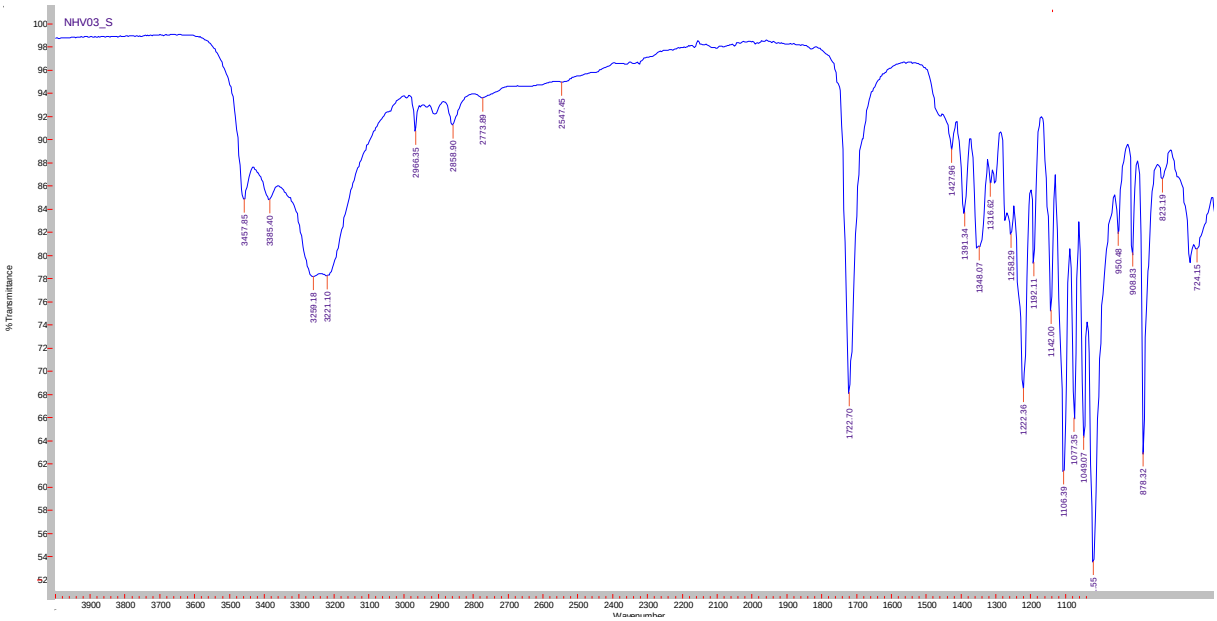

Fig. S28 FT-IR of **4**. Carbonyl signal correspond to a δ-lactone (1722 cm^{-1}).

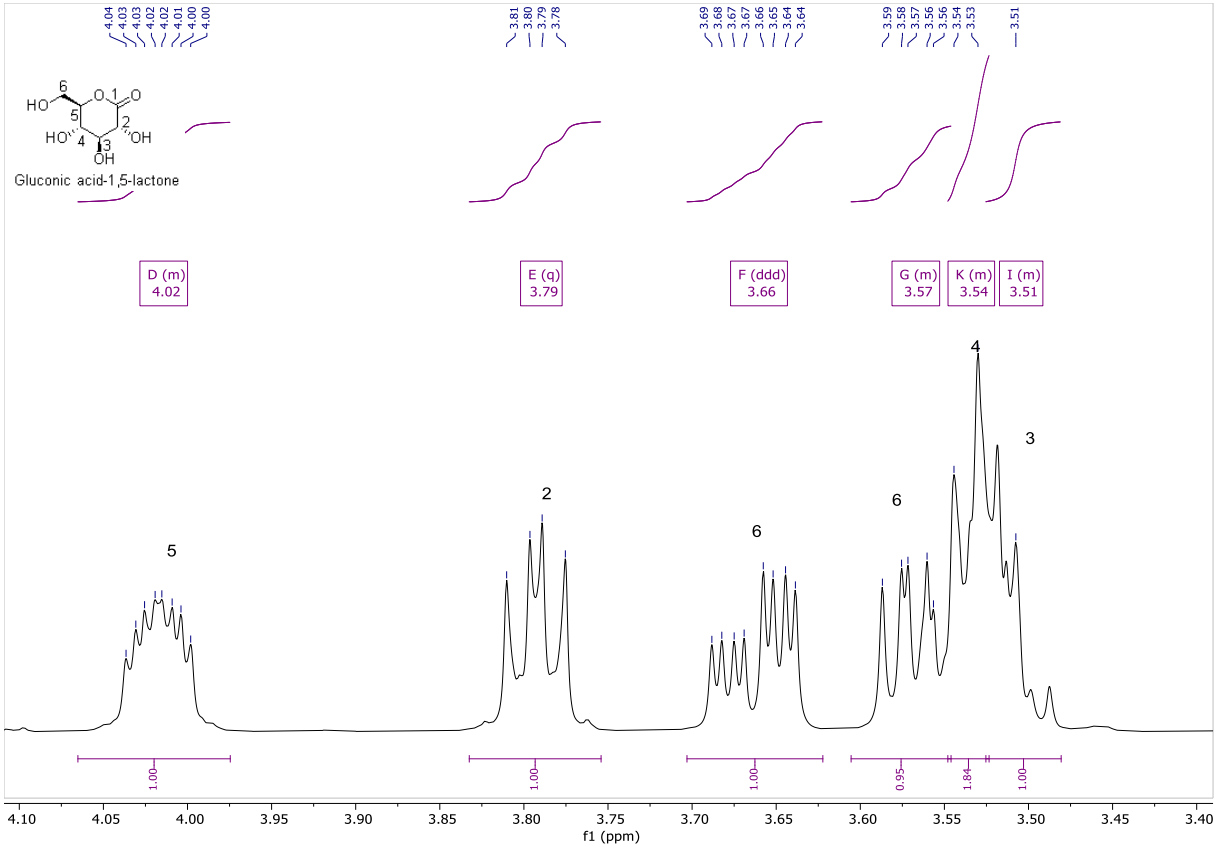

Fig. S29 ^{1}H NMR of **4** (400 MHz, DMSO) δ ppm: 4.07 – 3.97 (m, 1H), 3.79 (q, *J* = 8.4, 5.5 Hz, 1H), 3.66 (ddd, *J* = 12.2, 5.3, 2.4 Hz, 1H), 3.61 – 3.55 (m, 1H), 3.55 – 3.52 (m, 1H), 3.53 – 3.48 (m, 1H).

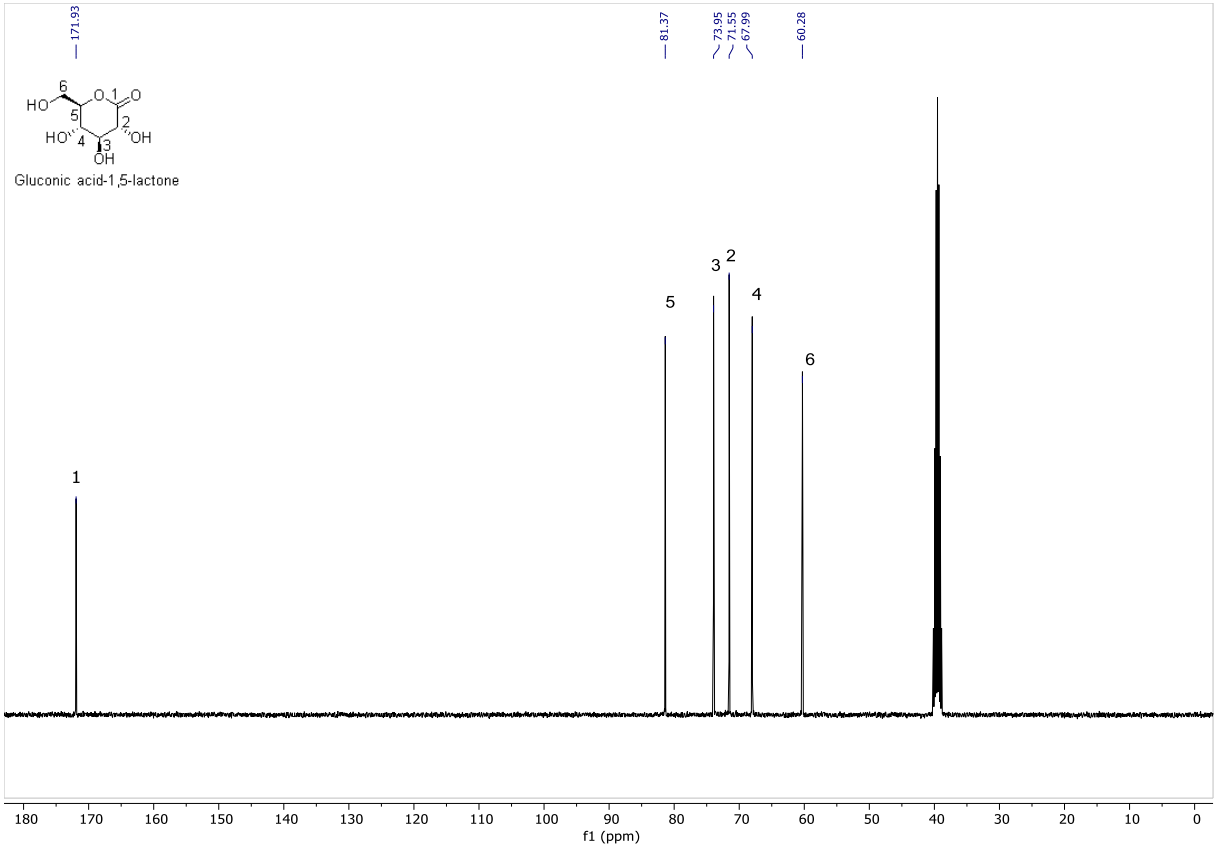

Fig. S30 ^{13}C-NMR of **4** (100.62 MHz, DMSO-D6) δ(ppm): 60.28, 67.99, 71.55, 73.95, 81.37, 171.93.

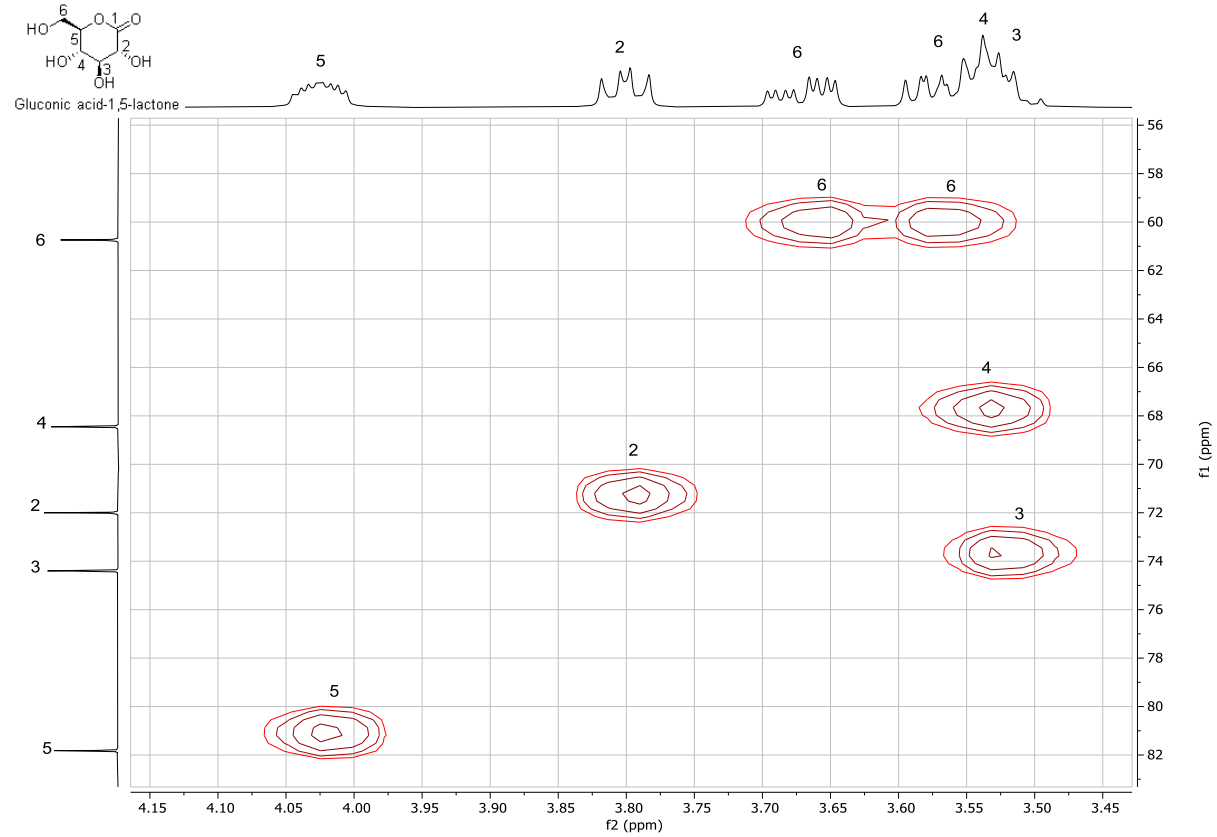

Fig. S31 HSQC-NMR of **4** (DMSO-D6)

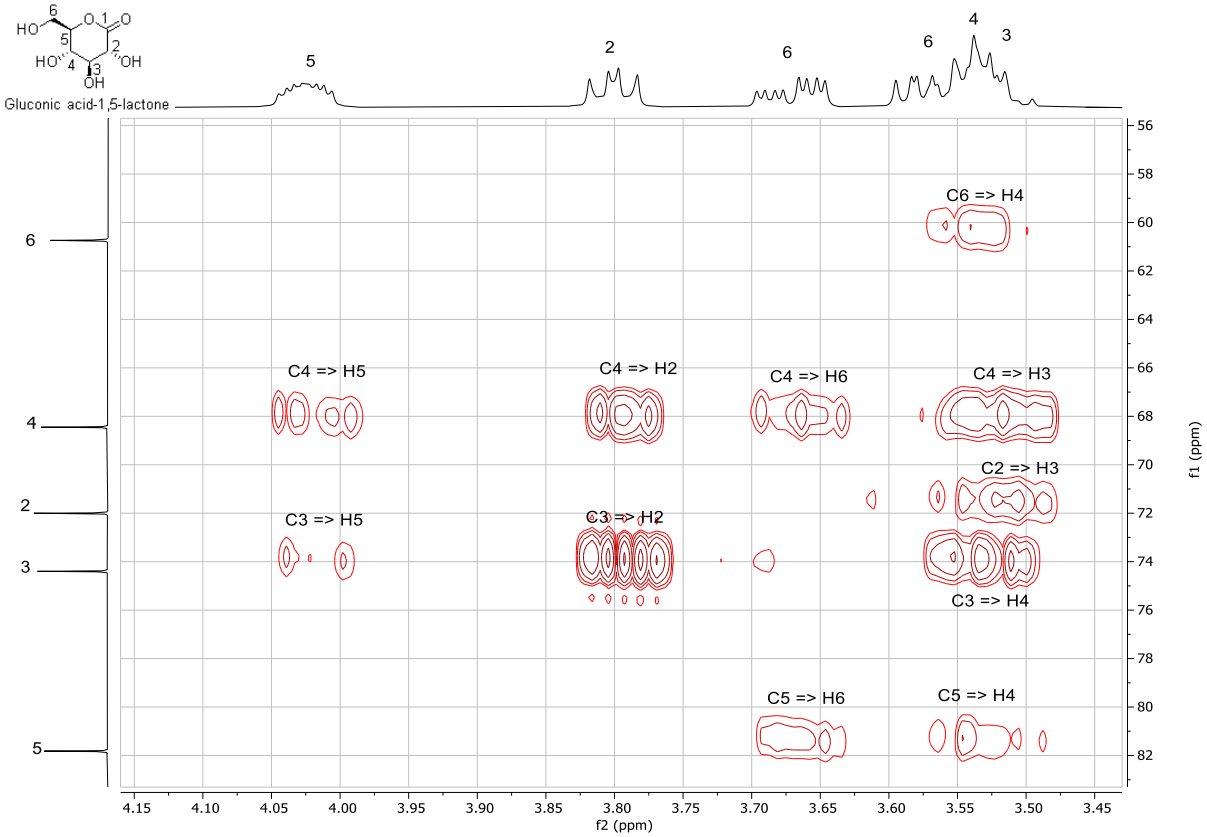

Fig. S32 HMBC-NMR of **4** (DMSO-D6)

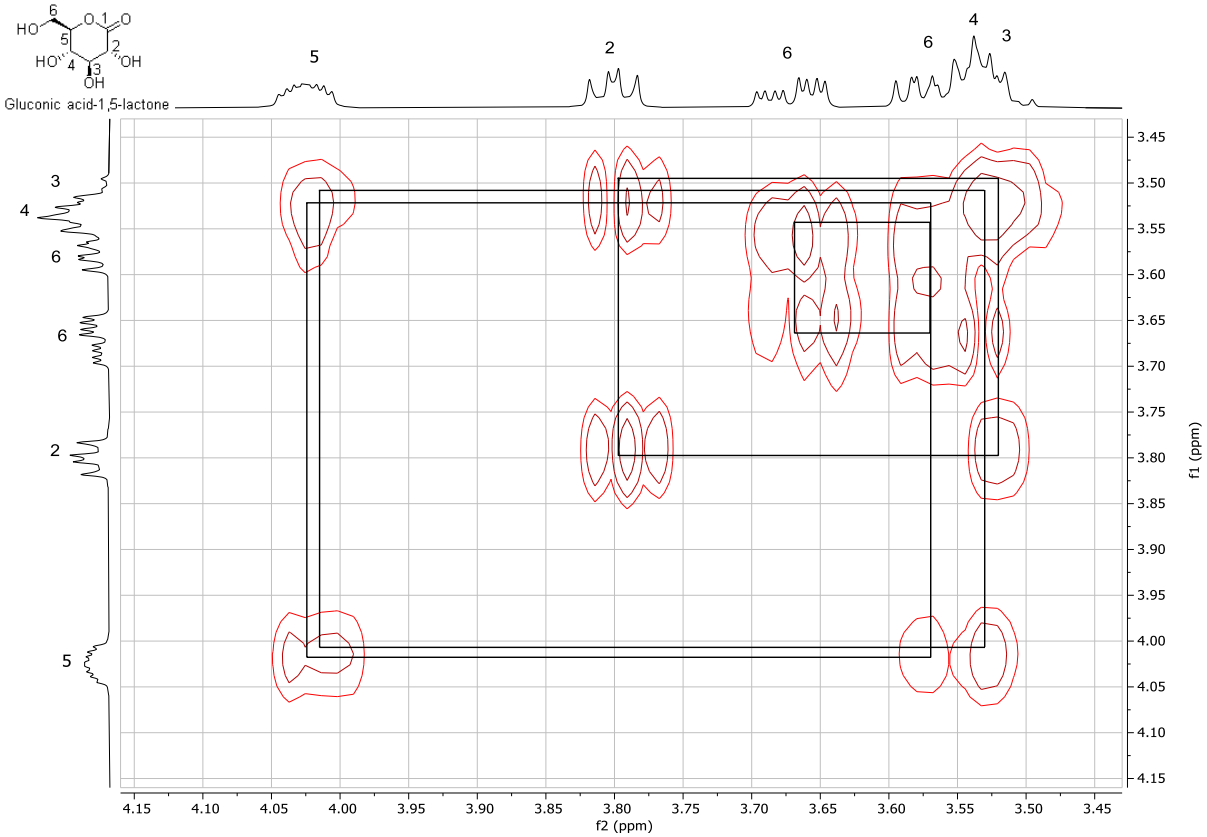

Fig. S33 COSY-NMR of **4** (DMSO-D6)

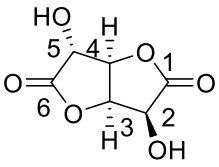

Glucaric acid-1,4;3,6-dilactone (5) The following procedure was adapted from Gehret *et al.*[38] In a 50 mL round bottom flask, calcium D-saccharate tetra hydrate (3.292 g, 10.2 mmol, 1.0 eq.) was suspended in 12 mL acetone/water (95/5 v/v%) using a magnetic stirrer. Sulfuric acid (1.0 g, 10.2 mmol, 1.0 eq.) was added to the suspension over a period of 25 min. The stirred mixture was heated at reflux for 4 hours. At no time did the mixture become homogenous. After that, the mixture was allowed to cool to RT and stirred for 2 hours. The suspension was filtrated over a type-3 glass filter and washed with 3x 15 mL acetone/water (95/5 v/v%). The mixture was concentrated using the rotary evaporator (30 °C; 285 mbar). The colourless solution was transferred into a 100 mL 3-neck flask and stored overnight in the refrigerator. The solution was stirred mechanically and heated (≤ 130 °C) under N_2-sparging for 2 hours. The thick syrup was allowed to reach RT, resulting in a dark brown glassy product (yield: 1.86 g, 104 % of theory). The hygroscopic product was exposed to air and had attracted water. Therefore, the syrup was again stirred mechanically and heated (≤ 130 °C) under N_2-sparging for 1.5 hours, resulting in a dark brown glassy product (yield 1.25 g, 70 % of theory). HPLC (UV and RI) of this product is provided in the HPLC overview at the end of this document (Fig. S60).

Gehret *et al.*[38] have published NMR data in acetone-D6, and Armstrong *et al*.[39] in D_2O, no previous records in DMSO-D6 have been published.

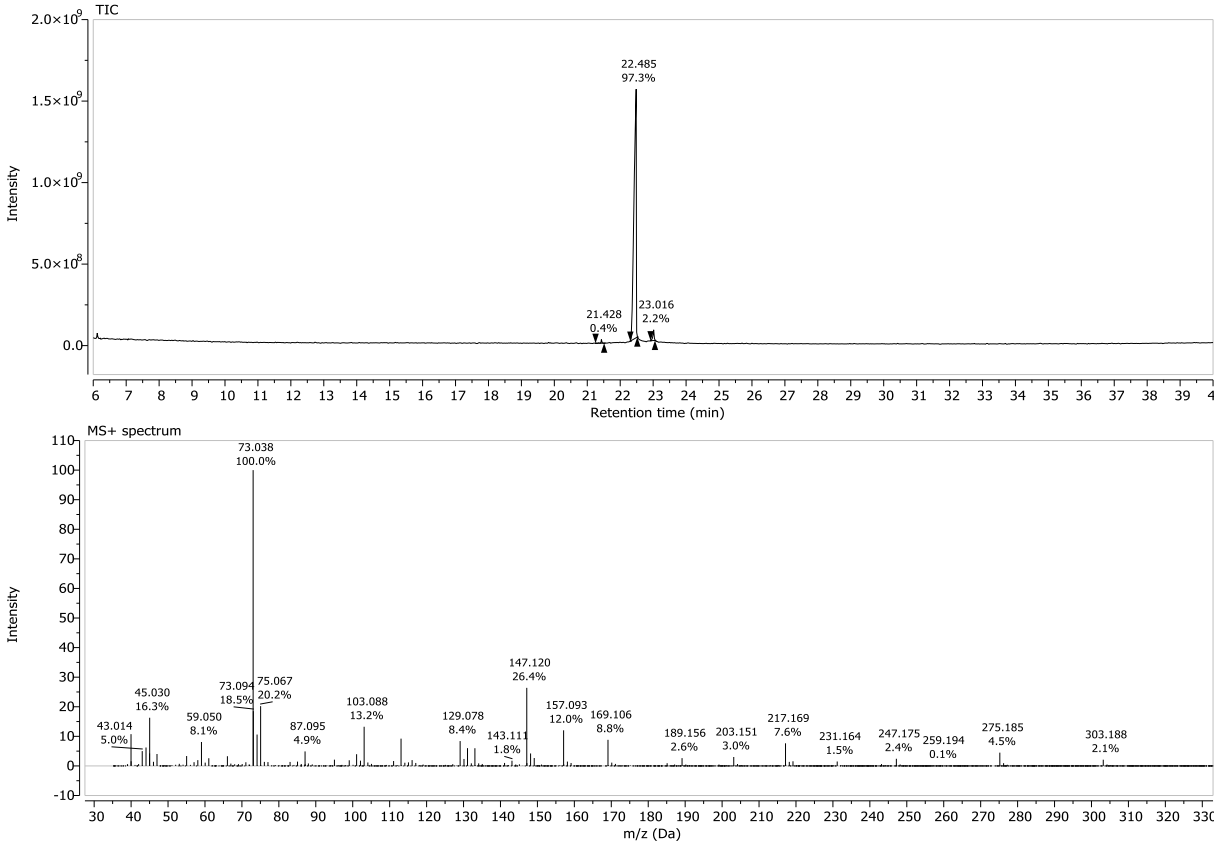

Fig. S34 GC-MS of **5** (silylated sample in pyridine): RT = 22.49 min. MS (GC-MS, 70 eV): *m/z* (%) = 303 (2.1) [M^+], 247 (2.4), 217 (7.6), 203 (3.0), 189 (2.6), 169 (8.8), 157 (12.0), 147 (26.4), 129 (8.4), 103 (13.2), 73 (100).

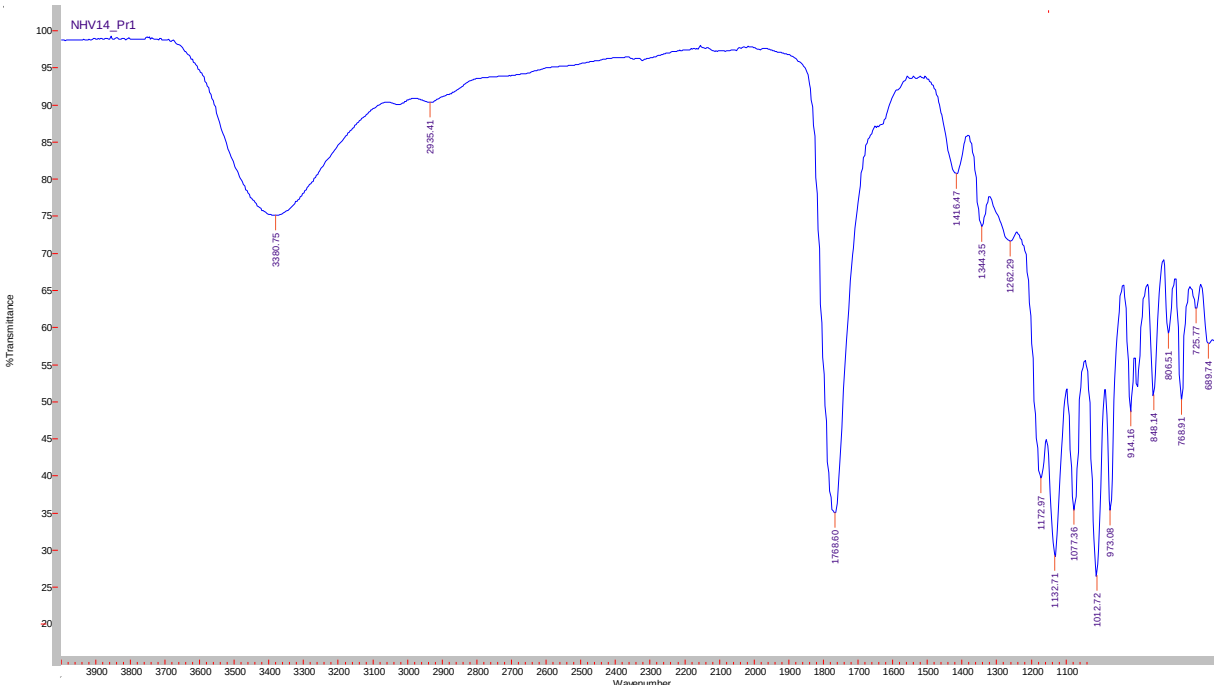

Fig. S35 FT-IR of **5**. Carbonyl signal correspond to a γ-lactone (1769 cm^{-1}).

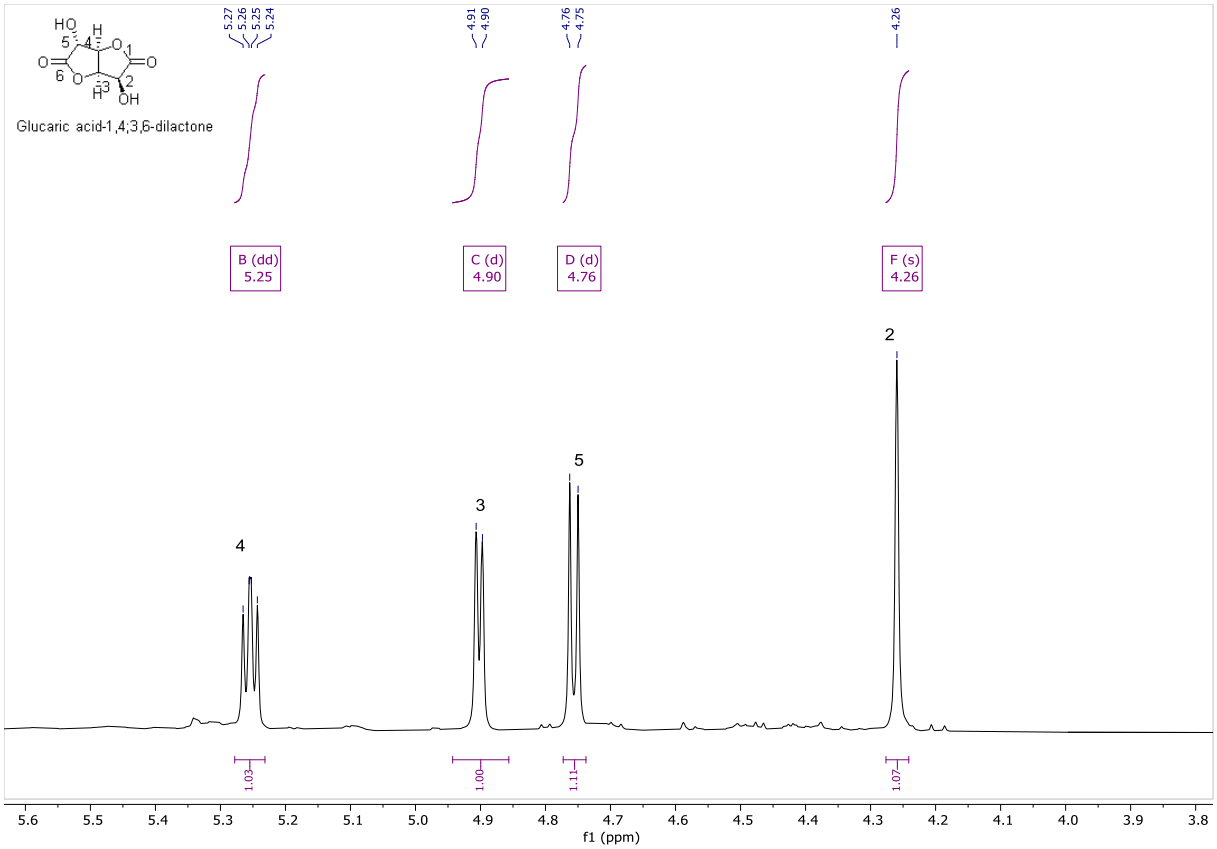

Fig. S36 ^{1}H NMR of **5** (400 MHz, DMSO) δ ppm: 5.25 (dd, *J* = 5.1, 3.6 Hz, 1H), 4.90 (d, *J* = 3.9 Hz, 1H), 4.76 (d, *J* = 5.1 Hz, 1H), 4.26 (s, 1H).

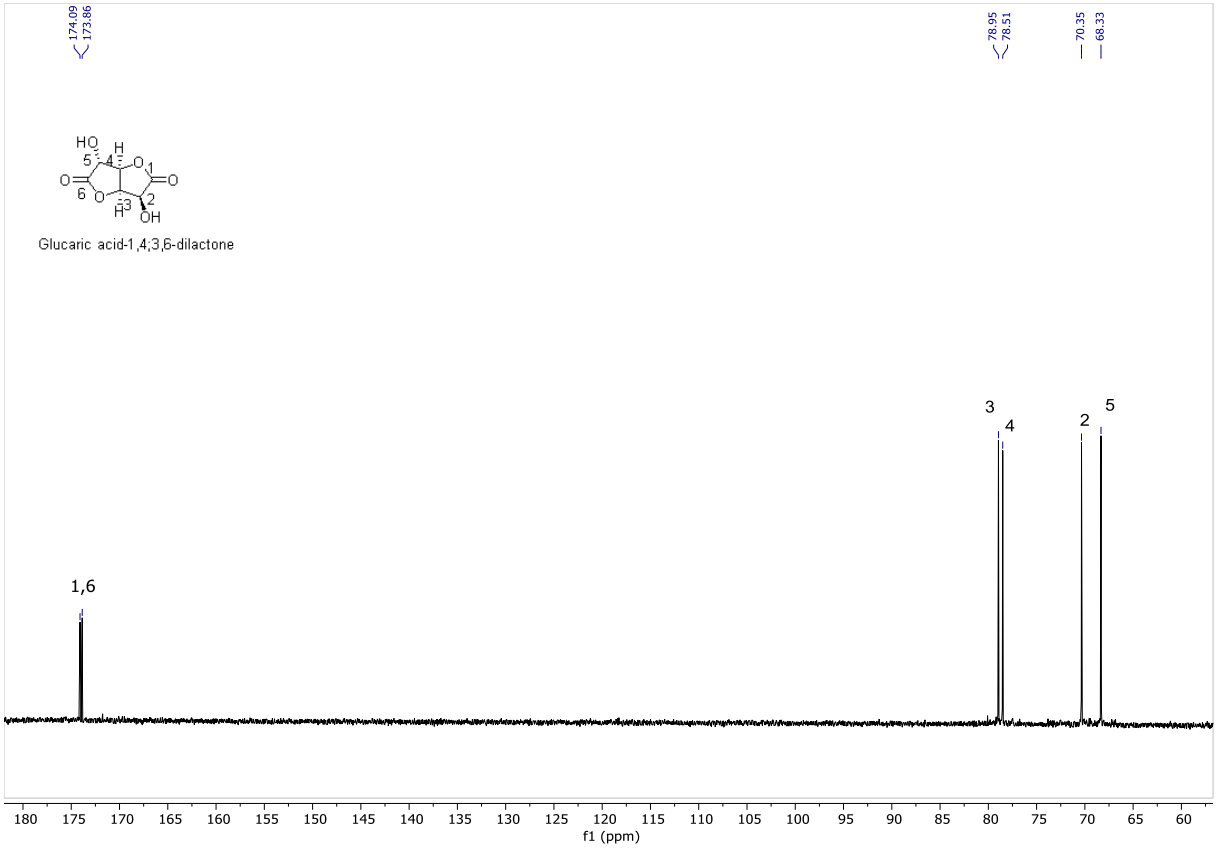

Fig. S37 ^{13}C-NMR of **5** (100.62 MHz, DMSO-D6) δ(ppm): 68.33, 70.35, 78.51, 78.95, 173.86, 174.09.

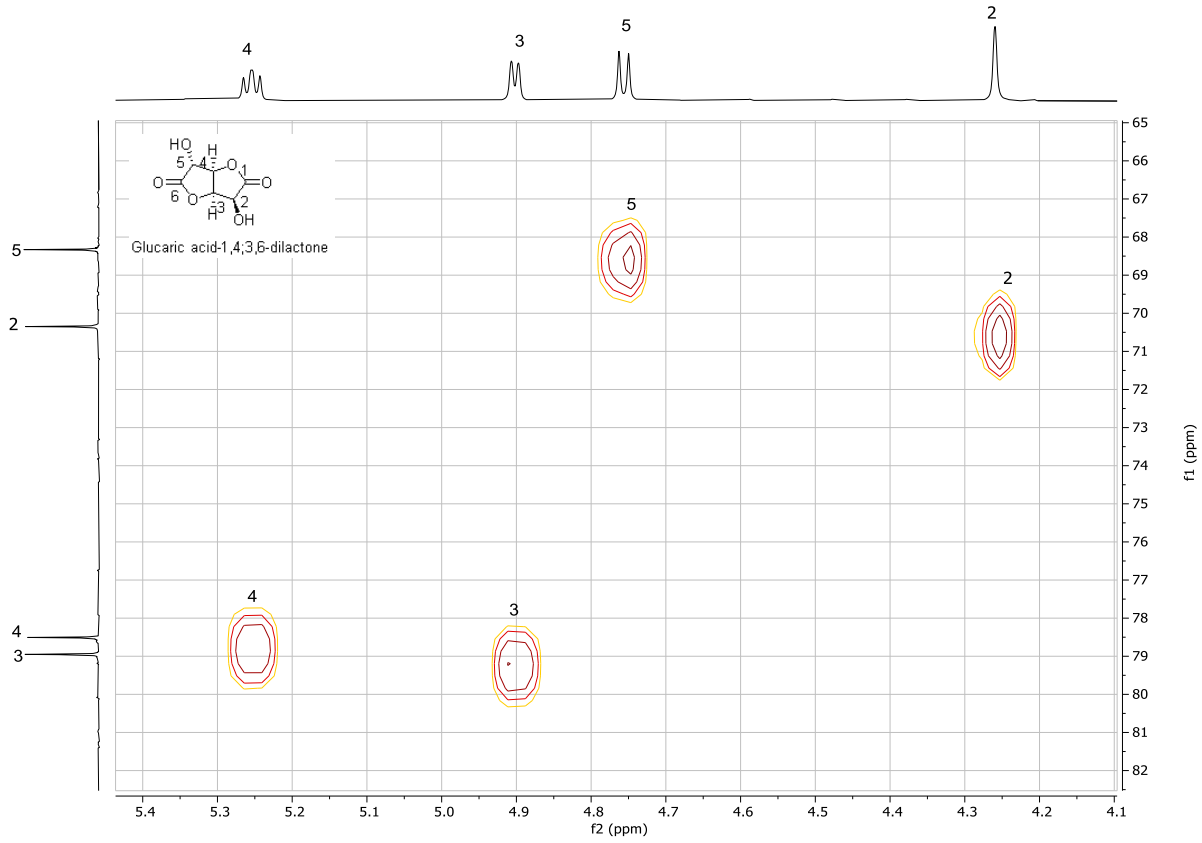

Fig. S38 HSQC-NMR of **5** (DMSO-D6)

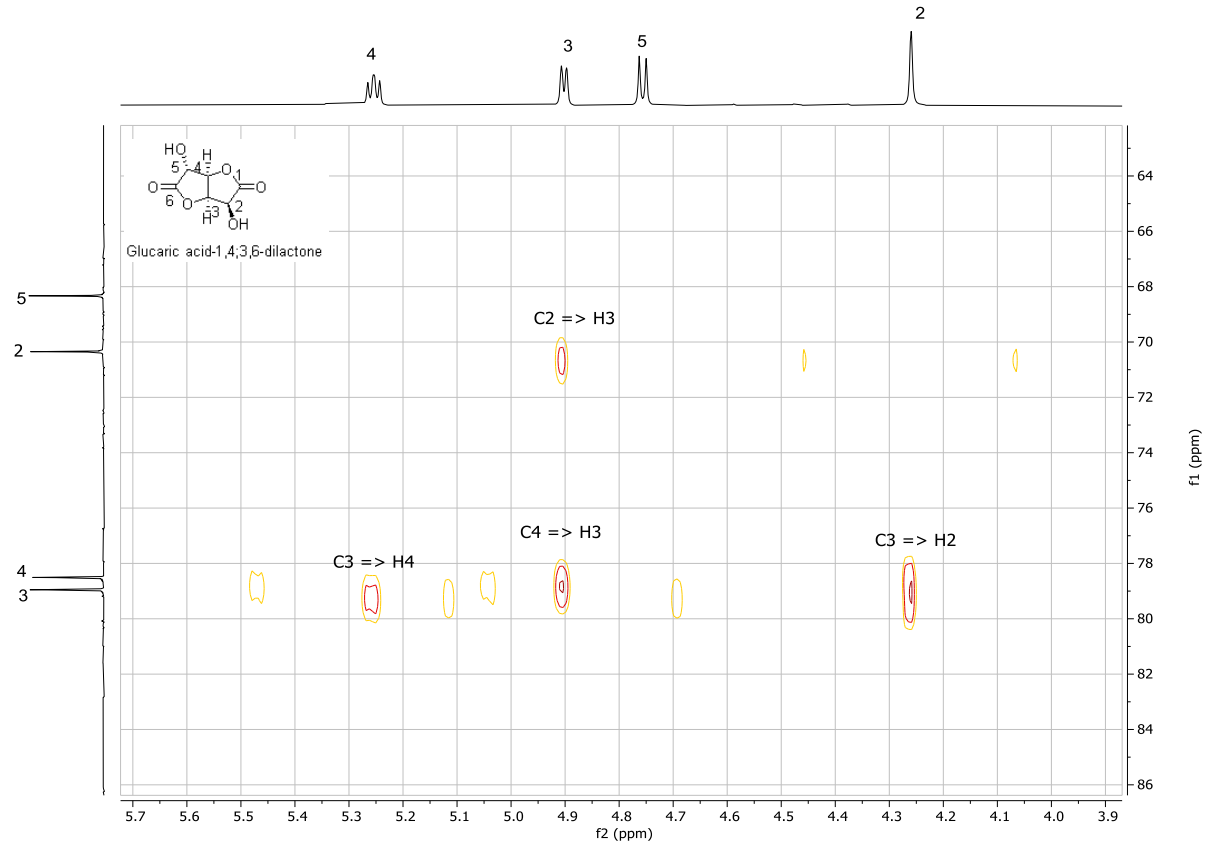

Fig. S39 HMBC-NMR of **5** (DMSO-D6)

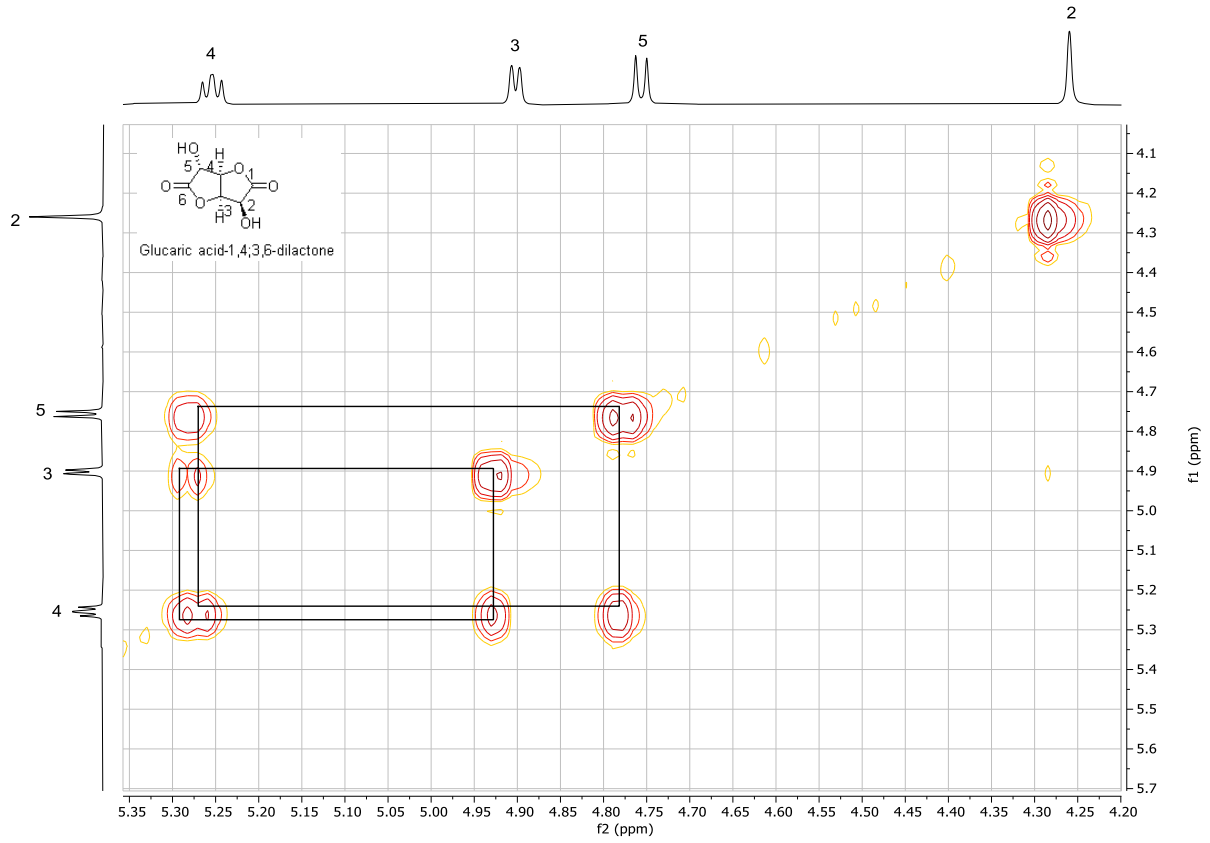

Fig. S40 COSY-NMR of **5** (DMSO-D6)

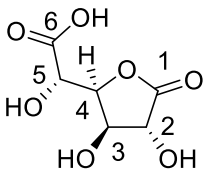

Glucaric acid-1,4-lactone (6) The following spectra were recorded from commercially sourced material. HPLC (UV and RI) of this product is provided in the HPLC overview at the end of this document (Fig. S61). Previous NMR data have been published in different solvents: Gehret *et al.*[38] in acetone-D6, and Armstrong *et al*.[39] in D_2O, while DMSO-D6 has not been reported.

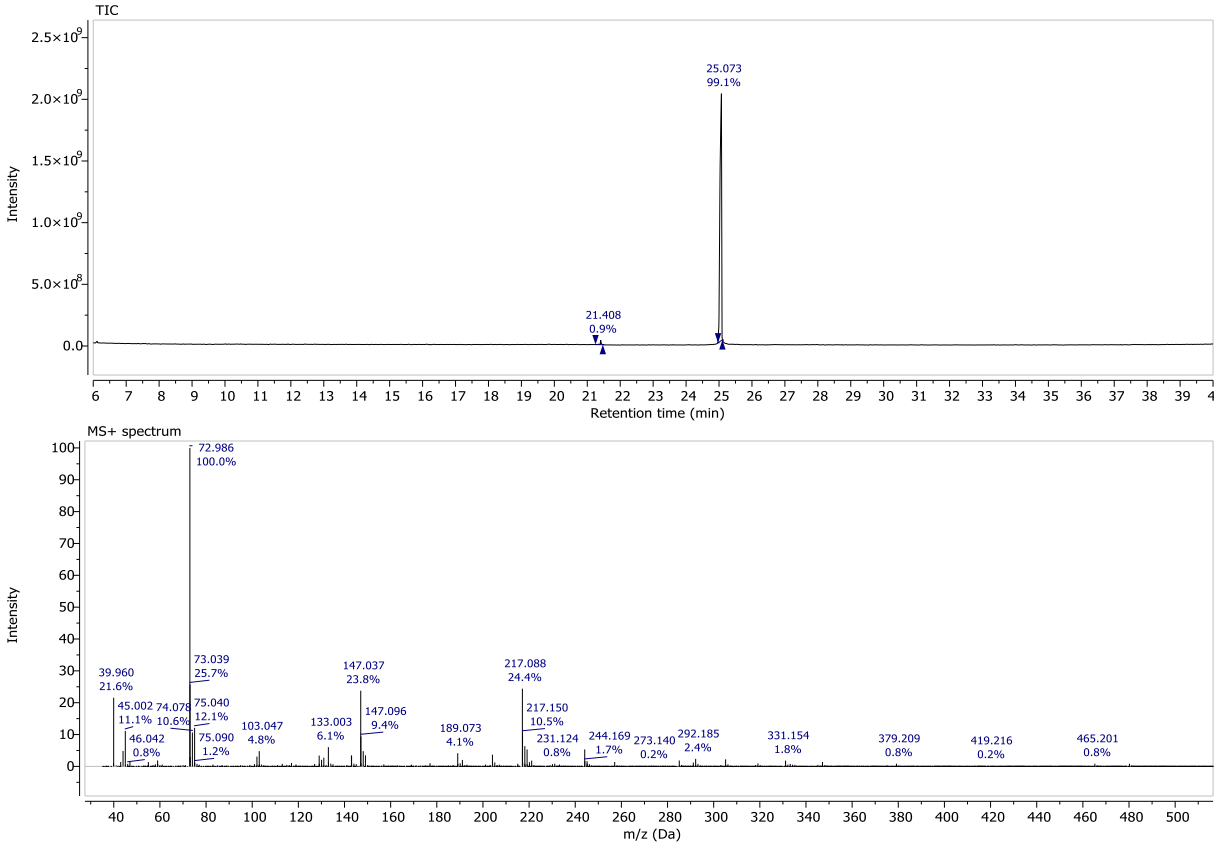

Fig. S41 GC-MS of **6** (silylated sample in pyridine): RT = 25.07 min. MS (GC-MS, 70 eV): *m/z* (%) = 481 (0.2) [M^+], 465 (0.8), 379 (0.8), 292 (2.4), 217 (24.4), 147 (23.8), 73 (100).

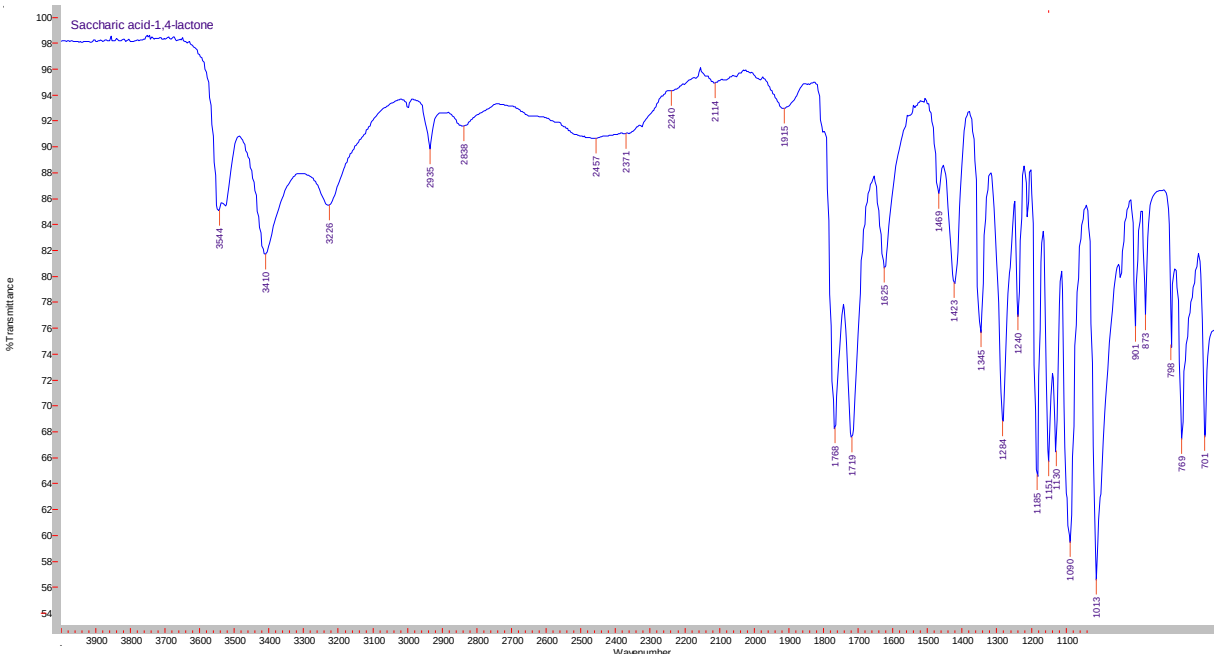

Fig. S42 FT-IR of **6**. Carbonyl signal correspond to the presence of a γ-lactone (1768 cm^{-1}) and a free carboxylic acid (1719 cm^{-1}).

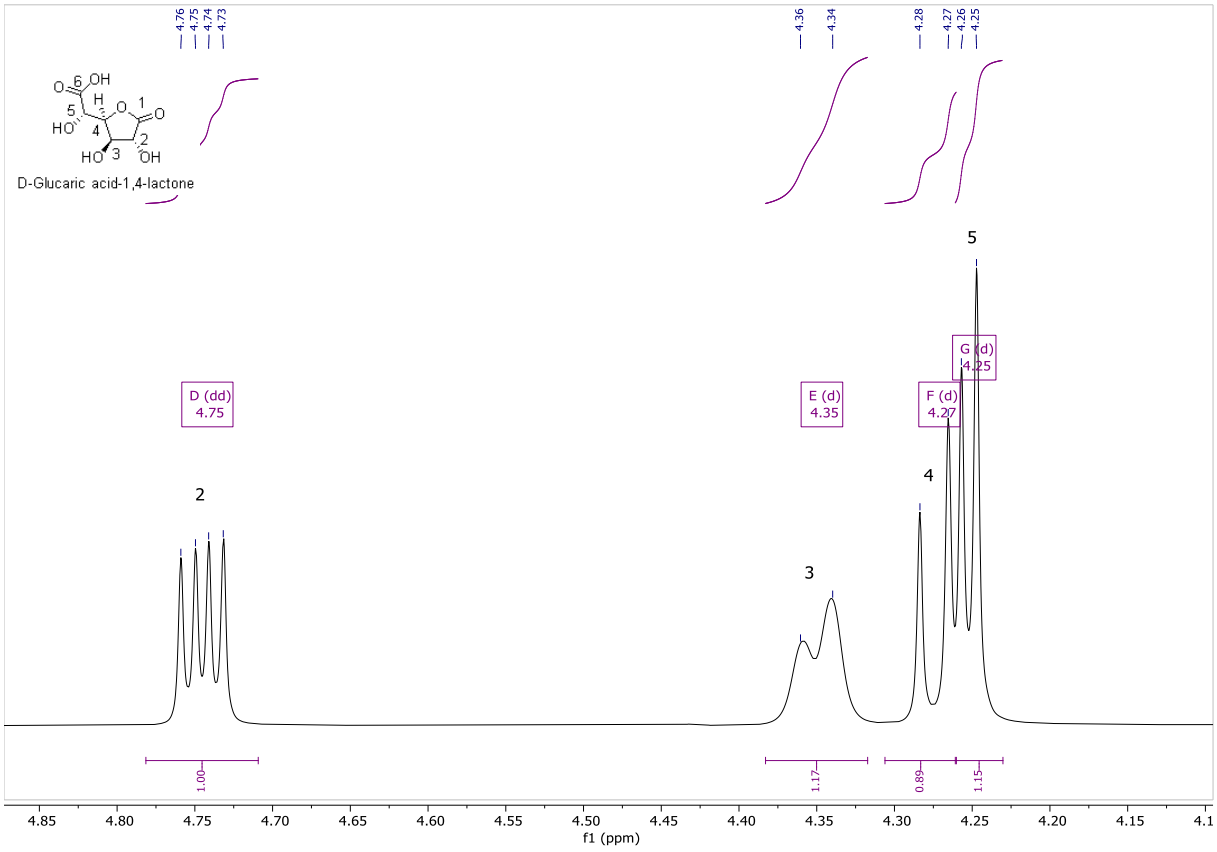

Fig. S43 ^{1}H NMR of **6** (400 MHz, DMSO) δ ppm: 4.75 (dd, *J* = 7.2, 3.8 Hz, 1H), 4.35 (d, *J* = 8.3 Hz, 1H), 4.27 (d, *J* = 7.3 Hz, 1H), 4.25 (d, *J* = 3.9 Hz, 1H).

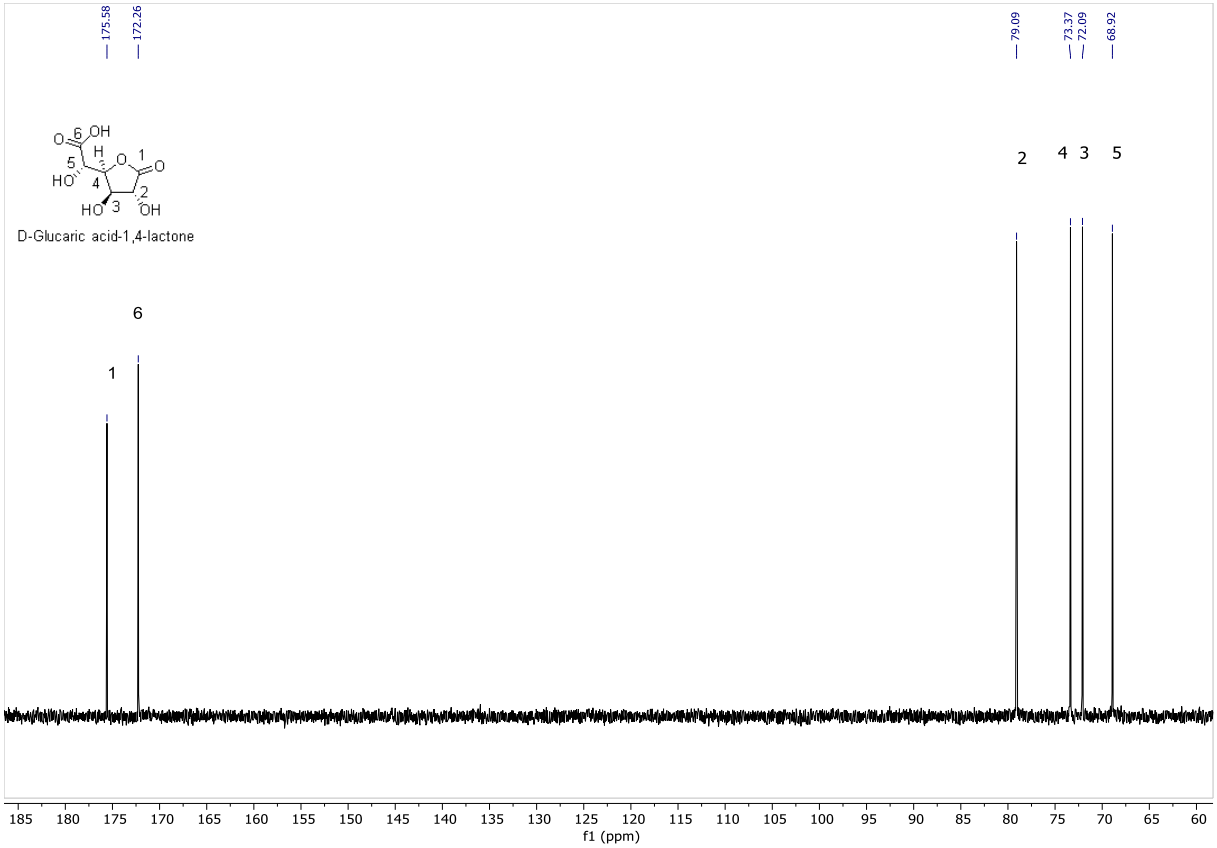

Fig. S44 ^{13}C-NMR of **6** (100.62 MHz, DMSO-D6) δ(ppm): 68.92, 72.09, 73.37, 79.09, 172.26, 175.58.

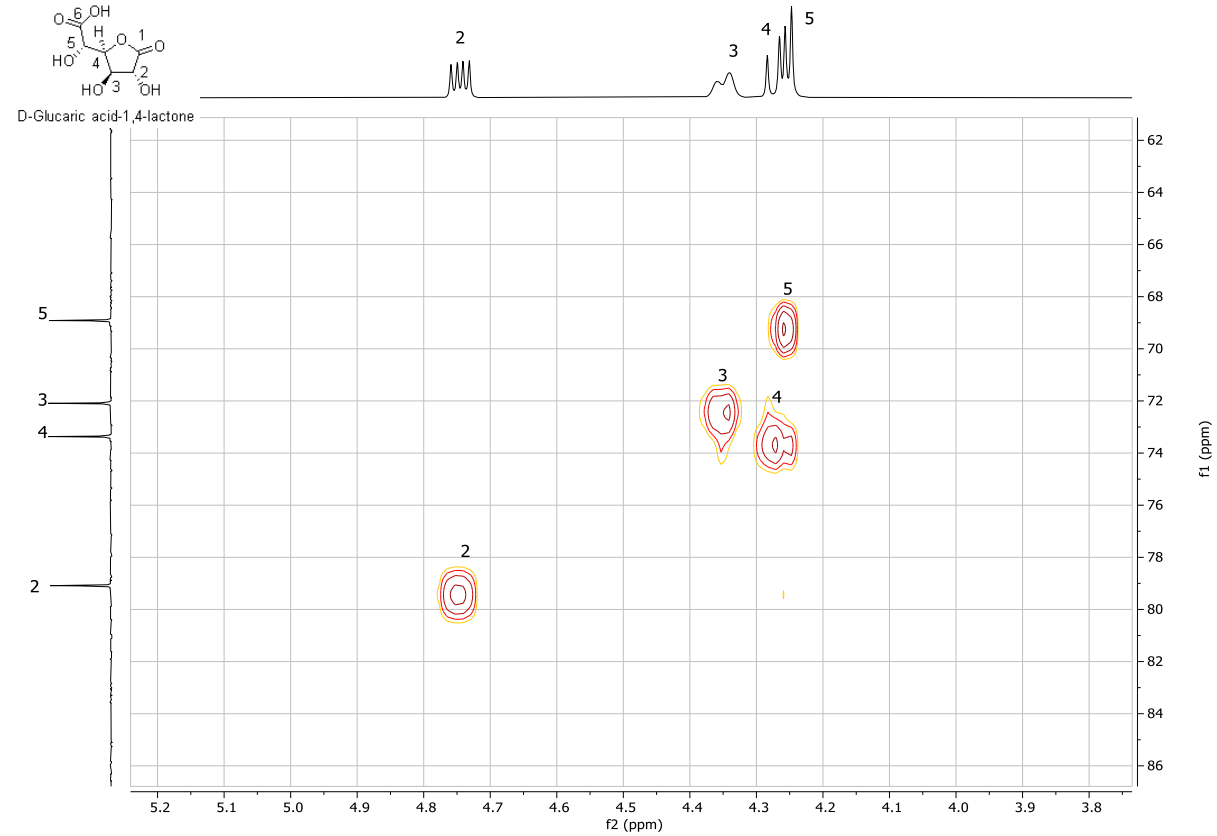

Fig. S45 HSQC-NMR of **6** (DMSO-D6)

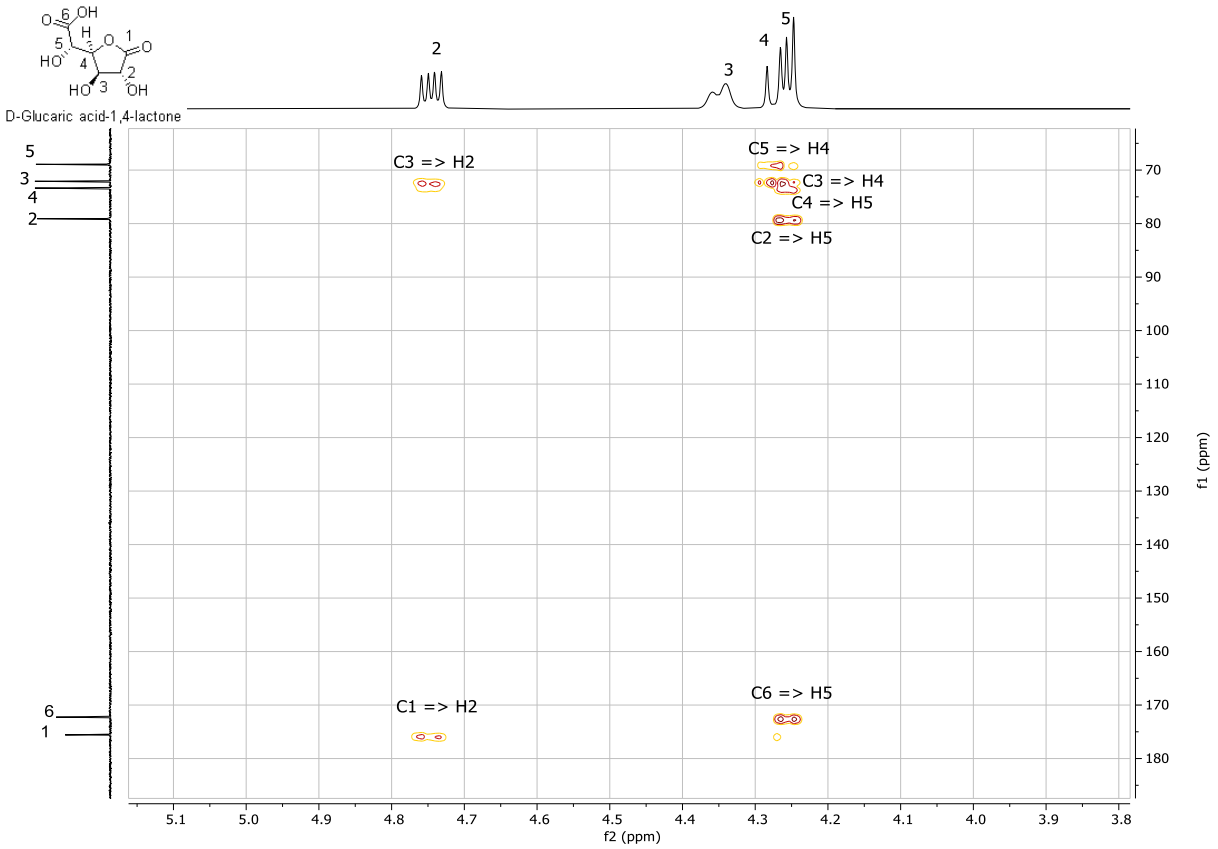

Fig. S46 HMBC-NMR of **6** (DMSO-D6)

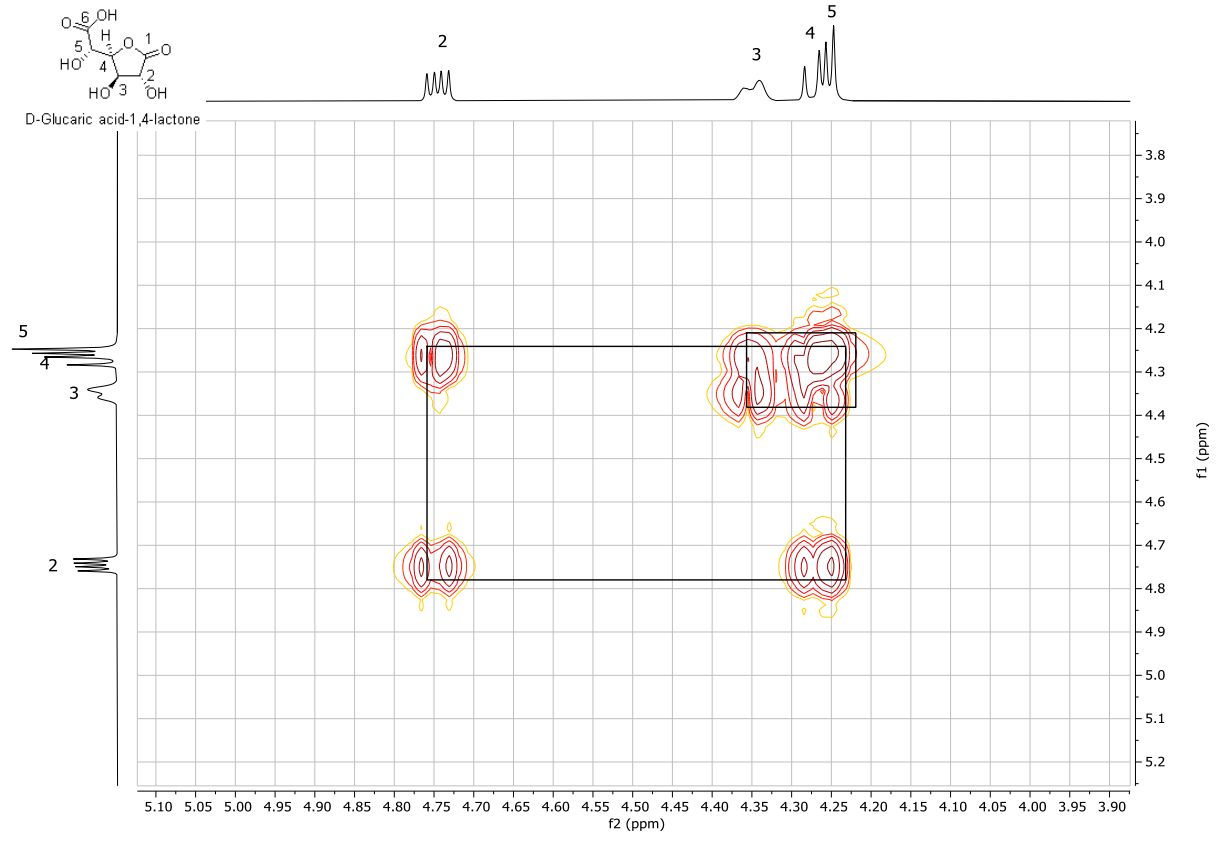

Fig. S47 COSY-NMR of **6** (DMSO-D6)

Table S3 Overview of HPLC retention times (UV and RI) for (commercial and in-house synthesized) reference compounds

Compound	**R_t UV (min)**	**R_t RI (min)**
D-Galacturonic acid	13.86	14.40
Galactaric acid (= mucic acid)	12.77	13.31
Galactaric acid-1,4-lactone (**1**)	12.88	13.43
D-Galactose	-	16.71
D-Galactonic acid	15.56	16.09
D-Galactonic acid-1,4-lactone (**2**)	15.57	16.10
D-Glucose	-	15.65
D-Gluconic acid	15.12	15.66
D-Gluconic acid-1,4-lactone (**3**)	15.24	15.78
D-Gluconic acid-1,5-lactone (**4**)	15.11	15.65
D-Glucuronic acid	12.75	13.29
D-Saccharic acid (= glucaric acid)	13.49	14.03
D-Glucaric acid-1,4;6,3-dilactone (**5**)	13.73	14.28
D-Glucaric acid-1,4-lactone (**6**)	13.63	14.16

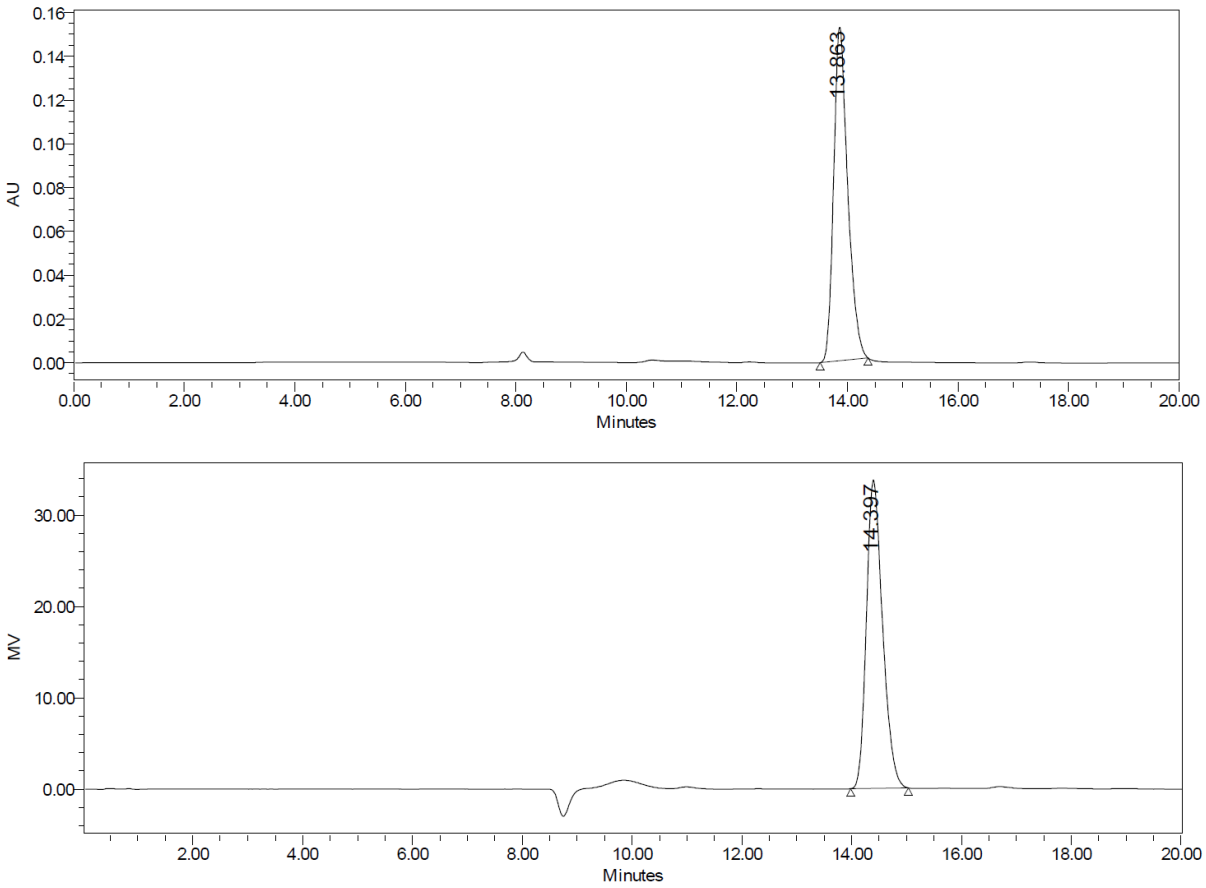

Fig. S48 HPLC of D-Galacturonic acid: UV (top); RI (bottom).

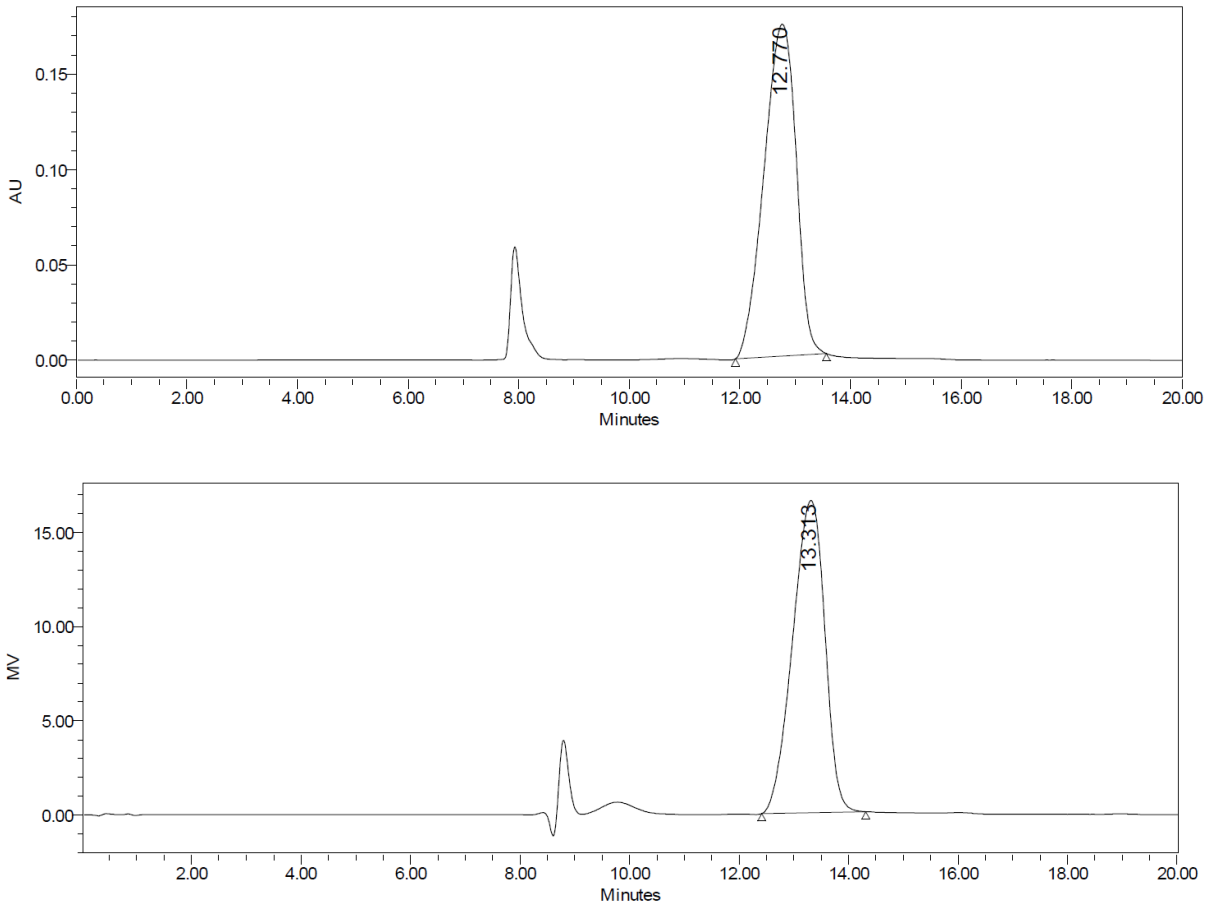

Fig. S49 HPLC of Galactaric acid (= mucic acid): UV (top); RI (bottom).

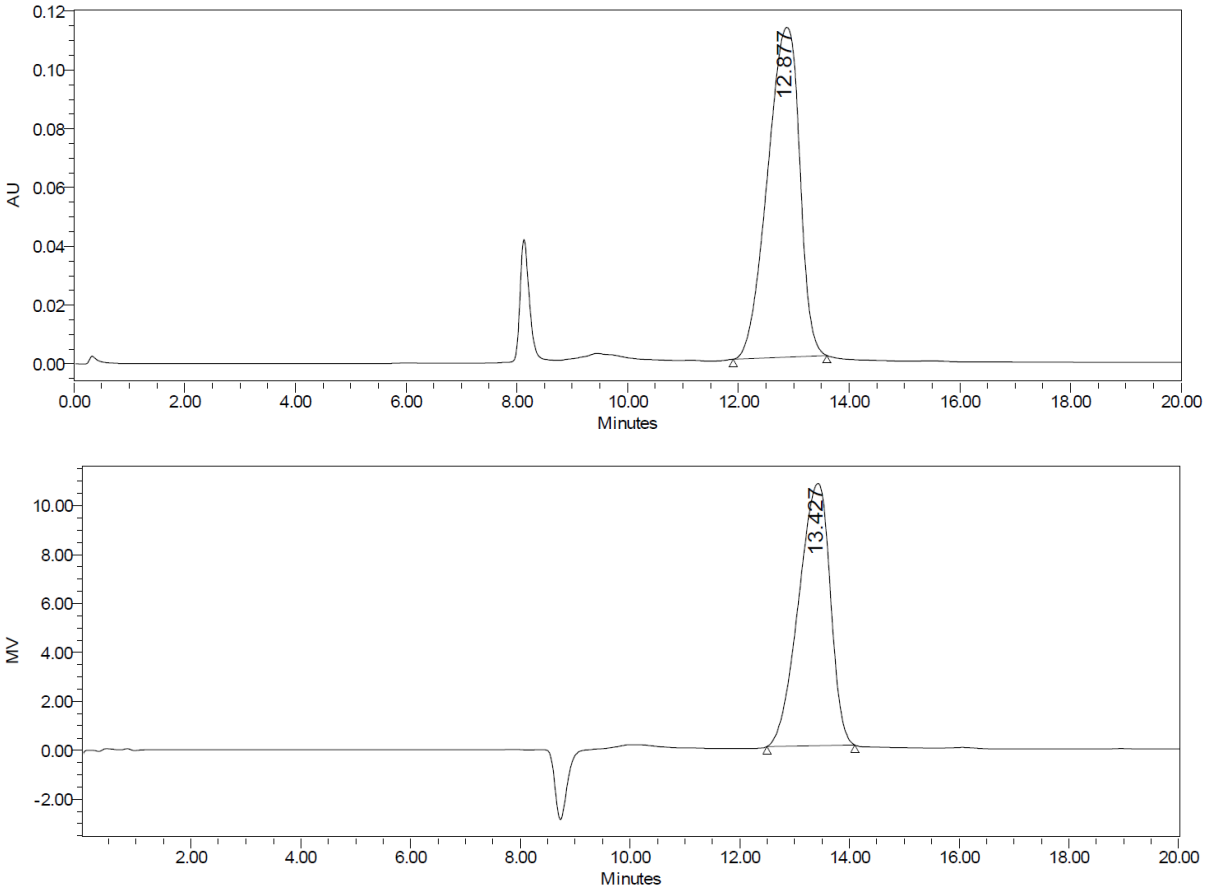

Fig. S50 HPLC of Galactaric acid-1,4-lactone (**1**): UV (top); RI (bottom).

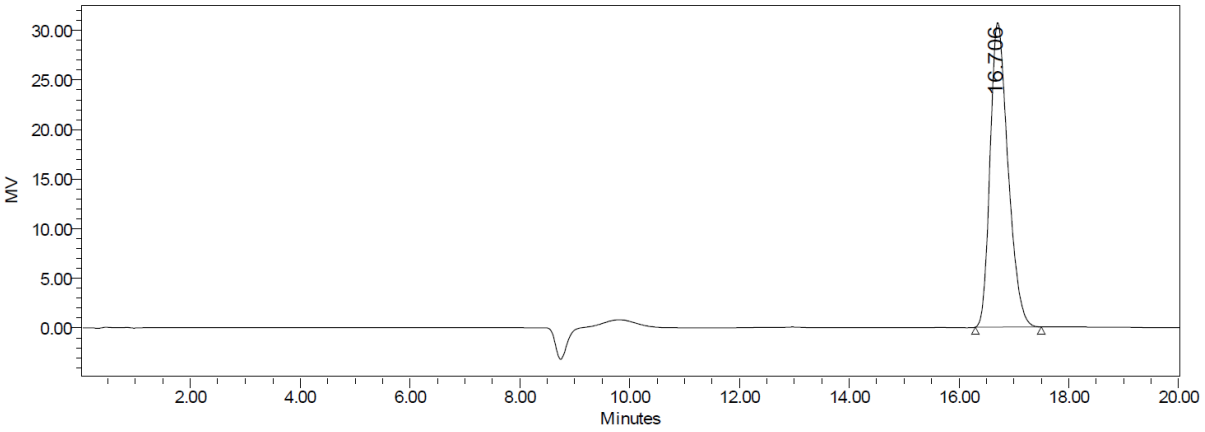

Fig. S51 HPLC of D-Galactose: RI (sample has no UV signal).

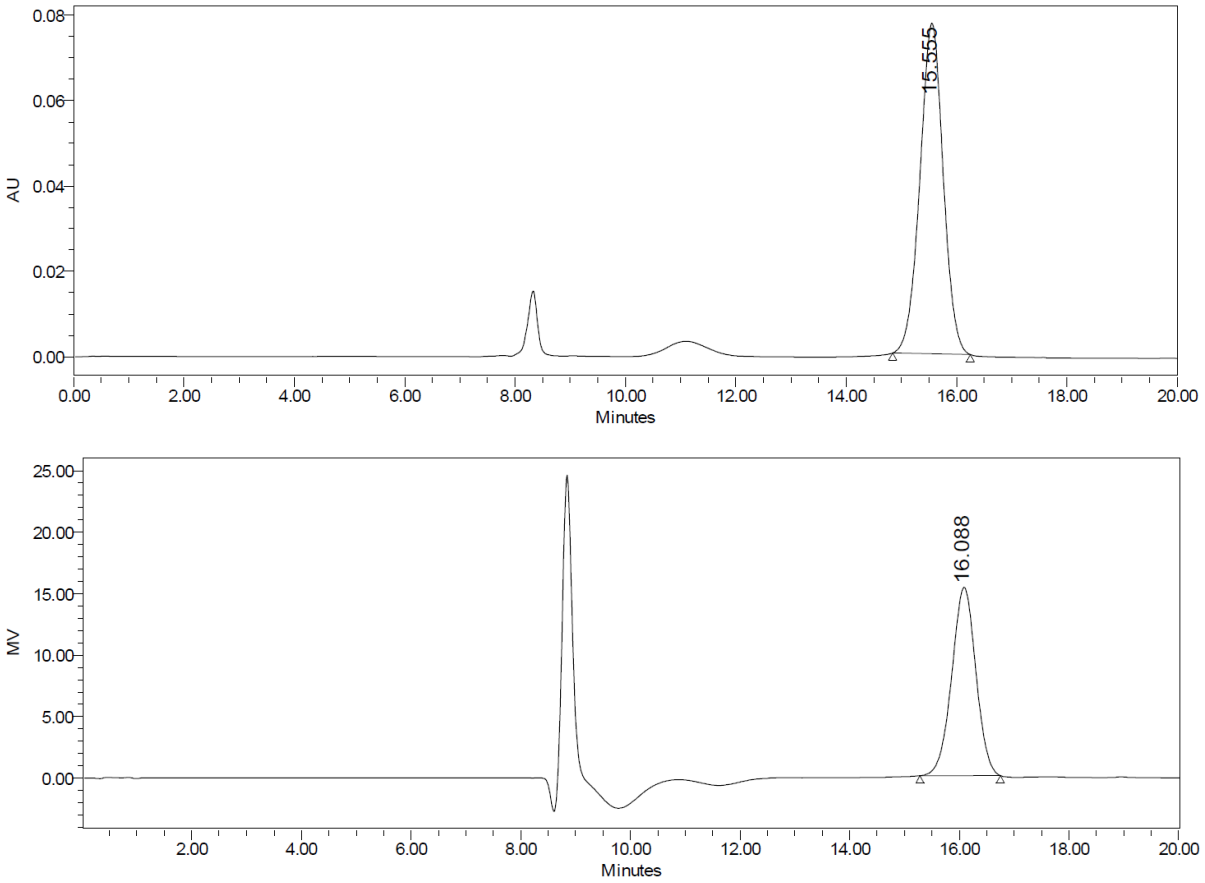

Fig. S52 HPLC of D-Galactonic acid: UV (top); RI (bottom).

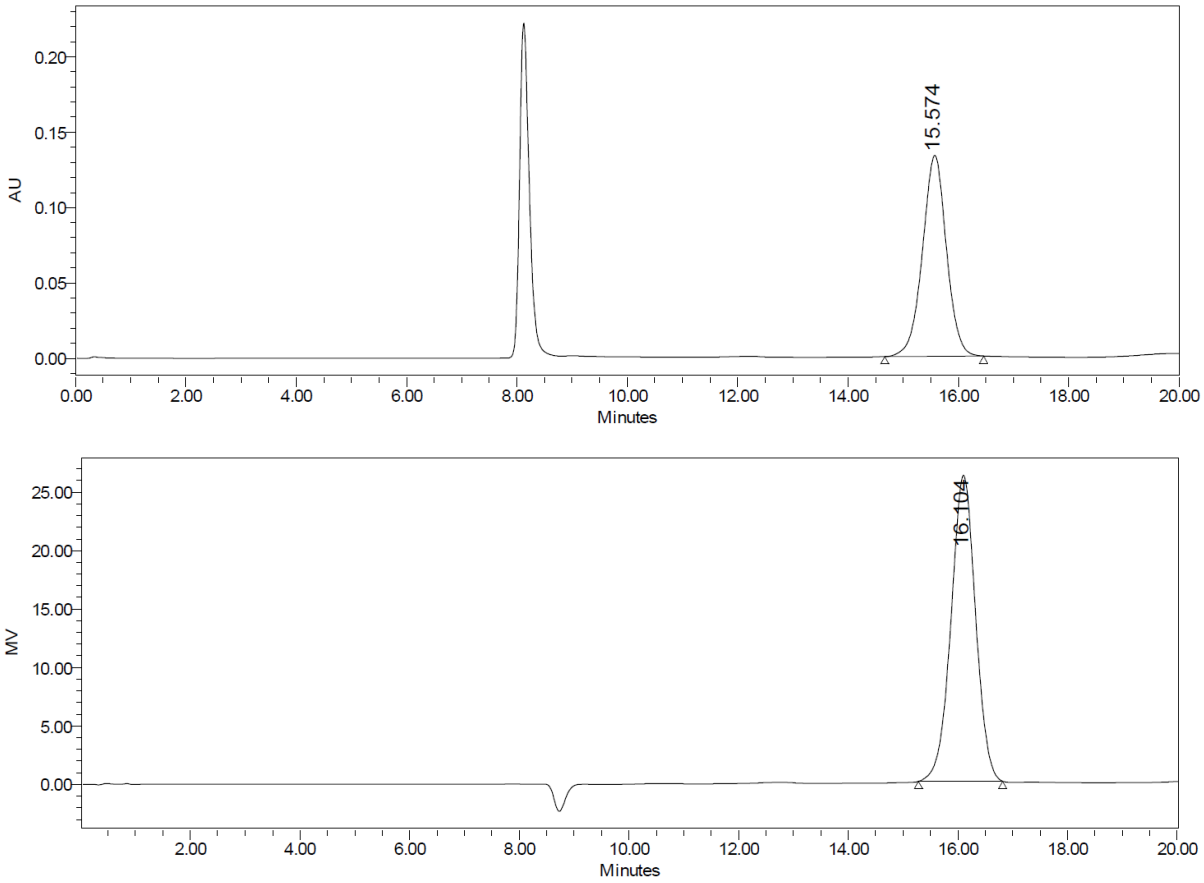

Fig. S53 HPLC of D-Galactonic acid-1,4-lactone (**2**): UV (top); RI (bottom).

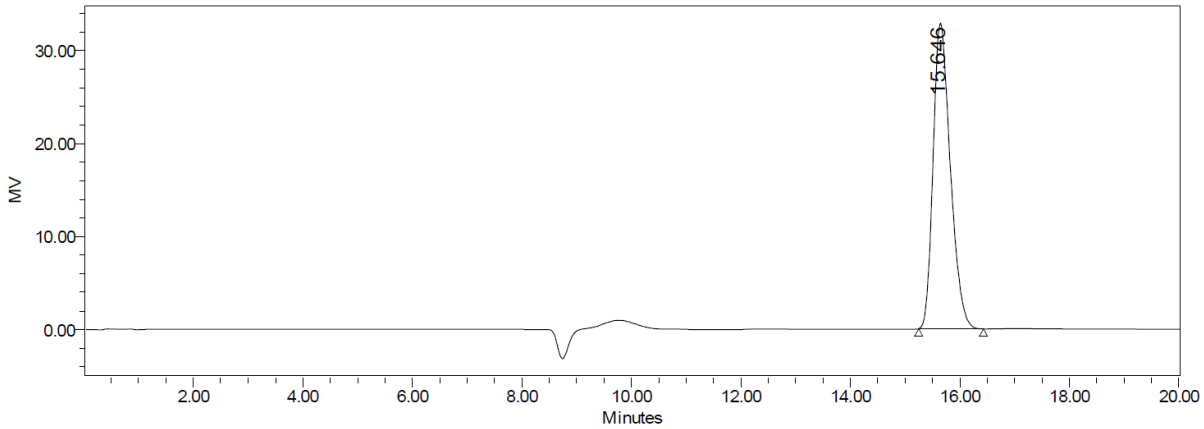

Fig. S54 HPLC of D-Glucose: RI (sample has no UV signal).

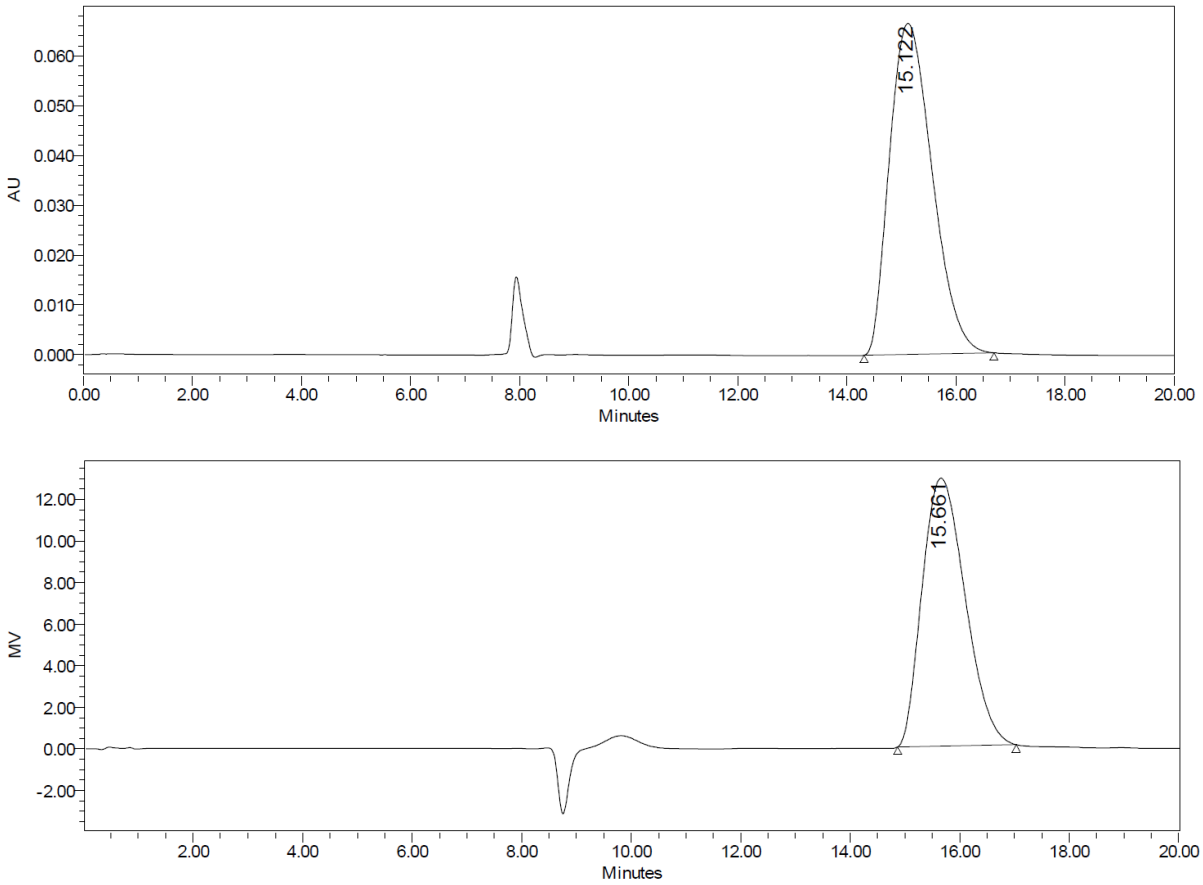

Fig. S55 HPLC of D-Gluconic acid: UV (top); RI (bottom).

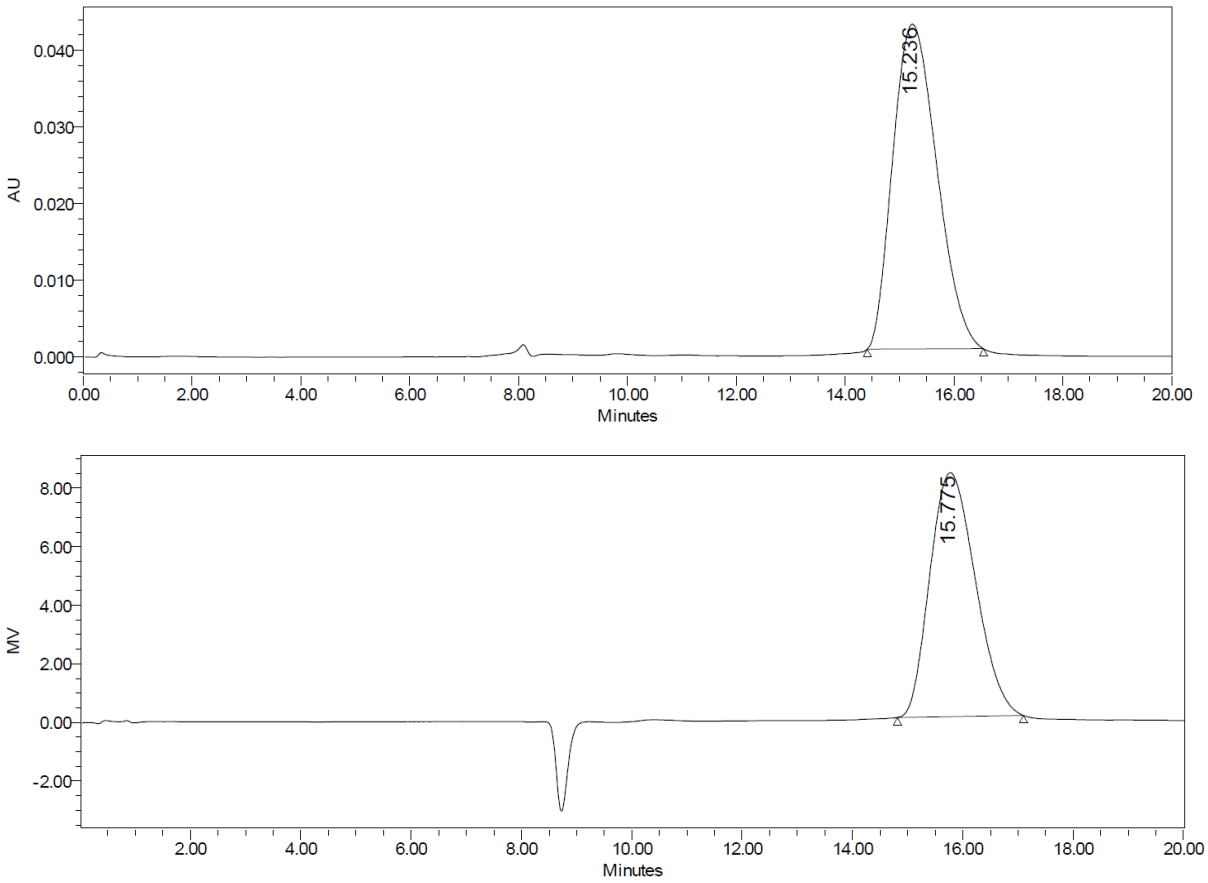

Fig. S56 HPLC of D-Gluconic acid-1,4-lactone (**3**): UV (top); RI (bottom).

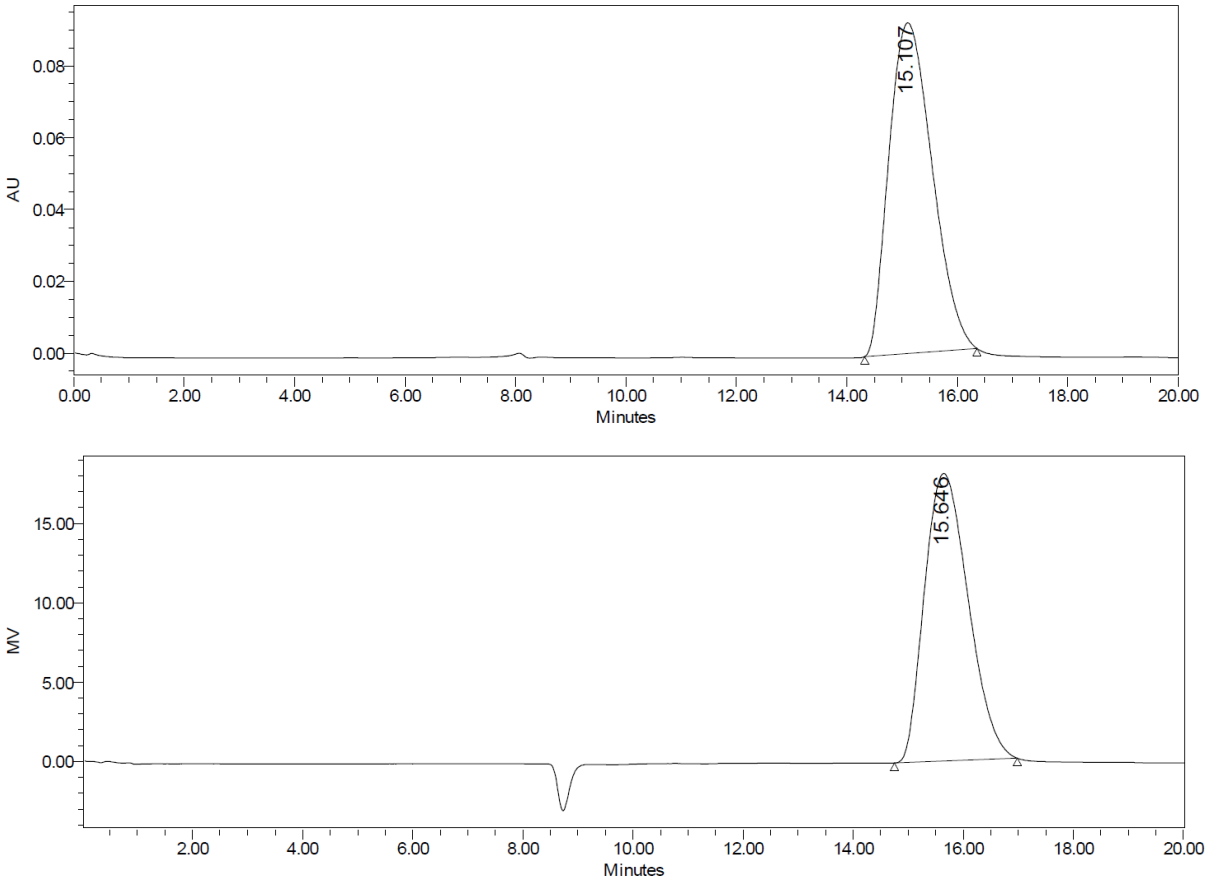

Fig. S57 HPLC of D-Gluconic acid-1,5-lactone (**4**): UV (top); RI (bottom).

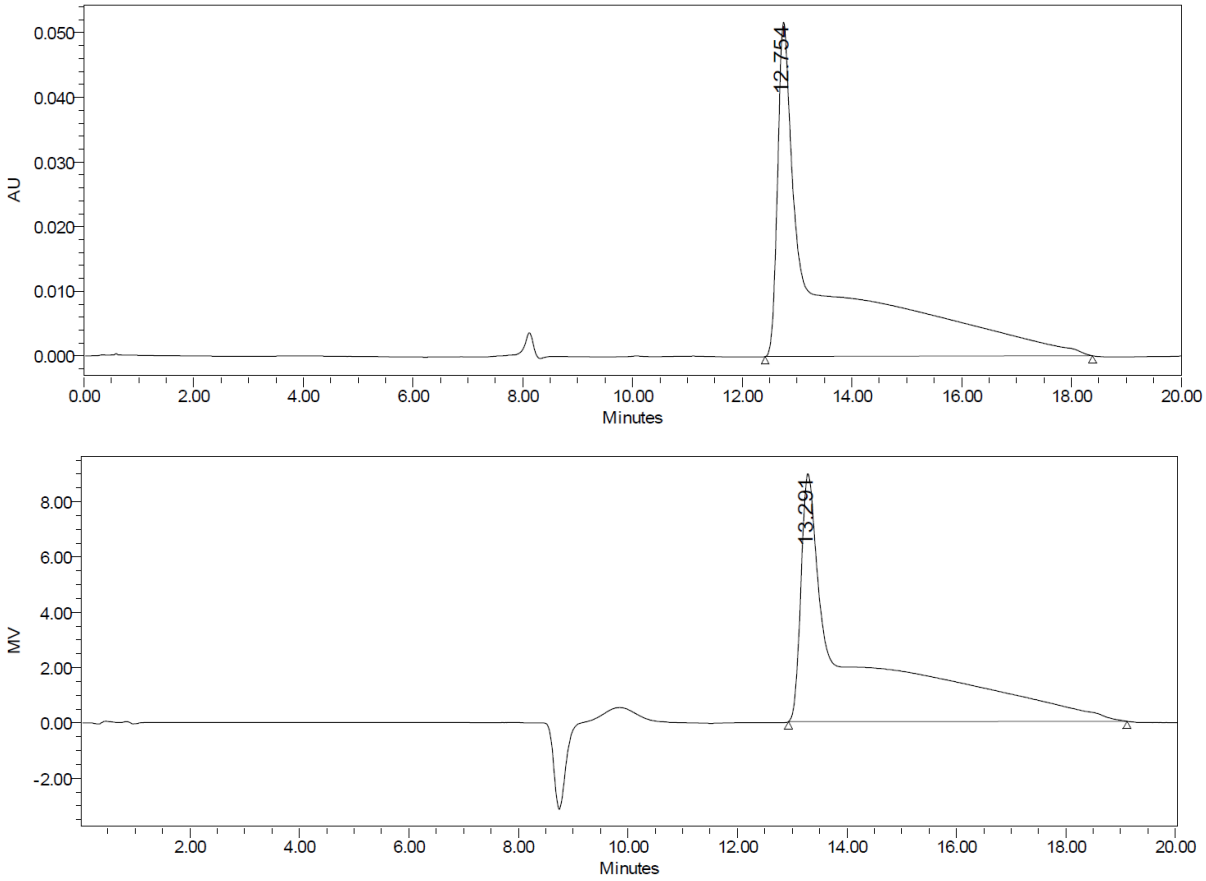

Fig. S58 HPLC of D-Glucuronic acid: UV (top); RI (bottom).

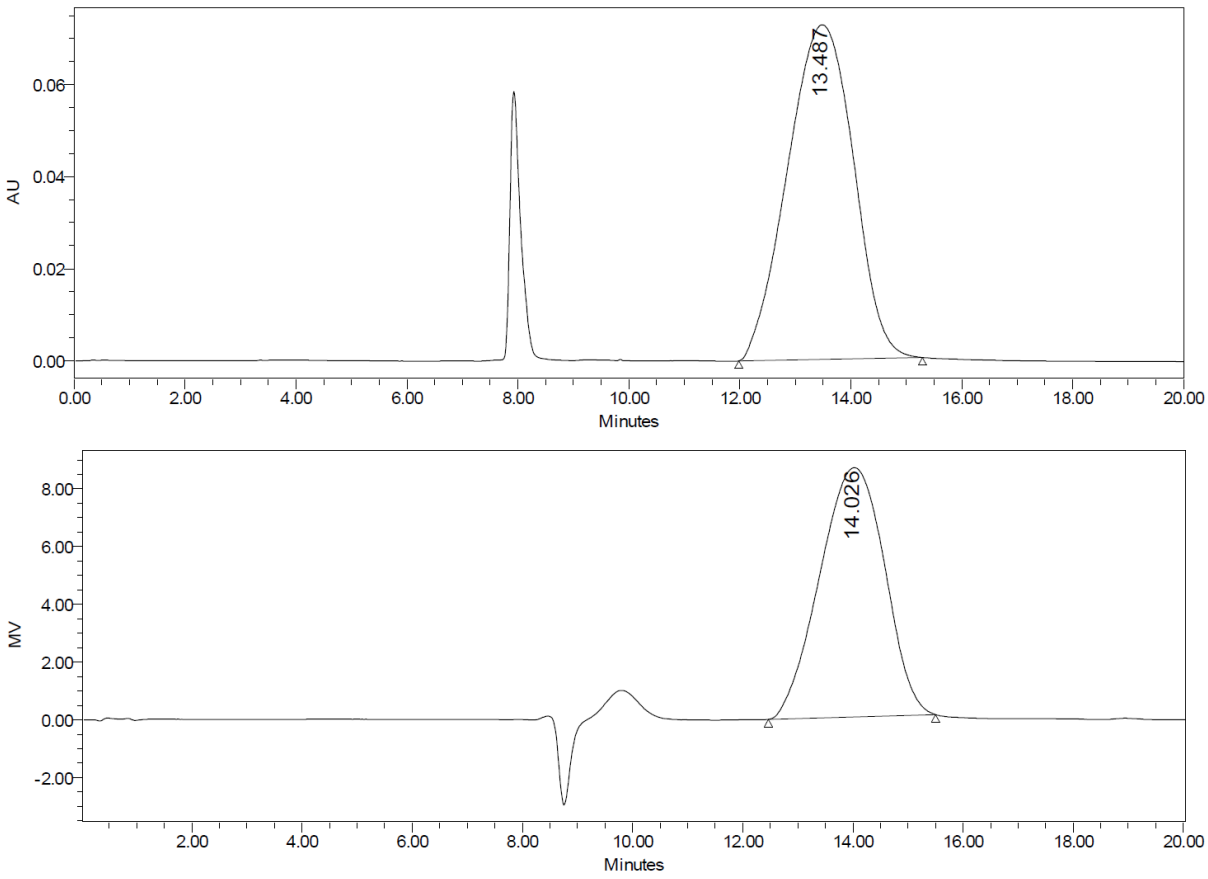

Fig. S59 HPLC of D-Saccharic acid (= glucaric acid): UV (top); RI (bottom).

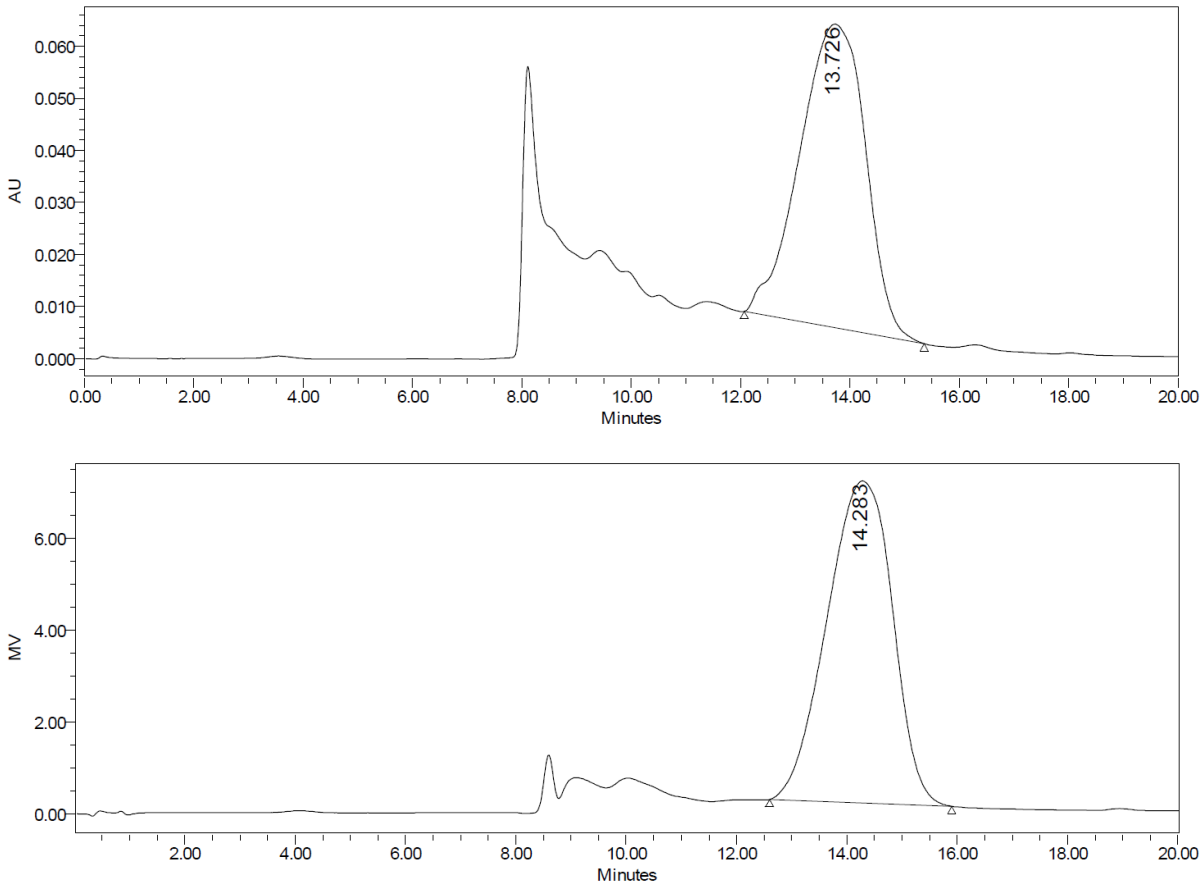

Fig. S60 HPLC of D-Glucaric acid-1,4;3,6-dilactone (**5**): UV (top); RI (bottom).

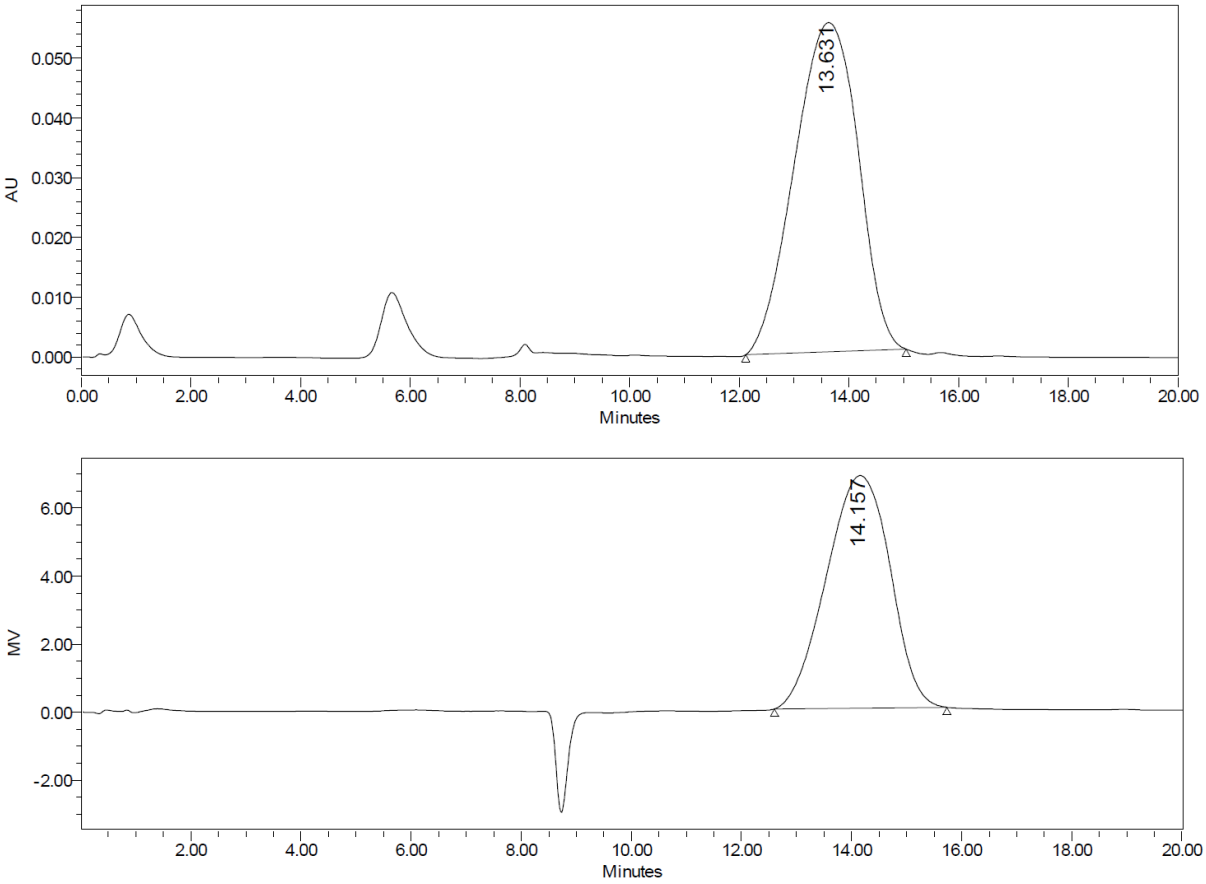

Fig. S61 HPLC of D-Glucaric acid-1,4-dilactone (**6**): UV (top); RI (bottom).

Section 3. References

1. B. T. Kusema, J.-P. Mikkola and D. Y. Murzin, *Catal. Sci. Technol.*, 2012, **2**, 423-431.
2. B. T. Kusema and D. Y. Murzin, *Catal. Sci. Technol.*, 2013, **3**, 297-307.
3. H. S. Isbell, *Bur. Stand. J. Res.*, 1932, **8**, 615-624.
4. H. S. Isbell and C. S. Hudson, *Bur. Stand. J. Res.*, 1932, **8**, 327-338.
5. H. S. Isbell and W. Pigman, *Bur. Stand. J. Res.*, 1933, **10**, 337-356.
6. F. P. Phelps, H. S. Isbell and W. Pigman, *J. Am. Chem. Soc.*, 1934, **56**, 747-748.
7. B. Beden, F. Largeaud, K. B. Kokoh and C. Lamy, *Electrochim. Acta*, 1996, **41**, 701-709.
8. F. K. Largeaud, K. B.; Beden, B.; Lamy, C., *J. Electroanal. Chem.*, 1995, **397**, 261-269.
9. J. T. Bouvier, F. P. Groninger-Poe, M. Vetting, S. C. Almo and J. A. Gerlt, *Biochemistry*, 2014, **53**, 614-616.
10. R. D. Armstrong, J. Hirayama, D. W. Knight and G. J. Hutchings, *ACS Catal.*, 2019, **9**, 325-335.
11. D. Horton, Z. Walaszek and I. Ekiel, *Carbohydr. Res.*, 1983, **119**, 263-268.
12. P. Collins and R. Ferrier, *Monosaccharides: Their Chemistry and Their Roles in Natural Products*, Wiley, First edn., 1995.
13. T. K. Lindhorst, *Essentials of Carbohydrate Chemistry and Biochemistry*, John Wiley & Sons, Third, Completely Resived and Enlarged edn., 2003.
14. M. L. Sinnott, *Carbohydrate Chemistry and Biochemistry: Structure and Mechanism*, Royal Society of Chemistry, Second edn., 2013.
15. A. E. Flood and S. Srisa-nga, *Asian Pacific Confederation of Chemical Engineering congress program and abstracts*, 2004, **2004**, 110-110.
16. A. G. Fadnis and S. K. Shrivastava, *Carbohydr. Res.*, 1982, **102**, 23-29.
17. J. R. Felty, Texas Tech Univesity, 1972.
18. T. Juĺík, P. Podešva, Z. Farka, D. Kováĺ, P. Skládal and F. Foret, *Electrochim. Acta*, 2016, **188**, 277-285.
19. M. Pasta, F. La Mantia and Y. Cui, *Electrochim. Acta*, 2010, **55**, 5561-5568.
20. N. L. Chauhan, V. Dameera, V. A. Juvekar, S. M. Mahajani, A. K. Suresh and A. Sarkar, *J. Electrochem. Soc.*, 2018, **165**, H196-H204.
21. Z. Zhang, P. Gibson, S. B. Clark, G. Tian, P. L. Zanonato and L. Rao, *J. Solution Chem.*, 2007, **36**, 1187-1200.
22. D. T. Sawyer and J. B. Bagger, *J. Am. Chem. Soc.*, 1959, **81**, 5302-5306.
23. N. M. Xavier, A. P. Rauter and Y. Queneau, *Top. Curr. Chem.*, 2010, **295**, 19-62.
24. L. Kerins, S. Byrne, A. Gabba and P. V. Murphy, *The Journal of Organic Chemistry*, 2018, **83**, 7714-7729.
25. S. Stojkovski, D. M. Whitfield, B. Sarkar, S. Stojkovski, R. J. Magee and B. D. James, *J. Inorg. Biochem.*, 1990, **39**, 125-136.
26. M. L. D. Ramos, M. M. M. Caldeira and V. M. S. Gil, *Carbohydr. Res.*, 1996, **286**, 1-15.
27. L. W. Jaques, J. B. Macaskill and W. Weltner, Jr., *J. Phys. Chem.*, 1979, **83**, 1412-1421.
28. A. Mirescu and U. Prüße, *Appl. Catal., B*, 2007, **70**, 644-652.
29. U. Prüße, K. Heidkamp, N. Decker, M. Herrmann and K. D. Vorlop, *Chemie Ingenieur Technik*, 2010, **82**, 1231-1237.
30. G. de Wit, J. J. de Vlieger, A. C. Kock-van Dalen, R. Heus, R. Laroy, A. J. van Hengstum, A. P. G. Kieboom and H. van Bekkum, *Carbohydr. Res.*, 1981, **91**, 125-138.
31. S. Rautiainen, P. Lehtinen, J. Chen, M. Vehkamaki, K. Niemela, M. Leskela and T. Repo, *RSC Adv.*, 2015, **5**, 19502-19507.
32. B. A. Lewis, F. Smith and A. M. Stephan, in *Methods in Carbohydrate Chemistry*, Academic Press, New York, 1963, vol. II, pp. 38-46.
33. V. Lemau de Talancé, E. Thiery, G. Eppe, S. E. Bkassiny, J. Mortier and S. P. Vincent, *J. Carbohydr. Chem.*, 2011, **30**, 605-617.
34. H. S. El Khadem, A. Crossman, D. Bensen and A. Allen, *J. Org. Chem.*, 1991, **56**, 6944-6946.
35. H. S. Isbell and H. L. Frush, *Bur. Stand. J. Res.*, 1933, **11**, 649-664 (Research Paper No. 613).
36. B. Asghari, P. Salehi, M. M. Farimani and S. N. Ebrahimi, *Rec. Nat. Prod.*, 2015, **9**, 276-283.
37. M. Bierenstiel and M. Schlaf, *Eur. J. Org. Chem.*, 2004, **2004**, 1474-1481.
38. T. C. Gehret, A. S. Frobese, J. S. Zerbe and H. K. Chenault, *J. Org. Chem.*, 2009, **74**, 8373-8376.
39. R. D. Armstrong, B. M. Kariuki, D. W. Knight and G. J. Hutchings, *Eur. J. Org. Chem.*, 2017, **2017**, 6811-6814.